Non-linear Flow in Unconsolidated Sandy Porous Media

An Experimental Investigation

M.Sc. Thesis

Submitted in partial fulfilment of the requirements for the degree of

M.Sc. Earth Surface and Water

Author	Roy Snoeijers
1st Supervisor	prof. dr. R.J. Schotting
2nd Supervisor	J.H. van Lopik, M.Sc.
Date	19-01-2016

Utrecht University

0. Abstract

With increasing pressure on water resources through climate change and anthropogenic influences, adequate freshwater management is essential. Important managing tools require efficient infiltration of freshwater into the subsurface. Fast, High Volume Infiltration (FHVI) is a novel infiltration technique that, if employed at its full potential, offers fast and efficient infiltration of freshwater into the subsurface. However, to date, the mechanisms and conditions enabling FHVI are not fully understood and its application is mainly based on trial and error. To overcome this barrier, research is initiated to accurately model FHVI. Due to the high injection pressures employed with FHVI, it is expected that non-linear flow behavior occurs around the injection well. Therefore, insight into this non-linear flow behavior is an adequate first step in understanding FHVI.

This research focusses non-linear Forchheimer flow in porous media similar to those in which FHVI is frequently applied (fine to course sands). An experimental setup that allows hydraulic head vs. superficial velocity measurements is used to analyze non-linear flow behavior in a variety of sandy porous media. Analysis is performed using the Forchheimer equation coefficients, statistical properties of the grain size distribution and the macroscopic parameters of the porous medium.

First, 11 fairly uniformly distributed calibrated reference porous media are tested. The porous medium with the smallest median grain size (U 0.2-0.5 [mm]) yielded the highest flow resistance with Forchheimer coefficients a and b being equal to $2.2369 \cdot 10^{-2}$ [day m^{-1}] and $1.8249 \cdot 10^{-6}$ [day^2 m^{-2}], respectively. The porous medium with the largest median grain size yielded the lowest flow resistance with Forchheimer coefficients a and b being equal to $9.268 \cdot 10^{-5}$ [day m^{-1}] and $8.2308 \cdot 10^{-8}$ [day^2 m^{-2}], respectively. In case of the reference porous media, flow resistance increased with decreasing median grain size.

Secondly, mixtures of the calibrated reference sand were prepared to investigate the effect of the shape of the grain size distribution on non-linear flow in porous media. The composites were prepared with their median grain size being equal to those of the reference porous media, but with a larger standard deviation or with the presence of one or multiple gaps in their distribution. It was found that the wider the grain size distribution, the larger the flow resistance. Especially the presence of a large fraction of fine material seemed to enhance the flow resistance. The most interesting results were obtained for the gap-graded porous media. For gap-graded porous medium N-U3, the Forchheimer coefficients a and b increased with 160.2 [%] and 200.8 [%], respectively, with respect to the fairly uniformly distributed reference porous medium U 0.4-0.8 [mm] with a similar median grain size.

Thirdly, the applicability of 7 existing empirical relations, for non-linear flow in porous media, to describe the experimental results of this study was assessed. In case of the reference porous media, it appeared that good fits were obtained by both the expressions by Kovács (1981) (for $d_{50} < \pm 1$[mm]) and Macdonald et al (1979) (for $d_{50} > \pm 1$[mm]). The empirical relations proved to be inadequate to describe non-linear flow in non-uniformly distributed porous media

(the composite porous media) as the empirical relations do not take the shape of the grain size distribution into account. It is recommended that modifications to these empirical relations are made if employed for non-linear flow in non-uniform porous media.

The outcome of this study is very useful within the context of FHVI. Great insight into non-linear flow in a variety of porous media is obtained. A subsequent step will be the application of the experimental data to a numerical model.

Table of Contents

0. Abstract 2
Table of Contents 4
List of Figures 6
List of Tables 8
Nomenclature 10
Acknowledgements 12
1. Introduction 13
2. Theory 16
2.1. Observation of Linear and Non-linear Flow in Porous Media 16
2.2. Proposed Physical Mechanisms for Non-linear Flow 18
2.3. Empirical Relations – Relating Hydraulic Gradient to Superficial Flow Velocity 19
3. Methodology 25
3.1. The Experimental Setup 25
3.2. The Sandy Porous Media 26
3.2.1. Grain Size Distribution Characterization 26
3.2.2. The Porous Media 27
3.2.2.1. Preparation Method 27
3.2.2.2. Reference Porous Media – Filtered/Calibrated Sands/Gravels 27
3.2.2.3. Composite/Mixed Porous Media 28
3.3. Note on Air Inclusion 32
3.4. Determination of the Macroscopic Hydraulic Parameters 32
3.4.1. Non-linear Flow Behavior – Forchheimer Coefficients 32
3.4.2. Non-linear Flow Behavior – Determination of the Onset of Non-linear Flow Behavior 33
3.4.3. Porosity 33
3.5. Determination of the Effect of the Grain Size Distribution on Non-linear Flow 34
3.6. Comparison Experimental Data with Empirical Expressions 34
4. Results 36

4.1. Non-linear Forcheimer Flow in the Reference Porous Media 36
4.2. Effect of Shape Grain Size Distribution on Non-Linear Flow in Porous Media .. 40
4.2.1. Comparison with U 0.4-0.8 [mm] 41
4.2.2. Comparison with U 0.71-1.25 [mm] 43
4.2.3. Other Comparisons 45
4.2.4. Relation Forchheimer Coefficients and Median Grain Size 49
4.2.5. The Effect of Porosity 50
4.3. Comparison of Experimental Data with Empirical i-q Relations 51
5. Discussion 54
5.1. Comparison Experimental Results with Existing Literature 54
5.2. Effect of the Grain Size Distribution on Non-linear Flow in Porous Media 55
5.2.1. Fraction of Fine Material 55
5.2.2. Grain Size Distribution versus Porosity for a Given Compaction 55
5.3. Uncertainty in the Experimental Data 56
5.4. Use of Empirical Relations 56
5.4.1. Fit of the Empirical Relation on the Data 56
5.4.2. Definition of the Length Parameter d 57
5.4.3. Effect of Shape and Roughness of Grains 57
5.5. Future Work 57
5.5.1. Account for the Effect of Grain Size Distribution 57
5.5.2. FHVI and Non-linear Flow Behavior 58
6. Conclusions 59
References 60
Appendix 66

List of Figures

Figure 1: Relation between the hydraulic gradient and the superficial flow velocity for the range of velocities in which Darcy's Law holds and for velocities below or above the threshold velocities that mark the limits of the applicability of Darcy's Law. Figure from Basak (1977a)……..**16**
Figure 2: Constants of Ergun equation according to analytical derivation by Du Plessis (1994; Eq. 12). Both Ergun equation constants A and B are dependent on porosity. Figures retrieved from Du Plessis (1994)……...**23**
Figure 3: The experimental setup. The white arrows indicate the flow direction. The porous medium is located in a cylindrical column in the middle of the setup. Water pressure is measured at four locations in the experimental setup using a pressure transmitter (see red arrow) and plastic wiring. PL is the water pressure measured left of the porous medium (red arrow), PR is the constant hydraulic head created by accumulation of water in the right vertical column which is equal to 0.55 [m]. The yellow hose supplies water from the reservoir (right bottom of the figure, see Appendix A.1 for a better image of the reservoir). The most right vertical segment serves as water outlet. Temperature is measured at the most-right red arrow……**25**
Figure 4: I-q relations based on the results of the experiments with reference porous media. Plotted are the data retrieved from the experimental analyses, the Forchheimer equation fit on the experimental data, and the Darcy equation based on the Forchheimer coefficient a. Color shading blue indicates presence of the Darcy regime, color shading green of the Forchheimer regime. For the fitted parameters and the goodness of fit, see Table 4……...**37**
Figure 5: Fitted Forchheimer coefficients a [day m^{-1}] of the experimental data vs. the median grain size [m] for the reference porous media. A fit on the data is shown in the form of a power law……**38**
Figure 6: Fitted Forchheimer coefficients b [day^2 m^{-2}] of the experimental data vs. the median grain size [m] for the reference porous media. A fit on the data is shown in the form of a power law……**39**
Figure 7: Grain size distributions and i-q curves shown for U 0.4-0.8 [mm], N-U1, N-U2, and N-U3……**43**
Figure 8: Grain size distributions and i-q curves shown for U 0.71-1.25[mm], N-U7, N-U8, N-U9, N-U10……**45**
Figure 9: Grain size distributions and i-q curves shown for U 0.5-1.0 [mm], U 0.63-1.0 [mm], U 0.8-1.25 [mm], U 1.0-1.6 [mm], N-U4, N-U5, N-U6, N-U11, N-U12, and N-U13……..**48**
Figure 10: Fitted Forchheimer coefficients a [day m^{-1}] of the experimental data vs. the median grain size [m] for the reference porous media. A fit on the data is shown in the form of a power law. Also the Forchheimer coefficients a for the composite porous media are given. No fit is made on these values……...…**49**
Figure 11: Fitted Forchheimer coefficients b [day^2 m^{-2}] of the experimental data vs. the median grain size [m] for the reference porous media. A fit on the data is shown in the form of a power

law. Also the Forchheimer coefficients b for the composite porous media are given. No fit is made on these values.....**50**
Figure 12: : i-q curves shown for U 0.2-0.63 [mm], and the empirical relations using the same n, d50, and ν as U 0.2-0.63 [mm].....**53**
Figure 13: i-q curves shown for U 5.0-8.0 [mm], and the empirical relations using the same n, d50, and ν as U 5.0-8.0 [mm].....**53**
Figure 14: Forchheimer coefficient a [s m^{-1}] versus the median grain size, d50 [m]. Data from Sidiropoulou et al. (2007), who summarized various datasets from previous studies, as well as this work's data are given. Power law fits are given for both datasets.....**54**
Figure 15: Forchheimer coefficient b [s^2 m^{-2}] versus the median grain size, d50 [m]. Data from Sidiropoulou et al. (2007), who summarized various datasets from previous studies, as well as this work's data are given. Power law fits are given for both datasets.....**55**

List of Tables

Table 1: Reference porous media used in this research. Characteristics of the grain size distribution are given in d_x, where x denotes the percentage of grains with a diameter smaller than the given diameter, in terms of the mean grain diameter (d_m), the variance (σ^2), standard deviation (σ) and skewness (d_{m3}/σ^3) of the grain size distribution. Furthermore the coefficient of curvature and the coefficient of uniformity are given……..**29**

Table 2: Composite porous media used in this research. This table shows the fractions of reference porous media present in each of the composite porous media……..**30**

Table 3: Composite porous media used in this research. Characteristics of the grain size distribution are given in d_x, where x denotes the percentage of grains with a diameter smaller than the given diameter, in terms of the mean grain diameter (d_m), the variance (σ^2), standard deviation (σ) and skewness (d_{m3}/σ^3) of the grain size distribution. Furthermore the coefficient of curvature and the coefficient of uniformity are given……..**31**

Table 4: Results of the experiments for the reference porous media in terms of the coefficients of the fitted Forchheimer equations, the goodness of the fits, the d_{50} of the porous media, the minimum and maximum Reynolds number encountered during the experiments and the Reynolds numbers indicating the transition from the Darcy regime to the Forchheimer regime according to the various definitions explained in the Methodology chapter, $Re_{F,1}$, $Re_{F,5}$, and $Re_{F,10}$-……**39**

Table 5: This table shows the statistical properties for porous media U 0.4-0.8 [mm], N-U1, N-U2, and N-U3 as also given in section 3.2. Results of the experiments for these porous media are given in terms of the coefficients of the fitted Forchheimer equations, the goodness of the fits, the d_{50} of the porous media, the minimum and maximum Reynolds number encountered during the experiments and the Reynolds numbers indicating the transition from the Darcy regime to the Forchheimer regime according to the various definitions explained in section 3.4, $Re_{F,1}$, $Re_{F,5}$, and $Re_{F,10}$. In case the Reynolds numbers are underlined, they fall within the range of measured Reynolds numbers……..**42**

Table 6: Relative error of Forchheimer equation coefficients a and b resulting from the experiments with composite porous media N-U1, N-U2, and N-U3 with respect to the Forchheimer equation coefficients a and b resulting from the experiments with reference porous medium U 0.4-0.8 [mm]……...…**42**

Table 7: This table shows the statistical properties for porous media U 0.71-1.25 [mm], N-U7, N-U8, N-U9, and N-U10 as also given in section 3.2. Results of the experiments for these porous media are given in terms of the coefficients of the fitted Forchheimer equations, the goodness of the fits, the d50 of the porous media, the minimum and maximum Reynolds number encountered during the experiments and the Reynolds numbers indicating the transition from the Darcy regime to the Forchheimer regime according to the various definitions explained in section 3.4, ReF,1, ReF,5, and ReF,10¬¬. In case the Reynolds numbers are underlined, they fall within the range of measured Reynolds numbers……...…**44**

Table 8: Relative error of Forchheimer equation coefficients a and b resulting from the experiments with the composite porous media N-U7, N-U8, N-U9 and N-U10 with respect to the Forchheimer equation coefficients a and b resulting from the experiments with reference porous medium U 0.71-1.25 [mm]……**44**
Table 9: This table shows the statistical properties for porous media U 0.5-1.0 [mm], U 0.63-1.0 [mm], U 0.8-1.25 [mm], U 1.0-1.6 [mm], N-U4, N-U5, N-U6, N-U11, N-U12 and N-U13 as also given in section 3.2. Results of the experiments for these porous media are given in terms of the coefficients of the fitted Forchheimer equations, the goodness of the fits, the d50 of the porous media, the minimum and maximum Reynolds number encountered during the experiments and the Reynolds numbers indicating the transition from the Darcy regime to the Forchheimer regime according to the various definitions explained in section 3.4, ReF,1, ReF,5, and ReF,10¬¬. In case the Reynolds numbers are underlined, they fall within the range of measured Reynolds numbers. a this porosity is not directly determined from the porous medium with which the non-linear flow experiment is performed through disturbance of the weighing process. The porosity of a porous medium with the same mixture is used instead……**46**
Table 10: : Relative error of Forchheimer equation coefficients a and b resulting from the experiments with the composite porous media N-U4, N-U5, N-U6, N-U11, N-U12, and N-U13 with respect to the Forchheimer equation coefficients a and b resulting from the associated experiments (similar median grain size) with reference porous media U 0.5-1.0 [mm], U 0.63-1.0 [mm], U 0.8-1.25 [mm], U 1.0-1.6 [mm]……..…**46**
Table 11: NOF values [-] for all investigated empirical expressions calculated relative to the Forchheimer equation fit on the experimental data. Shown for reference and composite porous media……**52**

Nomenclature

a	Coefficient Forchheimer equation [TL^{-1}]]
A	Constant Ergun equation [-]
A_c	Area cross section of column/porous medium [L^2]
α	Coefficient Ergun-Orning Equation [-]
b	Coefficient Forchheimer equation [$T^2L^{=2}$]
B	Constant Ergun equation [-]
β	Coefficient Ergun-Orning Equation [-]
c	Linear parameter Reynolds equation [L]
d	Representative length parameter [L]
d_{50}	Median grain diameter [L]
dh	Difference in hydraulic head over a porous medium [L]
d_i	Single grain size [L]
d_m	Mean grain diameter [L]
$d_{m3}\sigma^{-3}$	Skewness of grain size distribution [-]
dx	Length of a porous medium [L]
D(q)	Hydraulic gradient determined by Darcy equation for given q [-]
De_x	Deviation Forchheimer's (F(q)) from Darcy's (D(q) Equation [%]
F(q)	Hydraulic gradient determined by Forchheimer equation for given q [-]
g	Gravitational constant [LT^{-2}]
Δh	Difference in hydraulic head over the porous medium [L]
i	Hydraulic gradient [-]
k	Intrinsic permeability [L^2]
K	Hydraulic conductivity [LT^{-1}]
m_s	Mass of the solid matrix of the porous medium [M]
μ	Dynamic viscosity of water [$ML^{-1}T^{-1}$]
n	Porosity [-]
N	Sample size [-]
NU_a	Forchh. eq. coeff. a determined for a more well-graded or gap-graded porous medium [$TL^{=1}$]
NU_b	Forchh. eq. coeff. b determined for a more well-graded or gap-graded porous medium [$T^2L^{=2}$]
ν	Kinematic viscosity of water [L^2T^{-1}]
p_i	Probability of occurrence of single grain size d_i [-]
P_L	Pressure on left boundary porous medium [P]
P_R	Pressure on right boundary porous medium [P]
q	Superficial flow velocity or macroscopic flow velocity [LT^{-1}]
Q	Discharge through porous medium [L^3T^{-1}]
ρ_s	Density of the solid matrix [ML^{-3}]

ρ_w	Density of water [ML^{-3}]
σ	Standard deviation of grain size distribution [L]
σ^2	Variance of grain size distribution [L^2]
U	Velocity parameter Reynolds equation [LT^{-1}]
U_a	Forchh. eq. coeff. a determined for a reference porous medium [TL^{-1}]
U_b	Forchh. eq. coeff. b determined for a reference porous medium [T^2L^{-2}]
V_s	Volume of the solid matrix [L^3]
V_t	Total volume, volume of the column holding the porous medium [L^3]
x_i	Hydraulic gradient of experimental data for data point i [-]
Δx	Length of the porous medium [L]
y_i	Hydraulic gradient of empirical relation for data point i [-]

Acknowledgements

I would like to thank my supervisors, prof. dr. Ruud Schotting and Jan van Lopik, M.Sc., for giving me the opportunity to work together with them on the Fast, High Volume Infiltration project. It was a grand opportunity to combine pure scientific research with industry application. I am obliged to them for reviewing my thesis, improving my knowledge on the topic of non-linear flow in porous media, and providing feedback on my academic writing skills.

The author is obliged to STW and O2DIT for making this research possible within the context of the Fast, High Volume Infiltration project. Without their function as umbrella organizations, this thesis would not have existed.

Furthermore, I would like to express my sincere appreciation to Peter de Vet for the construction of the experimental setup used in this research and always being available to correspond about technical issues and improvement of the setup. I would also like to thank Thony van der Gon Netscher, ing. Van Dam, and mr. van Aken for their technical support. Regarding the experimental research I would like to thank Teun van Dooren, B.Sc. and Willem-Jan Dirkx, B.Sc. for providing me with new information on the experimental setup and helping me doing the experimental work. The occasional echoes of rock songs we played in the Van Unnik basement seemed to make the long lab days just a bit shorter.

I learned a great deal visiting the Wyenhütte and Ede sites where FHVI was put to practice and talking with the employees of the construction dewatering companies involved, mainly Thijs de Vet and Sjaak van Laan.

I would like to thank my parents, brother and girlfriend for always being there for me, in good and bad times, inside or outside the context of writing this thesis. Harm, Daniel and Mark, both the hydrology classes and the Utrecht nightlife wouldn't have been as good without you guys. Many thanks also to my friends outside of the department, mainly Geert, Bart and Jochem, for providing me with the necessary relaxation and making my Friday nights great.

1. Introduction

Management of freshwater resources is key for water security, safety, and ecosystem conservation. However, due to increased anthropogenic influence in the water cycle and changing boundary conditions as a result of climate change, management of these resources is developing into an increasingly complex problem on both local and global scale. In many regions on Earth, water shortage is faced, for instance in the form of alteration of precipitation patterns (e.g. Cao et al., 2010; Tsanis et al., 2011), overexploitation of existing resources (e.g. Wada et al., 2010; Scanlon, 2012), or salinization of groundwater resources (e.g. Oude Essink, 2001a; Werner et al., 2013). On the other hand, excess rainwater causes safety issues and ecosystem degradation on various locations globally (e.g. Loaiciga et al., 1996; Poesen and Hooke, 1997; Wilby and Keenan, 2012). A variety of freshwater management tools to minimize negative consequences of these global and local chances involve interaction with the subsurface. Examples are artificial aquifer recharge (AR), which can be applied to store excess precipitation (e.g. Patel et al., 2009) or to replenish exploited groundwater resources (e.g. Asano, 1985), and aquifer storage and recovery (ASR), for instance to bridge seasonal shortage of freshwater (e.g. Patel et al., 2009) or for wastewater treatment (e.g. Kanarek and Michail, 1996; Dillon et al., 2006). AR and ASR require efficient infiltration of water, just as a variety of other applications, such as groundwater remediation (e.g. Marryott, et al., 1993; Brusseau et al., 2007), aquifer thermal energy systems (ATES) (e.g. Palmer et al., 1992; Vandenbohede et al., 2011), the prevention of salt water intrusion into groundwater resources (e.g. Oude Essink, 2001b), and construction dewatering (e.g. Cashman and Preene, 2013).

During subsurface construction, it is necessary to (temporary) lower the groundwater level during excavation of a construction site in order to prevent damage and/or to improve conditions for construction (Powers et al., 2007; Cashman and Preene, 2013). Construction dewatering is used for this purpose. In some cases, the extracted groundwater is injected back into the same aquifer, as a result of legal factors, tax regulations or because of the possible danger of soil subsidence. Usually, re-injection of groundwater is done by means of an injection well with a large well screen, extending over the entire depth of the aquifer. Several Dutch and German dewatering companies have developed a new, more efficient, infiltration method, *Fast, High Volume Infiltration (FHVI).* These companies have encountered local injection points in the aquifer where infiltration was significantly easier compared to other points in the aquifer. Based on these findings, they use partially penetrating wells (FHVI-wells) with a small screen (usually 1 [m]) to efficiently inject large quantities of water in these local points in the aquifer. Because of the ease of infiltration, the impact on the local groundwater system is smaller than in case of regular re-infiltration, which allows the extracted groundwater to be injected closer to the location of extraction/the construction site, thereby reducing the footprint and lowering the costs of the construction dewatering. Unfortunately, to date, FHVI receives no solid scientific base and, as its application is largely based on trial and error, its market value is below its potential (STW, 2014).

Therefore, scientific research is required in order to give FHVI this scientific base and convince potential customers of the benefits of this infiltration method.

In order to accurately describe and use FHVI, adequate modeling of the infiltration method is necessary. Commonly, Darcy's Law, a linear relation between the pressure/hydraulic gradient and the flow velocity that describes creeping flow conditions, is applied to model flow around injection wells. This is a reasonable assumption when conventional infiltration wells are used, as injection rates and pressures (around 0.2 [bar]) are low enough to apply Darcy's Law. However, when the hydraulic gradient and flow velocity increase, Darcy's Law may become invalid. In literature it is frequently pointed out that at elevated flow velocities, the relation between the hydraulic gradient and the flow velocity becomes non-linear as a result of enhanced flow resistance (e.g. Forchheimer, 1901, Schneebeli, 1955). In case of FHVI, the well screen is an order of magnitude smaller and the injection pressures can be as high as 2 [bar]. Hence, Darcy's Law might not apply for FHVI and the possible existence of non-linear flow around the well screen needs to be taken into account. The occurrence of non-linear flow around (injection) wells has been frequently discussed in literature (e.g. Basak, 1977b; Wu, 2005). Many investigators have attempted to derive solutions for non-linear flow around the well screen (e.g. Basak, 1977b; Mathias et al., 2008), but often the presence of non-linear flow conditions is neglected (e.g. see Walton, 2007) or included in the well skin of the well (e.g. Zenner, 2009). For the purpose of modeling FHVI, it might be necessary to adequately model non-linear flow around the well screen.

To be able to determine to what extent non-linear flow could occur around FHVI-wells, an understanding of non-linear flow behavior in a wide range of sandy porous media (e.g. fine to course, poorly- to well-graded) is needed. Therefore, we have investigated non-linear flow behavior in a variety of sandy porous media by means of laboratory column experiments. Concerning the design of this research, attention is paid to the sandy porous media in which FHVI is applied, as well as the already existing literature on non-linear flow in porous media. It was found that most experimental data on (post-Darcy) non-linear flow in porous media is conducted for course porous media, such as coarse sands, gravels, large glass beads, etc. (e.g. see Sidiropoulou et al., 2007; Huang et al., 2013; Bağci et al., 2014; Sedghi-Asl et al., 2014). There seems to be relatively little experimental data available for finer sandy porous media. As the porous media in which FHVI is applied range greatly in grainsize (e.g. Hölscher Wasserbau GmbH, 2010; Fugro GeoServices B.V., 2012; Theo van Velzen BV, 2013), research into finer sandy porous media is of great benefit. Furthermore, in many studies on non-linear flow in porous media, a single value for median or mean grain size (d_{50}) is used to characterize grain size of the porous media. Relatively little research has been conducted on the effect of the grain size distribution on non-linear flow in porous media. As porous media occur in great variety in the subsurface (e.g. poorly-graded, well-graded, uniformly-graded, gap-graded), research on this topic is often of great value.

Considering the research gaps and the importance of aimed research for FHVI, this study focusses on the following research topics:

1) Generation of a database of non-linear flow experiments for 11 sand types with various grain sizes (d_{50}).
2) Analysis of the effect of the shape of the grain size distribution on non-linear flow in porous media. For a group of the 11 reference sand types, new porous media were created with a different shape of the grain size distribution (e.g. more well-graded or gap-graded) but with a similar median grain size (d_{50}).
3) Analyzing the applicability of various existing empirical expressions, relating hydraulic gradient to flow velocity at high flow velocities using fluid and porous medium properties (e.g. Ergun, 1952; Macdonald et al., 1979), to predict our experimental results. 7 of these expressions are used in this research.

To investigate the research topics above, laboratory column experiments are employed to obtain insight into the non-linear flow behavior for the porous media in consideration. For every porous media, the relation between the hydraulic gradient and the superficial flow velocity is investigated, as well as the media properties (porosity, grain size distribution). This is a common method applied to investigate non-linear flow in porous media (e.g. Bağci et al., 2014; Sedghi-Asl et al., 2014).

2. Theory

2.1. Observation of Linear and Non-linear Flow in Porous Media

Flow of fluids is initiated by a difference in mechanical energy of fluid at two distinct points in space. The mechanical energy of water at a certain point in space is also called the 'hydraulic head' and is the summation of the elastic potential energy, the gravitational potential energy and the kinetic energy. The difference in mechanical energy between water in one point in space and water in another point in space is accordingly called the 'hydraulic gradient.'

The first relation between the hydraulic gradient (or pressure gradient) and the flow velocity was constructed independently by Hagen (1839) and Poiseuille (1840) for laminar flow in capillary tubes, such as veins. Subsequently, Darcy (1856) was the first to point out a relationship between the hydraulic gradient and the superficial flow velocity (in literature also called: specific discharge, macroscopic velocity or Darcy flux) through a porous medium for a Newtonian fluid. He derived this equation (Eq. 1), a linear relationship between hydraulic gradient and the macroscopic velocity, empirically by performing column experiments.

$$q = -K\frac{dh}{dx} \tag{1}$$

Where q [m day^{-1}] is the superficial flow velocity, K [m day^{-1}] is the hydraulic conductivity, and dh/dx [-] is the hydraulic gradient over a porous medium.

According to many, this law marked the start of quantitative hydrogeology (e.g. Simmons, 2008). Darcy's Law is also widely applied in petroleum engineering (e.g. Yu and Lerche, 1995) and chemical engineering (e.g. Singh et al., 2003; Dufour et al., 2011). Although Darcy obtained his law empirically, Darcy's Law has been derived theoretically. Bear (1988) listed examples of derivations of Darcy's Law in case of fully saturated porous media. Other examples of derivations of Darcy's Law are: Neuman (1975) for homogeneous porous media and Whitaker (1986) for heterogeneous porous media. Derivations are also performed for more complex situations, e.g. in case the porous medium is composed of two weakly coupled solid phases (Santos and Sheen, 2008) or in case of slowly deforming porous media (e.g. Gray and O'Neill, 1976).

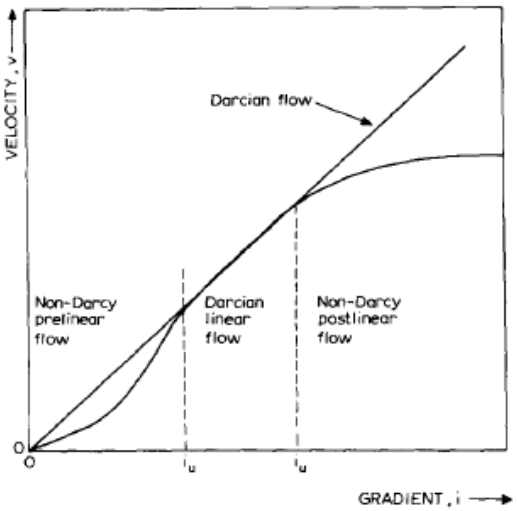

Figure 1: Relation between the hydraulic gradient and the superficial flow velocity for the range of velocities in which Darcy's Law holds and for velocities below or above the threshold velocities that mark the limits of the applicability of Darcy's Law. Figure from Basak (1977a).

Many experimental studies have observed deviation from Darcy's linear law when superficial flow velocity increases (e.g. Fancher et al., 1933; Schneebeli, 1955; Bağci et al., 2014). When a certain velocity threshold is exceeded, the flow resistance in the porous

medium increases in a way that the relation between the hydraulic gradient and the superficial flow velocity becomes non-linear, the hydraulic gradient increasing faster for a given change in flow velocity (see Figure 1). Forchheimer (1901), one of the earlier observes of this non-linearity, proposed an extension of the Darcy equation by adding a non-linear term (Eq. 2). a [day m^{-1}] and b [day^2 m^{-2}] are coefficients, often referred to as the 'Forchheimer coefficients'. When omitting the second term, Darcy's Law is obtained (as coefficient a is the inverse of K). The Forchheimer coefficients can be determined empirically. However, many modifications and different interpretations are given for the Forchheimer coefficients (see section 2.3.). Like Darcy's Law, Forchheimer's equation has been derived theoretically using a variety of physical boundary conditions (e.g. Giorgi, 1997; Chen et al., 2001).

$$-\frac{dh}{dx} = aq + bq^2 \tag{2}$$

Other relations have been derived to describe non-linear flow in porous media by relating the hydraulic gradient to the flow velocity. Of these relations, the Izbash equation is most frequently used (as given in Soni et al., 1978), but many more exist (e.g. see Bear, 1988; Skjetne and Auriault, 1999). In literature, there is discussion on whether the Forchheimer or Izbash relation is more appropriate to describe non-linear flow. Some studies indicate that the Izbash relation gives a better fit on their experimental data (e.g. Bordier and Zimmer, 2000). However, in general, the Forchheimer equation is used more frequently, partially because it also fits experimental data very well (e.g. Moutsopoulos et al., 2009; Sedghi-Asl et al., 2014) and because the Forchheimer equation is regarded as physically sound (Bordier and Zimmer, 2000), while the Izbash equation is very empirical in nature (Moutsopoulos et al., 2009).

Reynolds number (Reynolds, 1883) is used to determine whether flow is linear or non-linear, in other words, whether flow is in the Darcy regime or the Forchheimer regime, referring to the equations applied in the linear and non-linear regime, respectively. Reynolds derived his equation for open pipe flow (Eq. 3)

$$Re_{pipe} = \frac{c\rho_w U}{\mu} \tag{3}$$

in which c [L] denotes a linear parameter like the radius of a tube, U [L T^{-1}] is the velocity parameter, ρ_w [M L^{-3}] is the density of water, and μ [M L^{-1} T^{-1}] the dynamic viscosity of water.

Reynolds number has been adapted for use in porous media. A form commonly encountered in literature is the form in which c is chosen to be equal d_{50}, the median or mean grain diameter and U is chosen to be equal to the superficial flow velocity, q (Eq. 4). Although this definition of Reynolds number is frequently used, there is some discussion on the use of the linear parameter c and the velocity parameter (e.g. Bağci et al., 2014) and also, a fair amount of

studies use a different definition of Reynolds number (e.g. Green and Duwez, 1951; Ergun, 1952; Muljadi et al., 2015).

$$Re = \frac{d_{50}\rho_w q}{\mu} \tag{4}$$

A great amount of research has been devoted to obtain a single value for Reynolds number that marks the boundary between linear and non-linear flow, i.e. that marks the onset of non-linear flow. Unfortunately, up to date, this single value has not been found. This is partially due to the absence of a consensus on the definition of the Reynolds number (or other definition for the transition between linear and non-linear flow) (Zeng and Grigg, 2006). Chauveteau and Thirriot (1967) and Bear (1972) both indicate that previous works have shown that the threshold Reynolds number varies somewhere between 1 and 10. However, other reviews have discussed different threshold values, e.g. 0.1 and 75 (Scheidegger as cited in Zeng and Grigg, 2006), 1-15 as pointed out by Hassanizadeh and Grey (1987) who reviewed several experimental and numerical studies on the subject. According to Chauveteau and Thirriot (1967) it is impossible to reach consensus on one Reynolds number that marks the end of the linear Darcy regime, as the Reynolds number does not take the main driver behind flow regimes, the pore shape, into account. In fact, for the calculation of Reynolds number, it is assumed that the pore shape is exactly the same for every pore in the porous medium (Chauveteau and Thirriot, 1967), which is not a realistic assumption for natural porous media.

2.2. Proposed Physical Mechanisms for Non-linear Flow

At first the onset of non-linear flow behavior was assumed to be the effect of turbulence (e.g. Bear, 1988), but this was soon refuted by various investigators (see Bear, 1988). Many studies Hassanizadeh and Gray (1987) attribute the onset of non-linear flow to viscous drag forces, which are retarding forces (by a fluid) that results from the movement of an object through a fluid (Tipler and Mosca, 2008). In porous media flow, this can be characterized by retarding forces exerted on the pore walls (e.g. Hassanizadeh and Gray, 1987). It needs to be pointed out that even though the relation between the hydraulic gradient and the flow velocity is non-linear, the flow is still laminar and not yet turbulent (e.g. Hassanizadeh and Gray, 1987; Seguin et al., 1998).

After the onset of the Forchheimer regime, this regime can be regarded as a transition from linear laminar flow via non-linear laminar flow to fully turbulent flow, where flow resistance changes slowly from viscous forces-oriented to inertial forces-oriented (e.g. Chauveteau and Thirriot, 1967). Chauveteau and Thirriot (1967) have experimentally shown that increasing deformation of streamlines in an increasing amount of pores with increasing flow velocity occurs. According to their results this occurs for Reynolds numbers greater than 80. They attribute the deformation of streamlines to inertial forces. They show that with increasing flow velocity, turbulent flow appears in an increasing amount of pores, whilst in others laminar flow continues

to be present. This indicates that in the Forchheimer regime, flow steadily changes from laminar to non-laminar (i.e. turbulent), after a certain threshold (Re of 80 in case of Chauveteau and Thirriot, but different numbers exist) (Chauveteau and Thirriot, 1967). They show that at some critical velocity all flow in the porous medium completely dominated by inertial forces and is fully turbulent. This is the end of the Forchheimer regime and the start of the turbulent regime. As is the case for the transition from the linear laminar Darcy regime to the non-linear laminar Forchheimer regime, there exists no single Reynolds number that indicates the transition from the Forchheimer regime to the fully turbulent regime. Chauveteau and Thirriot attribute a Reynolds number of approximately 180 to this transition, but other proposed numbers exist. Many studies use the Forchheimer equation to model turbulent flow (e.g. Bağci et al., 2014). In this study, the occurrence of the turbulent flow regime is rare or absent (depending on the definition of the boundary between the Forchheimer regime and the turbulent regime) and therefore, if it is present at all, it will be described using Forchheimer's equation.

Interesting to note is that another non-linear regime is present for flow velocities lower than the lower threshold velocity (or Reynolds number) for Darcy's Law (see Figure 1). The regime is accordingly called the pre-Darcy regime. Little mention of pre-Darcy flow is made in literature, but its existence has been shown in multiple experimental studies (e.g. Zeng et al., 2012; Bağci et al., 2014; Dukhan et al, 2014). An early notion of pre-Darcy flow was made by King (1899), by stating that under some circumstances, the superficial velocity may increase more strongly than the hydraulic gradient, for water flow through sands or rock. Soni et al. (1978), referring to a previous work done by Basak (1977a), point out that, due to molecular forces, the pre-Darcy regime is characterized by a non-linear relationship between hydraulic gradient and superficial velocity of the fluid. Similar to King, they point out that it appears that for a part of the pre-Darcy regime, the velocity increases more than the hydraulic gradient proportionally. As will be shown later, no notion of the pre-Darcy regime is taken in the current work, since the Reynolds numbers encountered during the experiments are significantly larger than the proposed upper boundary Reynolds number for pre-Darcy flow: Fand et al. (1987) proposed a maximum Reynolds number of 10^{-5} (as cited in Bağci et al., 2014).

2.3. Empirical Relations – Relating Hydraulic Gradient to Superficial Flow Velocity

Parameters a [$day m^{-1}$] and b [$day^2 m^{-2}$] of the Forchheimer equation, Eq. 2, can be determined empirically through experimental investigation. Empirical determination of the Forchheimer equation coefficients suffices in some cases. However, great interest has been expressed in the recent decades in (general) solutions for the coefficients. As Macdonald et al. (1979) point out, it is convenient to be able to calculate the superficial flow velocity when the hydraulic gradient or pressure gradient is known and vice versa. Unfortunately, the derivation of analytical solutions to the coefficients seems to be nearly impossible, due to, for instance, the complexity of the flow pattern (Macdonald et al., 1979) and the complexity of porous media geometry (Hlushkou and Tallarek, 2006). Nevertheless, scientists and engineers have attempted to develop (semi-)empirical expressions for Forchheimer equation coefficients a and b in terms of porous medium properties,

such as intrinsic permeability, porosity, etc., and flow properties, as viscosity (e.g. Ergun, 1952; Ward, 1964; Irmay, 1964, Macdonald et al., 1979). In many experimental frameworks, including the one in this study, it is possible to determine these macroscopic porous medium/fluid parameters. Therefore, these empirical relations are a popular tool to characterize non-linear flow in porous media. In this section, the most important empirical relations are described.

The best known empirical equation relating the hydraulic gradient to superficial flow velocity is the Ergun equation (Ergun, 1952), Eq. 5,

$$-\frac{dh}{dx} = 150\frac{(1-n)^2\nu}{gn^3d^2}q + 1.75\frac{(1-n)}{gn^3d}q^2 \tag{5}$$

where n [-] is the porosity of the porous medium, ν [m^2day^{-1}] the kinematic viscosity of the fluid, g [$mday^2$] the gravitational constant, and d [m] a representative length parameter, usually the median grain size (in this study this is chosen to be the median grain size). The physical roots of the Ergun (1952) equation become apparent in an earlier work by Ergun and Orning (1949). The Ergun equation is based on the Kozeny-Carman model (Kozeny, 1927; Carman, 1937), which is a geometric permeability model for flow in porous media based on conduit flow (Dullien, 1979). The Kozeny-Carman equation (Eq. 6, from Bear (1988)) relates the hydraulic conductivity or intrinsic permeability of a porous medium to the pore diameter and porosity,

$$k = \frac{d_m^2}{180}\frac{n^3}{(1-n)^2} \tag{6}$$

where d_m is the mean particle size. Hence, also the hydraulic gradient or pressure gradient can be related to these macroscopic fluid and porous medium parameters (see Ergun and Orning, 1949). The Kozeny-Carman equation is based on the assumption that a porous medium can be represented as an aggregation of capillary tubes and the Navier-Stokes equation can be applied onto (e.g. Chapuis and Aubertin, 2003). The Kozeny-Carman equation is only valid for creeping laminar flow (e.g. Ergun and Orning, 1949), which means that also the relation between hydraulic gradient and the macroscopic parameters can only be used to estimate the intrinsic permeability for Darcian flow. Ergun and Orning (1949) added an additional term to the 'Kozeny-Carman' term to extend the relation between hydraulic/pressure gradient and the macroscopic parameter for use for non-linear flow. This term is based on the addition of a term for kinetic energy loss concerning capillary flow, in a similar way as was done by Brillouin (1907) (see Ergun and Orning, 1949). Subsequently, two parameters, α and β are added to the first and second term respectively as correction factors for the frequency of kinetic losses. The Ergun-Orning equation is commonly given in the form of Eq. 7 (e.g. Bear, 1988).

$$-\frac{dh}{dx} = 180\alpha\frac{(1-n)^2\nu}{gn^3d^2}q + \frac{3\beta(1-n)}{4gn^3d}q^2 \tag{7}$$

Ergun (1952) subsequently derived this (semi-)empirical relation (Eq. 5) using data from 640 experiments including a variety of small diameter (<1.5 [mm]) (almost) spherical granular materials (mono-sized), including sand and glass spheres (Allen et al. and Ergun as cited in Koekemoer and Luckos (2015)). Through his analysis he was able to assign constant values to the correction factors of the Ergun-Orning equation (Eq. 7). The Ergun equation is easier in use than the Ergun-Orning equation as no knowledge of the correction factors is needed and the hydraulic gradient can be calculated solely from macroscopic parameters.

The study by Ergun is considered a pioneering study regarding this topic and forms the base of numerous new empirical expressions relating hydraulic gradient to superficial flow velocity (e.g. Macdonald et al., 1979; Kovács, 1981; Ozahi et al., 2008), often referred to as Ergun-type equations (e.g. Sabiri and Comiti, 1995; Huang et al., 2013; Nield and Bejan, 2013). Despite the many corrections to the Ergun equation, it is still considered to be able to give a good prediction of an experimental hydraulic gradient – superficial flow velocity relation for packed beds of granular material (e.g. see Chhabra and Srinivas, 1990; Kunii and Levenspiel as cited in Koekemoer and Luckos (2015)).

It has been shown by various workers (e.g. Fand et al. and Kececioglu and Jiang as cited in Bağci et al., 2014), that Ergun's constants are not valid for all porous media. Hence, there is development of Ergun-type equations in several studies, either to fit a studies experimental data or to propose a general form of Ergun's equation that is applicable to a wider range of porous media. According to Standish and Drinkwater (as cited in Li and Ma, 2011), a variety of factors influence the value of the Ergun equation constants for non-linear flow in packed beds, including how the porous medium is packed, the uniformity of the grain size distribution, and the shape of the particles in consideration.

The study by Macdonald et al. (1979) is considered to be one of the most influential works on modification of the Ergun equation (Nemec and Levec, 2005). Their equation is shown in Eq. 8, in case of smooth particles.

$$-\frac{dh}{dx} = 180\frac{(1-n)^2\nu}{gn^{3.6}d^2}q + 1.8\frac{(1-n)}{gn^{3.6}d}q^2 \tag{8}$$

Their adaptation is considered of great additional value because particles of non-spherical shape are taken into account in their analysis (Macdonald et al., 1979; Nemec and Levec, 2005). The first modification is the proposition of a constant value of 180 instead of the 150 proposed by Ergun for the linear term and the proposition of a constant value between 1.8 and 4.0 instead of the 1.75 proposed by Ergun for the non-linear term, where 1.8 is used for smooth particles and 4.0 for the roughest particles. Another modification introduced by Macdonald and his colleagues is to use $n^{3.6}$ instead of n^3 for both the linear and non-linear term. This alteration is based upon empirical analysis in their work and is supposed to enhance the possibility to use constant values for the Ergun equation to predict the hydraulic/pressure gradient.

Another widely used modification of Ergun's equation is the equation by Kovács (1981). Kovács used a large dataset in a range of Reynolds numbers of 10-100 (as cited in Sidiropoulou et al., 2007; Sedghi- Asl et al., 2014) and proposed the expression in Eq. 9. It needs to be noted that the expression is derived for homodisperse spherical particles (Sidiropoulou et al., 2007).

$$-\frac{dh}{dx} = 144\frac{(1-n)^2\nu}{gn^3d^2}q + 2.4\frac{(1-n)}{gn^3d}q^2 \tag{9}$$

The proposed modifications presented so far mainly include an empirical correction to the constants of the Ergun equation (Eq. 5; A = 150, B = 1.75). A different approach is followed by Du Plessis (1994). He attempted to derive the numerical constants for the linear and non-linear terms analytically. For the derivation of the non-linear flow component of the equation, he introduced local flow recirculation in pore spaces, which induces drag forces. His derivation of a non-linear flow equation, physically proven, appears to be remarkably close the empirical Ergun equation. His quantification of the Ergun equation constants (A = 150 in Ergun equation; B = 1.75 in Ergun equation) are given by Eq. 10 and Eq. 11 for the linear and non-linear terms, respectively. Graphically, these relationships between the numerical value of A and B and porosity are depicted in Figure 2. Dependency of the constants on porosity has been suggested by more authors (e.g. Macdonald et al., 1979). With expressions for A and B included, the modified Ergun equation becomes as depicted in Eq. 12.

$$A = \frac{41n^2}{(1-n)^{2/3}(1-(1-n)^{1/3})(1-(1-n)^{2/3})} \tag{10}$$

$$B = \frac{n^2}{(1-(1-n)^{2/3})^2} \tag{11}$$

$$-\frac{dh}{dx} = \frac{41n^2}{(1-n)^{2/3}(1-(1-n)^{1/3})(1-(1-n)^{2/3})}\frac{(1-n)^2\nu}{gn^3d^2}q + \frac{n^2}{(1-(1-n)^{2/3})^2}\frac{(1-n)}{gn^3d}q^2 \tag{12}$$

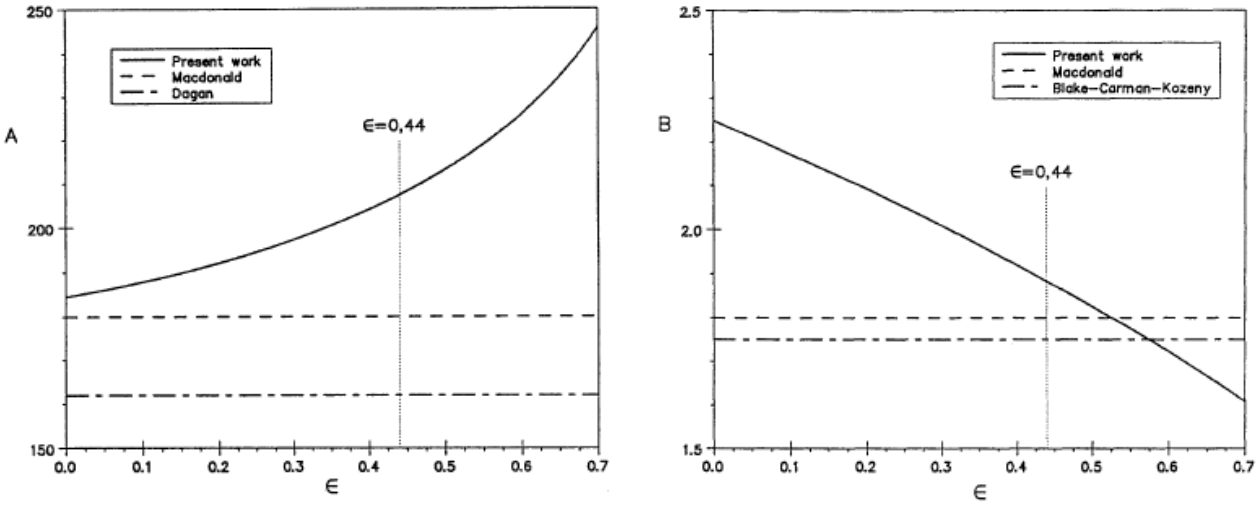

Figure 2: Constants of Ergun equation according to analytical derivation by Du Plessis (1994; Eq …). Both Ergun equation constants A and B are dependent on porosity. Figures retrieved from Du Plessis (1994).

Two empirical relations relating the hydraulic gradient to superficial flow velocity that are different from the Ergun-type equations are those given by Schneebeli (1955):

$$-\frac{dh}{dx} = 1100\frac{\nu}{gd^2}q + 12\frac{1}{gd}q^2 \tag{13}$$

$$-\frac{dh}{dx} = 1100\frac{\nu}{gd^2}q + 30\frac{1}{gd}q^2 \tag{14}$$

Schneebeli proposed Eq. 13 and Eq. 14 for spheres and chunks of granite, respectively. Ward (1964) proposed Eq. 15 by analyzing a dataset on non-linear flow experiments in 20 different porous media ranging in nature from glass beads to sand and gravel and ranging in particle diameter from 0.273 [mm] to 16.1 [mm] (as cited from Sidiropoulou et al., 2007).

$$-\frac{dh}{dx} = 360\frac{\nu}{gd^2}q + 10.44\frac{1}{gd}q^2 \tag{15}$$

None of these empirical relations do not include a porosity term, which distinguishes them from the Ergun-type equations.

Sidiropoulou et al. (2007) proposed Eq. 16 to model non-linear flow in porous media.

$$-\frac{dh}{dx} = 0.003333d^{-1.500403}n^{0.060350}q + 0.194325d^{-1.265175}n^{-1.141417}q^2 \tag{16}$$

Sidiropolou et al. (2007) investigated a different methodology to determine the parameters of the Forchheimer equation (Eq. 2) leading to a relation relating the hydraulic gradient to superficial flow velocity severely different from the Ergun-type equations. Using the numerical

representation of the Forchheimer equation coefficients a and b, the porosity, and (representative) grain size from a large set of data from earlier works it was attempted to derive expressions for Forchheimer equation coefficients a and b. Using multiple regression analysis of on the one hand the coefficients a and b versus on the other hand the porosity and the (representative) grain size they found Eq. 16 as expression for the Forchheimer equation relating the hydraulic gradient to the superficial flow velocity.

3. Methodology

For this study, an experimental setup is developed that allows measurement of the volumetric flow rate (Q in [$m^3\ h^{-1}$] through an unconsolidated packed sandy porous medium for hydraulic gradients (i) ranging from 1 to 62 [m m^{-1}]. This allows for the generation of i-q curves, a common approach for the analysis of non-linear flow in porous media (e.g. Bağci et al., 2014; Sedghi-Asl et al., 2014), as it allows for an empirical determination of Forchheimer equation coefficients a [m day^{-1}] and b [$m^2\ day^{-2}$]. Furthermore, using these type of experiments, other characteristics of the porous medium, as the porosity and characteristics of the grain size distribution can be determined from simple analysis and/or data provided by the manufacturer of the granular material.

3.1. The Experimental Setup

The setup is shown in Figure 3. The core of the setup is a cylindrical Plexiglas column (l: 0.507 [m], ø: 0.098 [m]) containing a porous medium consisting of sand and/or gravel which is prepared under saturated conditions. The packed sand in the Plexiglas column is sealed in place by a fibrous filter and a metal filter. Both filters have a larger permeability than any of the porous media used. A complete description of the seal design can be found in Appendix A.1. On the left side of the column water pressure can be elevated, through water injection, up to a maximum ranging between 1.2 [bar] and 3.2 [bar] (± 12 [m] and 32 [m] hydraulic head, respectively). On the right side, a constant hydraulic head of 0.55 [m] is established, allowing for a steep hydraulic gradient (up to 62 [m m^{-1}] for the finest sand). An outlet navigates the water into a reservoir (± 1 [m^3]), also serving as a water supply reservoir for the setup. Water is pumped from this reservoir via a hose into the setup. Three degassing valves ensure full saturation of the porous medium.

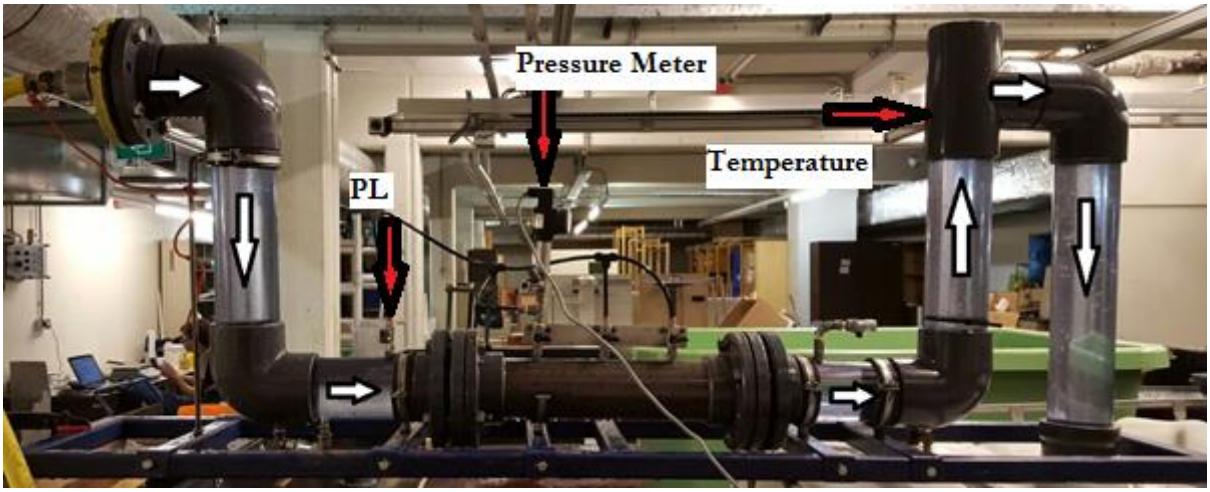

Figure 3: The experimental setup. The white arrows indicate the flow direction. The porous medium is located in a cylindrical column in the middle of the setup. Water pressure is measured at four locations in the experimental setup using a pressure transmitter (see red arrow) and plastic wiring. P_L is the water pressure measured left of the porous medium (red arrow), P_R is the constant hydraulic head created by accumulation of water in the right vertical column which is equal to 0.55 [m]. The yellow hose supplies water from the reservoir (right bottom of the figure, see Appendix A.1 for a better image of the reservoir). The most right vertical segment serves as water outlet. Temperature is measured at the most-right red arrow.

Water pressure measurements [bar] are taken using a BD Sensors pressure transmitter and a BD Sensors PA 430 display. Water pressure is measured left of the porous medium, just before it enters the porous medium. Also, water pressure is measured at 0.1275 [m], 0.2550 [m], and 0.3825 [m] from the left boundary of the porous medium. For the data analysis and according results in the next chapters, however, the three pressures measured along the porous medium will not be used. Discharge measurements [m^3/h] are taken between the pump and the water inlet into the setup using a SVM F2 Energy Meter. Water temperature measurements are taken in the outlet of the porous medium (see Figure 3) using an ASTM 17C thermometer or an ASTM 90C thermometer.

Before each experiment, the column containing the porous medium (packed under saturated conditions) was mounted to the other Plexiglas columns of the setup. This was done under saturated conditions in a second reservoir (see Appendix A-1). After installation, the saturated columns were placed onto an emplacement (blue metal structure in Figure 3), where it is mounted to the rest of the setup. The setup is flushed with water from the setup's reservoir for a period of 15 [min] before initiating an experiment. Excess air, present in the setup (not the porous medium) is released from the setup by means of the air valves.

To be able to construct an i-q curve, the volumetric flow rate (Q) is determined for a variety of hydraulic gradients over the porous medium. The volumetric flow rate is measured for 1 [min] and 45 [sec] (in case of absence of or very small variation in Q) or over 2 [min] and 30 [sec] (in case of larger variations in Q). During the experiment, the temperature of the water flowing through the porous medium was measured and controlled to be 20 [°C] by altering the water temperature in the reservoir.

3.2. The Sandy Porous Media

3.2.1. Grain Size Distribution Characterization

A variety of sandy/gravelly porous media are used in this research. To be able to link the grain size distribution to the experimental results, it is chosen to characterize the porous media by means of their statistical properties. Eq. 17, 18, 19, and 20 give the mean (d_m), the variance (σ^2), the standard deviation (σ), and the skewness ($d_{m3}\ \sigma^{-3}$), respectively (see Nomenclature for meaning symbols in the equations).

$$d_m = \frac{1}{N}\sum_{i=1}^{N} d_i \tag{17}$$

$$\sigma^2 = \sum_{i=1}^{N} p_i (d_i - d_m)^2 \tag{18}$$

$$\sigma = \sqrt{\sigma^2} = \sqrt{\sum_{i=1}^{N} p_i (d_i - d_m)^2} \tag{19}$$

$$\frac{d_{m3}}{\sigma^3} = \frac{\sum_{i=1}^{N} p_i (d_i - d_m)^3}{\sigma^3} \tag{20}$$

Furthermore, the coefficient of uniformity, C_U (Eq. 21), and the coefficient of curvature, C_C (Eq. 22), are used as indicators of the shape of the porous media. Definitions of these coefficients are given by ASTM, 2006. The coefficient of uniformity, is a measure of the uniformity of the distribution. The higher this value, the more uniform the distribution is. The coefficient of curvature is a measure of the shape of the distribution, with a value outside the range of 1-3 indicating a roughly shaped distribution. d_x is the grain size for which x [%] of the grain sizes in the sample are smaller than d_x (e.g. d_{50} is median grain size).

$$C_u = \frac{d_{60}}{d_{10}} \tag{21}$$

$$C_c = \frac{(d_{30})^2}{d_{10} \cdot d_{60}} \tag{22}$$

3.2.2. The Porous Media

3.2.2.1. Preparation Method

The porous media tested in the experimental setup are unconsolidated packed beds of granular material, more specifically, sands and gravels. All porous media have been packed using a combination of the drizzle method, as described by Rietdijk et al. (2010), and the compaction-undercompaction method from Mitchell et al. (1976). For a detailed description of this packing method, the reader is referred to Van Dooren (2015). In case of packing porous media consisting of sand/gravel mixtures, the drizzle method by Rietdijk et al. (2010) had to be applied in a higher rate to minimize layer formation due to varying settling rates for particles of varying size. Van Dooren (2015) has analyzed the reproducibility of porous media using this packing method. In this study, grain density in terms of porosity as well as non-linear flow behavior in terms of Forchheimer coefficient a and b has been investigated for three of the reference calibrated sandy porous media from Table 1: U 0.2-0.63 [mm], U 0.4-0.8 [mm], and U 0.63-1.0 [mm]. It was found that for this particular packing method the maximum relative error in porosity, Forchheimer coefficient a, and Forchheimer coefficient b between various prepared porous media amounted to 1.102 [%], 2.053 [%], and 3.106 [%]. This implies that this packing method can be used to produce reproducible porous media and that measurements using these porous media can be mutually compared. It is assumed that the porosity distribution in the porous medium is homogeneous which leads to a uniform flow distribution (Nemec and Levec, 2005).

3.2.2.2. Reference Porous Media – Filtered/Calibrated Sands/Gravels

In total, 11 reference porous media are used in this research. The reference porous media are a single filtered/calibrated sand/gravel as provided by the manufacturer, Filcom. The characteristics of the reference porous media are given in Table 1. The notation for these porous media is U x-y [mm], where x and y are approximately minimum and maximum grain sizes (in [mm]) as provided by Filcom. The reference porous media are generally uniformly distributed with a

narrow grain size distribution (small standard deviation), with increasing grain size the grain size distribution becomes slightly wider. All reference porous media are approximately normally distributed. The finest and coarsest porous media used in this research are U 0.2-0.5 [mm] and U 5.0 -8.0 [mm], respectively. The grain size distributions of the reference porous media are provided by Filcom. As the sand/gravel is sieved by Filcom using a limited amount of sieves, the grain sizes are subdivided into ranges of grain sizes with an associated percentage of presence in the total sample. In this research it is assumed that every individual grain size (accuracy: 0.001 [mm]) within a range of grain sizes has an equal contribution to the total sample. I.e. the combined contribution of a range of grain sizes is divided by the amount of individual grain sizes within that range. In Appendix A.2, the grain size distributions for all reference porous media are given.

3.2.2.3. Composite/Mixed Porous Media

In total, 13 composite porous media are used in this research. The composite porous media consist of a mixture of 2 or more of the filtered/calibrated sands as provided by Filcom. The composite porous media are created with the purpose of being able to investigate the effect of the shape of the grain size distribution on non-linear flow in porous media. Therefore, the composite porous media are created such that the median grain size, d_{50}, is equal to the median grain size of one of the reference porous media. In this research two types of composite porous media can be distinguished:

1) Composite porous media that are more well-graded their associated reference porous media (larger σ and larger C_U), but are, just as the reference porous media, approximately normally distributed (similar C_c). The composite porous media have smaller grain sizes for d_{10} and larger grain sizes for d_{90}, for instance.
2) Composite porous media that are gap-graded, i.e. which grain size distributions are characterized by at least two distinct peaks. Compared to their associated reference cases, these composite porous media have a significantly larger σ and C_U, and a significantly smaller C_C (different shape of grain size distribution).

The characteristics of the composite porous media (e.g. d_{10} and d_{90}) are given in Table 3. In Table 2 can be seen how the single filtered/calibrated sands/gravels are mixed to create the composites. The notation for the composite porous media is N-Ux, where x is a number between 1 and 13, referring to a specific composite porous medium. In Appendix A.2, the grain size distributions for all composite porous media are given.

Table 1: Reference porous media used in this research. Characteristics of the grain size distribution are given in d_x, where x denotes the percentage of grains with a diameter smaller than the given diameter, in terms of the mean grain diameter (d_m), the variance (σ^2), standard deviation (σ) and skewness (d_{m3}/σ^3) of the grain size distribution. Furthermore the coefficient of curvature and the coefficient of uniformity are given.

Porous Medium	d_5 [mm]	d_{10} [mm]	d_{20} [mm]	d_{30} [mm]	d_{40} [mm]	d_{50} [mm]	d_{60} [mm]	d_{70} [mm]	d_{80} [mm]	d_{90} [mm]	d_{95} [mm]
U 0.2-0.5 [mm]	0,259	0,293	0,327	0,353	0,371	0,389	0,406	0,423	0,452	0,484	0,499
U0.2-0.63 [mm]	0,251	0,276	0,317	0,343	0,366	0,388	0,409	0,431	0,461	0,491	0,531
U 0.4-0.8 [mm]	0,435	0,47	0,515	0,547	0,58	0,612	0,644	0,678	0,713	0,767	0,794
U 0.5-1.0 [mm]	0,494	0,532	0,588	0,632	0,673	0,714	0,757	0,8	0,849	0,917	0,975
U 0.63-1.0 [mm]	0,684	0,722	0,76	0,797	0,819	0,84	0,861	0,882	0,908	0,958	0,983
U 0.7-1.25 [mm]	0,727	0,795	0,862	0,909	0,948	0,988	1,03	1,073	1,116	1,174	1,224
U 0.8-1.25 [mm]	0,846	0,893	0,938	0,98	1,016	1,048	1,08	1,112	1,152	1,205	1,244
U 1.0-1.6 [mm]	1,03	1,125	1,209	1,268	1,315	1,361	1,409	1,466	1,522	1,579	1,626
U 1.0-2.0 [mm]	1,078	1,163	1,263	1,343	1,422	1,503	1,583	1,672	1,773	1,911	1,986
U 1.7-2.5 [mm]	1,545	1,718	1,861	1,967	2,046	2,113	2,18	2,248	2,318	2,407	2,465
U 5.0-8.0 [mm]	4,83	5,16	5,622	5,865	6,108	6,343	6,548	6,764	7,011	7,46	7,741

Porous Medium	μ [mm]	σ^2 [mm^2]	σ [mm]	$\mu^3\sigma^{-3}$ [-]	C_C	C_U
U 0.2-0.5 [mm]	0,39013	0,00743146	0,08621	1,13	1,05	1,39
U0.2-0.63 [mm]	0,3885	0,00752983	0,08677	0,13	1,04	1,48
U 0.4-0.8 [mm]	0,61481	0,01309855	0,11445	0,05	0,99	1,37
U 0.5-1.0 [mm]	0,7227	0,02521434	0,15879	0,8	0,99	1,42
U 0.63-1.0 [mm]	0,83726	0,00898706	0,0948	-0,34	1,02	1,19
U 0.7-1.25 [mm]	0,9848	0,02799444	0,16732	-0,39	1,01	1,30
U 0.8-1.25 [mm]	1,04942	0,02019108	0,1421	1,05	1,00	1,21
U 1.0-1.6 [mm]	1,35413	0,03802139	0,19499	-0,84	1,01	1,25
U 1.0-2.0 [mm]	1,51717	0,08470849	0,29105	0,07	0,98	1,36
U 1.7-2.5 [mm]	2,07432	0,09830148	0,31353	-1,53	1,03	1,27
U 5.0-8.0 [mm]	6,27616	0,92742614	0,96303	-1,25	1,02	1,27

Table 2: Composite porous media used in this research. This table shows the fractions of reference porous media present in each of the composite porous media.

Porous Medium	U 0.2-0.5	U 0.2-0.63	U 0.4-0.8	U 0.5-1.0	U 0.63-1.0	U 0.7-1.25	U 0.8-1.25	U 1.0-1.6	U 1.0-2.0	U 1.7-2.5	U 5.0-8.0
N-U1	0	0,15	0,5	0,35	0	0	0	0	0	0	0
N-U2	0	0,3	0,3	0,4	0	0	0	0	0	0	0
N-U3	0	0,5	0	0	0	0	0	0	0	0,5	0
N-U4	0,05	0,05	0,27	0,34	0,1	0,19	0	0	0	0	0
N-U5	0	0,33	0	0,33	0	0	0	0	0	0,34	0
N-U6	0	0	0,15	0,24	0,19	0,42	0	0	0	0	0
N-U7	0	0,04	0,05	0,12	0,09	0,36	0,04	0,17	0,13	0	0
N-U8	0	0,02	0,05	0,08	0,1	0,1	0,65	0	0	0	0
N-U9	0	0	0	0,09	0,12	0,5	0,12	0,17	0	0	0
N-U10	0	0,05	0,095	0,285	0,06	0	0	0,46	0,05	0	0
N-U11	0	0,02	0,03	0,1	0,08	0,23	0,225	0,215	0,1	0	0
N-U12	0,02	0	0,01	0,12	0,08	0,17	0,295	0,22	0,085	0	0
N-U13	0	0	0	0,1	0	0,2	0	0,04	0,55	0,11	0

Table 3: Composite porous media used in this research. Characteristics of the grain size distribution are given in d_x, where x denotes the percentage of grains with a diameter smaller than the given diameter, in terms of the mean grain diameter (d_m), the variance (σ^2), standard deviation (σ) and skewness (d_{m3}/σ^3) of the grain size distribution. Furthermore the coefficient of curvature and the coefficient of uniformity are given.

Porous Medium	d_5 [mm]	d_{10} [mm]	d_{20} [mm]	d_{30} [mm]	d_{40} [mm]	d_{50} [mm]	d_{60} [mm]	d_{70} [mm]	d_{80} [mm]	d_{90} [mm]	d_{95} [mm]
N-U1	0,341	0,404	0,478	0,53	0,575	0,617	0,659	0,702	0,756	0,826	0,889
N-U2	0,304	0,347	0,413	0,474	0,532	0,586	0,639	0,692	0,754	0,834	0,896
N-U3	0,275	0,316	0,366	0,408	0,46	0,619	1,862	2,046	2,18	2,318	2,407
N-U4	0,373	0,444	0,532	0,597	0,656	0,713	0,772	0,833	0,899	1,001	1,098
N-U5	0,299	0,341	0,407	0,48	0,596	0,718	0,854	1,754	2,054	2,252	2,356
N-U6	0,511	0,569	0,658	0,731	0,791	0,841	0,887	0,944	1,007	1,103	1,164
N-U7	0,479	0,606	0,755	0,847	0,919	0,993	1,081	1,177	1,323	1,516	1,647
N-U8	0,558	0,681	0,816	0,889	0,94	0,988	1,032	1,076	1,119	1,178	1,229
N-U9	0,658	0,74	0,828	0,885	0,938	0,99	1,049	1,11	1,186	1,344	1,477
N-U10	0,445	0,529	0,64	0,738	0,839	1,006	1,225	1,327	1,427	1,541	1,598
N-U11	0,564	0,689	0,823	0,904	0,975	1,045	1,116	1,203	1,333	1,507	1,611
N-U12	0,579	0,705	0,833	0,912	0,981	1,048	1,115	1,197	1,323	1,495	1,595
N-U13	0,679	0,811	0,975	1,116	1,241	1,363	1,49	1,623	1,784	1,992	2,184

Porous Medium	d_m [mm]	σ^2 [mm^2]	σ [mm]	$\mu^3\sigma^{-3}$ [-]	C_C	C_U
N-U1	0,6186	0,0282	0,1680	0,34	1,06	1,63
N-U2	0,5901	0,0357	0,1888	0,41	1,01	1,84
N-U3	1,2314	0,7634	0,8737	0,14	0,28	5,89
N-U4	0,7215	0,0477	0,2184	0,29	1,04	1,74
N-U5	1,0720	0,5803	0,7618	0,67	0,79	2,50
N-U6	0,8384	0,0412	0,2030	0,12	1,06	1,56
N-U7	1,0323	0,1224	0,3498	0,40	1,10	1,78
N-U8	0,9607	0,0434	0,2084	-0,40	1,12	1,52
N-U9	1,0140	0,0579	0,2406	0,39	1,01	1,42
N-U10	1,0328	0,1574	0,3967	0,06	0,84	2,32
N-U11	1,0709	0,1024	0,3201	0,33	1,06	1,62
N-U12	1,0715	0,0966	0,3108	0,32	1,06	1,58
N-U13	1,3860	0,2049	0,4527	0,21	1,03	1,84

3.3. Note on Air Inclusion

As full saturation of the porous medium is wished in case of these experiments, the effect of air inclusion on flow through porous media is investigated for porous media U 0.2-0.5 [mm], U 0.63-1.0 [mm], U 1.0-1.6 [mm], U 1.7-2.5 [mm], U 5.0-8.0 [mm], N-U1, and N-U10 in a side-research. The exact same porous media used for the saturated experiment were exposed to air for approximately 20 [min] prior to initiation of the experiments. Air was able to intrude via the porous filters secluding the porous media. It was found that Forchheimer coefficients a and b for these exposed porous media all lie within an uncertainty range of 0 to 5 [%] (4,83 [%] and 4,49 [%] maximum deviation for coefficients a and b, respectively). The air inclusion induced in these experiments is expected to be many times higher than in case of 'accidental' air inclusion during a fully saturated experiment. It is expected that in case air has been accidently included in the porous medium, it does not affect the Forchheimer parameters by more than 5 [%].

3.4. Determination of the Macroscopic Hydraulic Parameters

3.4.1. Non-linear Flow Behavior – Forchheimer Coefficients

Using the measured data from each experiment, important macroscopic parameters can be determined. The applied water pressure and the measured discharge can be converted to a hydraulic gradient (i) and the superficial flow velocity (q) using Eq. 23 and Eq. 24, respectively.

$$i = -\frac{\Delta h}{\Delta x} \qquad \Delta h = \frac{(P_R - P_L) \cdot 10^5}{\rho_w g} \tag{23}$$

$$q = \frac{Q}{A_c} \tag{24}$$

where Δh [m] represents the difference in hydraulic head between the left and right side of the porous medium, Δx [m] the length of the porous medium, P_L and P_R the water pressure on the left and right side of the porous medium [bar], respectively, ρ_w the water density which is 998.2 [kg m^{-3}] at 20 [°C] (Vanoni, 2006), g is the gravitational constant and is assumed to be equal to 9.81 [m s^{-2}], Q is the discharge through the porous medium [m^3 day^{-1}], and A is the cross section of the cylinder holding the porous medium [m^2]. Converting the measured data (P_L and Q) to values for i and q, enables a plot of i vs. q.

On the experimental i-q plot, the Forchheimer equation (Eq. 2) is fitted using the Method of Least Squares. This results in having numerical values for Forchheimer equation coefficients a [day m^{-1}] and b [day^2 m^{-2}]. From coefficient a, the intrinsic permeability [m^2], can be calculated using Eq. 25.

$$\kappa = \frac{K\mu}{\rho_w g} = \frac{\mu}{a\rho_w g} \tag{25}$$

where κ [m^2] is the permeability, K [m day^{-1}] the hydraulic conductivity (for Darcian flow), and μ the dynamic viscosity of water at 20 [°C] which is equal to 86.24 [kg m^{-1} day^{-1}], and ρ_w is the density of water at 20 [°C].

The Darcy equation, as in Eq. 26, is graphed on the same plot as is the experimental data and the Forchheimer equation fit using the empirically determined value of the permeability.

$$q = -\frac{1}{a}\frac{dh}{dx} \tag{26}$$

3.4.2. Non-linear Flow Behavior – Determination of the Onset of Non-linear Flow Behavior

For every porous media, the Forchheimer fit and the Darcy plot are used to determine the moment of onset of non-linear flow. The transition is marked by means of the Reynolds number. In the *Theory* chapter, it is pointed out that no generally accepted definition of the critical Reynolds number marking the transition from the Darcy regime to the Forchheimer (Forchheimer) regime exists present day. Therefore, it is chosen to mark the end of the Darcy regime and the beginning of the non-linear regime by a certain deviation of the Forchheimer equation fit from the Darcy equation. The deviation can be calculated using Eq. 27.

$$De_x = \frac{F(q) - D(q)}{D(q)} \cdot 100[\%] \tag{27}$$

where De_x [%] denotes the deviation of the Forchheimer fit from the Darcy equation in percentage, x being the percentage of deviation allowed, F(q) the Forchheimer equation fit, and D(q) the Darcy equation fit. In this research, the allowed deviation De_x was determined beforehand to be equal to and be compared between 1 [%], 5 [%], and 10 [%]. These are criterion frequently encountered in literature to indicate the end of the Darcy regime (e.g. Wahyudi et al., 2002). With a known De_x, a critical superficial velocity can be determined which marks the transition from the Darcy to the non-linear regime. This velocity is used to determine a critical Reynolds number using Eq. 4.

3.4.3. Porosity

The mass of the solid matrix of each porous medium, m_S, is determined by oven-drying the porous media at 105 [°C] and weighing the dry mass. The porosity is subsequently determined by using Eq. 28.

$$n = 1 - \frac{V_s}{V_t} \qquad V_s = \frac{m_s}{\rho_s} \tag{28}$$

where n [-] is the porosity, V_S [m^3] is the volume of the solid matrix, V_t [m^3] the volume of the column or volume of the porous medium being equal to $3.84691 \cdot 10^{-3}$ [m^3], m_s [kg] the dry mass of the solid matrix, and ρ_s the density of the solid phase being equal to $2.66 \cdot 10^3$ [kg m^{-3}].

3.5. Determination of the Effect of the Grain Size Distribution on Non-linear Flow

The outcome of the non-linear flow experiments is compared between the reference porous media (U x-y [mm]) and the composite porous media (N-Ux) with a similar median grain size (d_{50}). The comparison is performed by means of analyzing the effect of the grain size distribution on the coefficients of the fitted Forchheimer equation. So in fact, there is looked at the effect of grain size distributions on the hydraulic gradient – superficial flow relationship. Taking the Forchheimer coefficients a and b for the reference porous media as the reference value (U_a or U_b) and taking the Forchheimer coefficients a and b for the composite porous media as the 'deviating' values (NU_a or NU_b), the relative error between the Forchheimer coefficients of the reference porous media and the Forchheimer coefficients of the composite porous media can be determined using Eq. 29 and Eq. 30.

$$Relative\ Error\ a = \frac{NU_a - U_a}{U_a} \tag{29}$$

$$Relative\ Error\ b = \frac{NU_b - U_b}{U_b} \tag{30}$$

3.6. Comparison Experimental Data with Empirical Expressions

The Forchheimer equation fits of both reference and composite porous media will be compared to empirical expressions relating the hydraulic head to the superficial velocity. We have tested the empirical expressions by Ergun (1952; Eq. 5), Macdonald et al. (1979; Eq. 8), Kovács (1981; Eq. 9), Du Plessis (1994; Eq. 12), Schneebeli (1955; Eq. 14), Ward (1964; Eq. 15), and Sidiropoulou et al. (2007; Eq. 16). Comparison of the empirical relations with the Forchheimer equation fit on the data will be performed by means the Normalized Objective Function (NOF), as described in Moutsopoulos et al. (2009). For the determination of the NOF, Eq. 31, 32, and 33 are used. In these equations, RMSE represents the root mean squared error [-], x_i [-] represents the experimentally determined hydraulic gradient for data point i, y_i [-] represents the empirically determined hydraulic gradient using one of the empirical relations for data point i, N [-]is the sample size which is equal to the number of measurements for the experimental results in consideration plus one extra data point for the origin, (0,0) (e.g. N = 15 for U 0.2-0.5 [mm] as the superficial flow velocity was determined for 14 different gradients during the experiment, plus the data point for the origin), and X is the mean of the experimental hydraulic gradient determined for a single i-q curve.

$$RMSE = \sqrt{\frac{\sum_{i=1}^{N}(x_i - y_i)^2}{N}} \tag{31}$$

$$X = \frac{1}{N}\sum_{i=1}^{N} x_i \tag{32}$$

$$NOF = \frac{RMSE}{X} \tag{33}$$

The closer the NOF is to 0, the better the ability of the empirical relation to 'predict' or 'mimic' the experimental data.

4. Results

The results of this work are subdivided into three major sections:

1) Characterization of non-linear flow in the 11 sandy reference porous media (U 0.2-0.5 [mm] tot 5.0-8.0 [mm]) as given in Table 1.
2) Comparisons of non-linear flow in the reference porous media on the one hand and composite porous media (N-Ux) on the other hand. Porous media with similar values for d_{50} are compared to determine the effect of the shape of the grain size distribution on non-linear flow in porous media.
3) Comparison of the experimentally determined i-q curves for all porous media created with existing empirical relations (see section 2.3.).

4.1. Non-linear Forcheimer Flow in the Reference Porous Media

The first step in this research is to analyze non-linear Forchheimer flow in the reference porous media as provided by the manufacturer. The results from these porous media serve as reference for subsequent analyses. The flow is analyzed by means of i-q curves (see section 3.4). Results can be seen in Figure 4. The Forchheimer equation (Eq. 2) was used to fit the data. The poorest fit resulted in a R^2-coefficient of 0.99953, which indicates that the Forchheimer fit and the experimental data are in excellent agreement (see Table 4). Similar values for the R^2-coefficient are acquired in studies similar to this work (Bağci et al., 2014; Sedghi-Asl et al., 2014).

Values of Forchheimer coefficients a and b for the fit on each dataset can be retrieved from Table 4. U 0.2-0.5 [mm], the finest porous medium used in this work, yielded the highest value for coefficient a ($2.2369 \cdot 10^{-2}$ [day m^{-1}]) and, therefore, the lowest permeability ($5.2744 \cdot 10^{-11}$ [m^2]). Regarding coefficient b, U 0.2-0.5 [mm] yielded the highest value ($1.8249 \cdot 10^{-6}$ [$day^2 m^{-2}$]). The lowest a-coefficient acquired for the reference porous media was for the medium U 5.0-8.0 [mm], the a-coefficient being equal to $9.268 \cdot 10^{-5}$ [$day m^{-1}$] and the permeability being equal to $1.2729 \cdot 10^{-8}$ [m^2]. Regarding coefficient b, U 5.0-8.0 [mm] yielded the lowest value (8.2308^{-8} [$day^2 m^{-2}$]). It comes as no surprise that both Forchheimer coefficients decrease with increasingly coarser material as the resistance to flow generally decreases with increasing grain size. Interesting to note is that the ratio of coefficient a to coefficient b decreases with increasingly coarser material. This is an indication that the non-linear term in Eq. 2, becomes increasingly more important with increasing grain size. Similarly, the linear term becomes less important with increasing grain size.

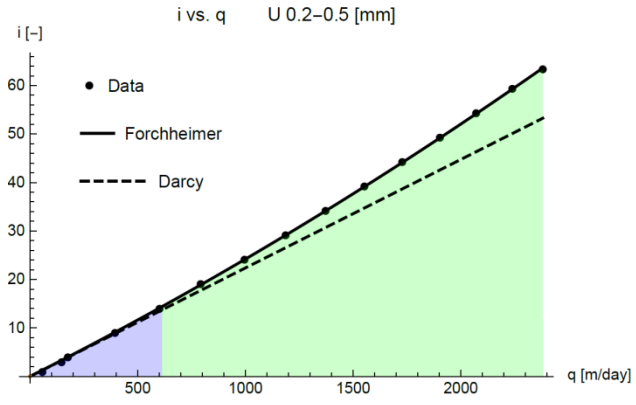
i vs. q U 0.2–0.5 [mm]
i [–]
Data
Forchheimer
Darcy
q [m/day]

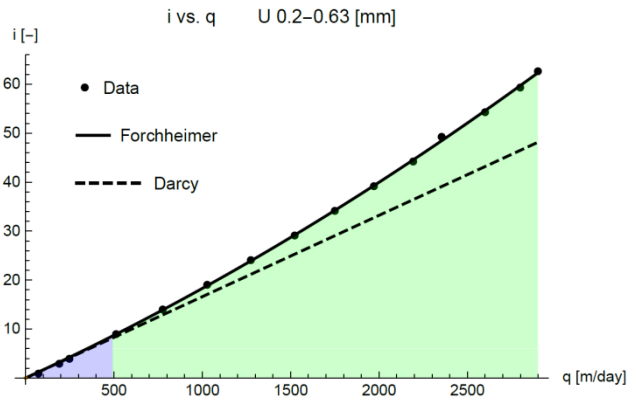
i vs. q U 0.2–0.63 [mm]
i [–]
Data
Forchheimer
Darcy
q [m/day]

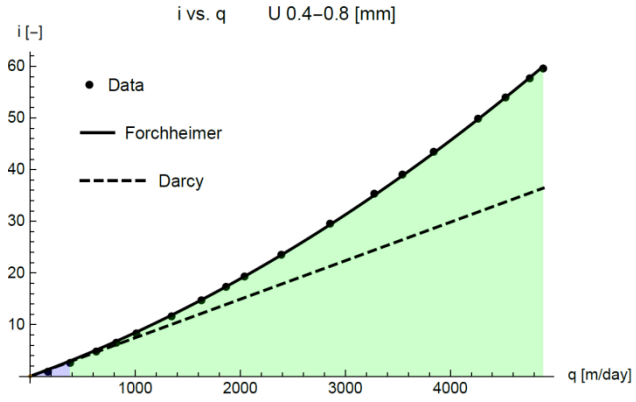
i vs. q U 0.4–0.8 [mm]
i [–]
Data
Forchheimer
Darcy
q [m/day]

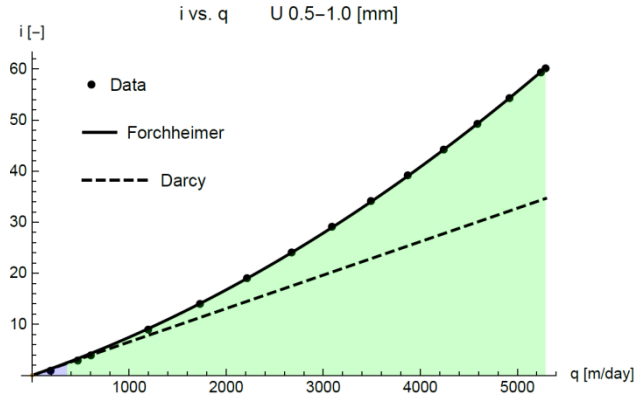
i vs. q U 0.5–1.0 [mm]
i [–]
Data
Forchheimer
Darcy
q [m/day]

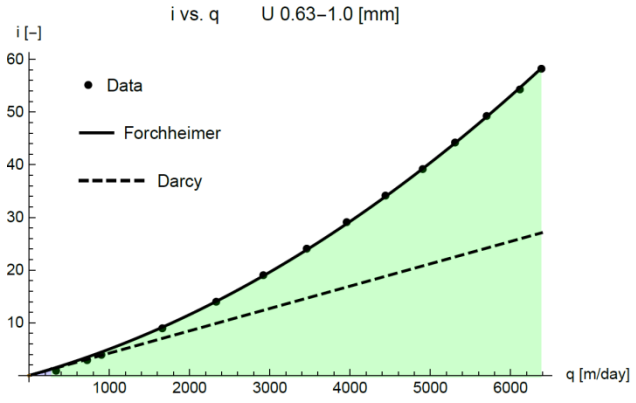
i vs. q U 0.63–1.0 [mm]
i [–]
Data
Forchheimer
Darcy
q [m/day]

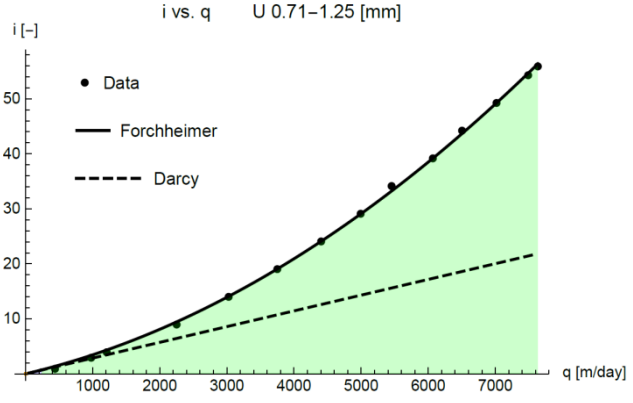
i vs. q U 0.71–1.25 [mm]
i [–]
Data
Forchheimer
Darcy
q [m/day]

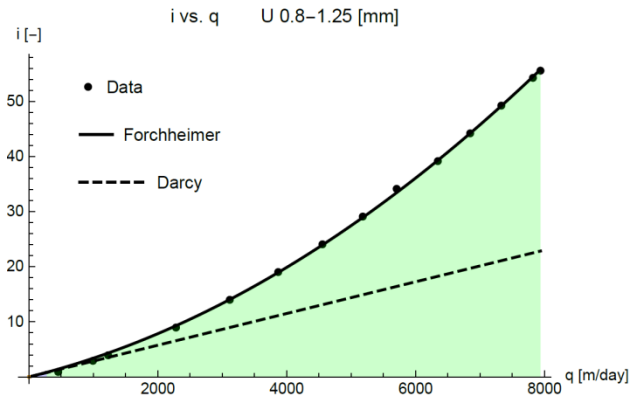
i vs. q U 0.8–1.25 [mm]
i [–]
Data
Forchheimer
Darcy
q [m/day]

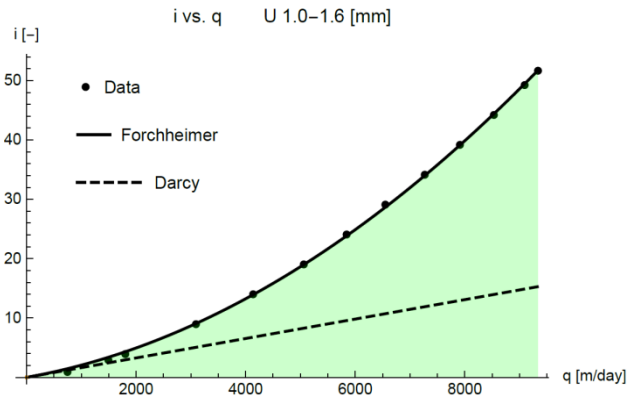
i vs. q U 1.0–1.6 [mm]
i [–]
Data
Forchheimer
Darcy
q [m/day]

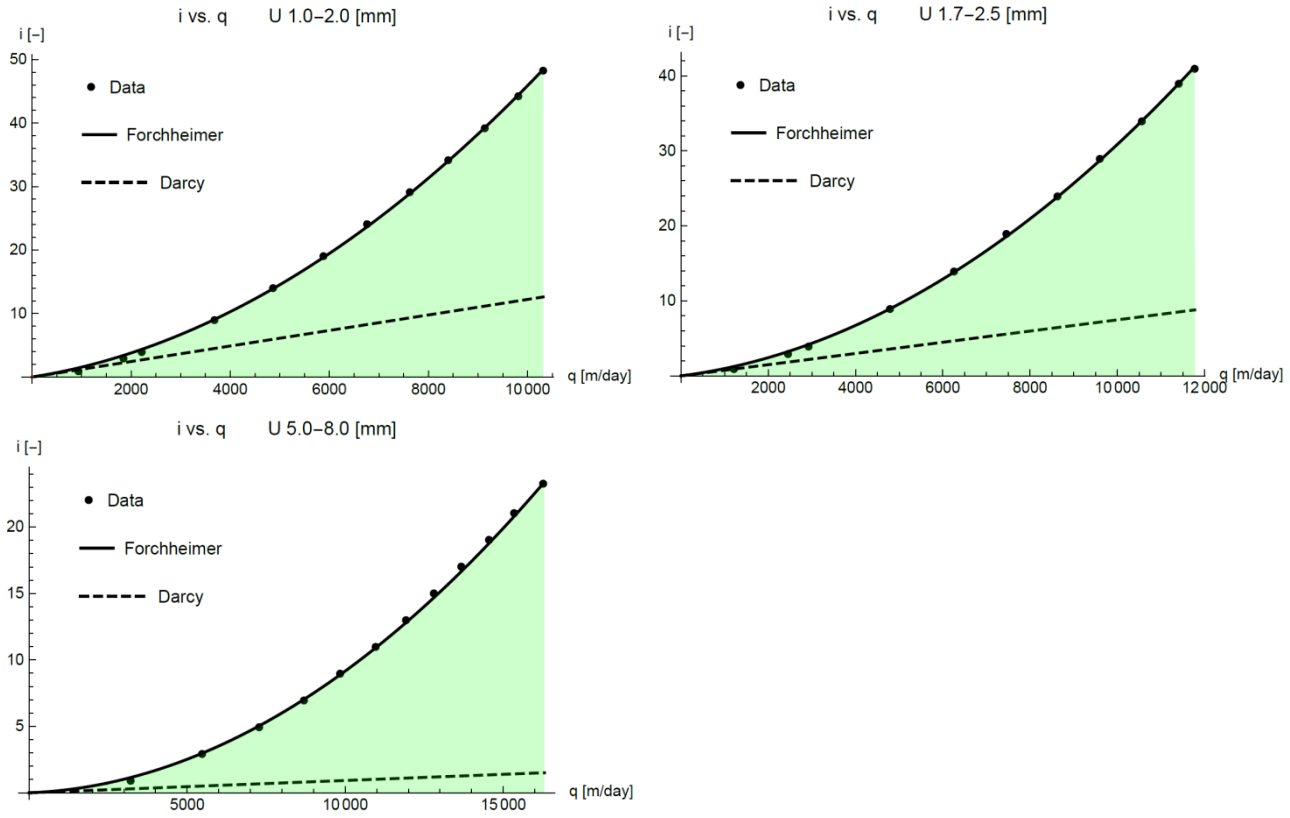

Figure 4: I-q relations based on the results of the experiments with reference porous media. Plotted are the data retrieved from the experimental analyses, the Forchheimer equation fit on the experimental data, and the Darcy equation based on the Forchheimer coefficient a. Color shading blue indicates presence of the Darcy regime, color shading green of the Forchheimer regime. For the fitted parameters and the goodness of fit, see Table 4.

In Figures 5 and 6, the relations between the median grain size and the Forchheimer equation coefficients a and b, respectively, can be seen. On both datasets, power functions are fitted. Both the data and fits show the drastic increase of the Forchheimer coefficients with decreasing median grain size and, hence, increasing flow resistance. A plot with all i-q curves for the reference porous media is given in Appendix A-3 to visualize the effect of the changing coefficients.

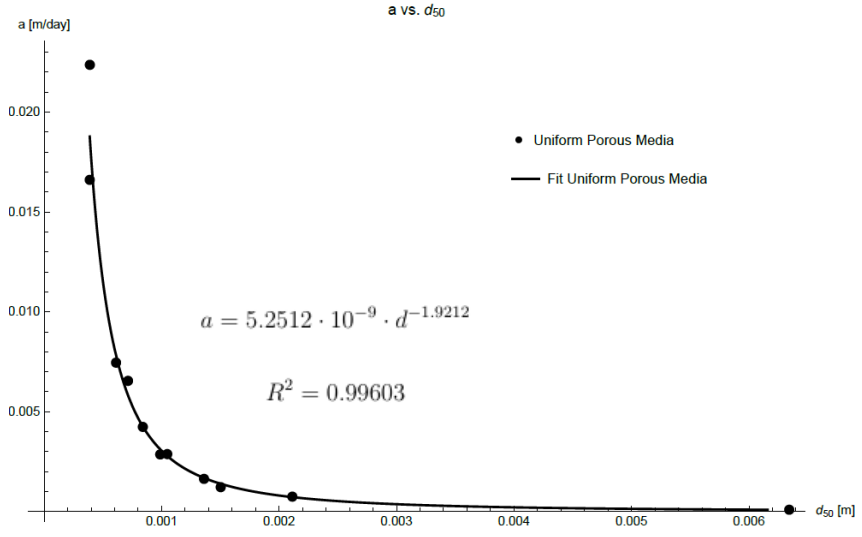

Figure 5: Fitted Forchheimer coefficients a [day m^{-1}] of the experimental data vs. the median grain size [m] for the reference porous media. A fit on the data is shown in the form of a power law.

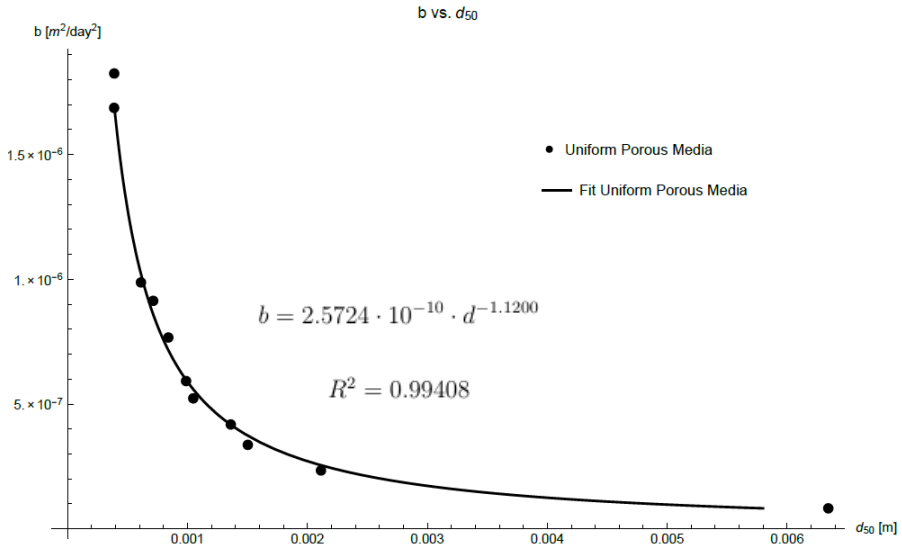

Figure 6: Fitted Forchheimer coefficients b [day^2 m^{-2}] of the experimental data vs. the median grain size [m] for the reference porous media. A fit on the data is shown in the form of a power law.

Table 4: Results of the experiments for the reference porous media in terms of the coefficients of the fitted Forchheimer equations, the goodness of the fits, the d_{50} of the porous media, the minimum and maximum Reynolds number encountered during the experiments and the Reynolds numbers indicating the transition from the Darcy regime to the Forchheimer regime according to the various definitions explained in the Methodology chapter, $Re_{F,1}$, $Re_{F,5}$, and $Re_{F,10}$.

Porous Medium	d_{50} [m]	a [daym^{-1}]	b [day^{2}m^{-2}]	R^2 [-]
U 0.2-0.5 [mm]	0,000389	2,2369E-02	1,8249E-06	0,99992
U0.2-0.63 [mm]	0,000388	1,6609E-02	1,6870E-06	0,99977
U 0.4-0.8 [mm]	0,000612	7,4570E-03	9,8748E-07	0,99994
U 0.5-1.0 [mm]	0,000714	6,5458E-03	9,1361E-07	0,99991
U 0.63-1.0 [mm]	0,00084	4,2400E-03	7,6666E-07	0,99974
U 0.7-1.25 [mm]	0,000988	2,8612E-03	5,9233E-07	0,99953
U 0.8-1.25 [mm]	0,001048	2,8787E-03	5,2293E-07	0,99972
U 1.0-1.6 [mm]	0,001361	1,6373E-03	4,1821E-07	0,99973
U 1.0-2.0 [mm]	0,001503	1,2225E-03	3,3655E-07	0,99964
U 1.7-2.5 [mm]	0,002113	7,4680E-04	2,3390E-07	0,99974
U 5.0-8.0 [mm]	0,006343	9,2689E-05	8,2308E-08	0,99959

Porous Medium	d_{50} [m]	Re_{min} [-]	Re_{max} [-]	$Re_{F,1}$ [-]	$Re_{F,5}$ [-]	$Re_{F,10}$ [-]
U 0.2-0.5 [mm]	0,000389	0,26	10,72	0,55	2,76	5,52
U0.2-0.63 [mm]	0,000388	0,33	13,02	0,44	2,21	4,42
U 0.4-0.8 [mm]	0,000612	1,21	34,59	0,53	2,67	5,35
U 0.5-1.0 [mm]	0,000714	1,58	43,72	0,59	2,96	5,92
U 0.63-1.0 [mm]	0,00084	3,28	62,07	0,54	2,69	5,38
U 0.7-1.25 [mm]	0,000988	5,02	87,29	0,55	2,76	5,52
U 0.8-1.25 [mm]	0,001048	5,51	96,28	0,67	3,34	6,68
U 1.0-1.6 [mm]	0,001361	11,78	147,06	0,62	3,08	6,17
U 1.0-2.0 [mm]	0,001503	16,33	179,44	0,63	3,16	6,32
U 1.7-2.5 [mm]	0,002113	29,65	287,92	0,78	3,90	7,81
U 5.0-8.0 [mm]	0,006343	248,34	1196,78	0,83	4,13	8,25

Eq. 26 was used to plot the Darcy equation in all figures. For each i-q curve, using Eq. 27, the critical superficial velocity for a certain deviation of the Forchheimer fit from the Darcy equation is determined for a deviation of 1 [%] (De_1), 5 [%] (De_1), & 10 [%] (De_{10}) (see section 3.4). The critical velocities are used to determine critical Reynolds numbers ($Re_{F,1}$ [-],$Re_{F,5}$ [-], & $Re_{F,10}$ [-]) that mark the boundary between the Darcy (linear laminar) regime and the Forchheimer (non-linear laminar) regime. Values of these critical Reynolds numbers are given in Table 4. In Figure 4, the section of the i-q curve for which the Darcy regime (blue color shading) applies and the section of the curve for which the Forchheimer regime (green color shading) applies are given using critical Reynolds number $Re_{F,5}$. As is expected, the Darcy regime is better represented for the porous media consisting of finer material. The flow resistance is higher for these cases compared to the coarser cases leading to a steeper i-q curve (see Figure 4 or Figure A-6). Flow velocities are relatively low which enhances the encounter of linear laminar flow (Darcian flow).

The minimum and maximum Reynolds numbers are determined for each experiment using the minimum and maximum flow velocities measured during each experiment. It appears that, for the measurements made, the Darcy regime is not present in case of each porous media. Also, the presence of the Darcy regime seems to be highly dependent on the allowed deviation of the Forchheimer fit from the Darcy equation. In Table 4, Reynolds numbers are underlined if they fall within the range of Reynolds numbers (superficial velocities) measured during the experiments. In case of no underlining, the Reynolds number falls outside of the measured range, thereby indicating that the Darcy regime has not been observed during the experiment. The values of the Reynolds numbers, whether inside or outside of the range of measured data, are in excellent agreement with the ranges of Reynolds numbers proposed in the literature (see section 2.1.) for each of the three definitions of Reynolds number. No notion of the pre-Darcy regime is taken during the experiments.

4.2. Effect of Shape Grain Size Distribution on Non-Linear Flow in Porous Media

In this section the results regarding effect of the shape of the grain size distribution on non-linear flow in porous media will be presented. Composite porous media have been constructed with similar values for median grain size (d_{50}) as the reference porous media, discussed in the previous section, but with a different grain size distribution (different σ, C_U and C_C). The same non-linear flow experiments as conducted for the reference porous media, resulting in similar i-q curves. By analyzing both the differences in grain size distribution and in non-linear flow behavior, using the cases of the reference porous media as reference, it is attempted to derive some general results on the effect of the shape of grain size distributions on non-linear flow. The results are summarized in three sections:

1) Comparison of reference porous medium U 0.4-0.8 [mm] with composite porous media N-U1 and N-U2 (more well-graded) and the composite porous medium N-U3 (gap-graded). All these porous media have median grain sizes around 0.612 [mm].

2) Comparison of reference porous medium U 0.71-1.25 [mm] with composite porous media N-U7, N-U8, and N-U9 (more well-graded) and composite porous medium N-U10 (gap-graded). All these porous media have median grain sizes around 0.988 [mm].
3) Summary of other comparisons made:
    a. Comparison of reference porous medium U 0.5-1.0 [mm] with composite porous medium N-U4 (more well-graded) and composite porous medium N-U5 (gap-graded). All these porous media have median grain sizes around 0.714 [mm].
    b. Comparison of reference porous medium U 0.63-1.0 [mm] with composite porous medium N-U6 (more well-graded). All these porous media have median grain sizes around 0.840 [mm].
    c. Comparison of reference porous medium U 0.8-1.25 [mm] with composite porous media N-U11 and N-U12 (more well-graded). All these porous media have median grain sizes around 1.048 [mm].
    d. Comparison of reference porous medium U 1.0-1.6 [mm] with composite porous medium N-U13 (more well-graded). All these porous media have median grain sizes around 1.361 [mm].

4.2.1. Comparison with U 0.4-0.8 [mm]

Porous media N-U1 and N-U2 have similar grain size distribution shapes as the reference case, U 0.4-0.8 [mm], but are more widely distributed, i.e. more well-graded (see Figure 7). This can be seen in higher values for C_C and C_U (more well-graded) as well as in the increase in standard deviation for both cases (see Table 5). Concerning the non-linear flow behavior, both more well-graded porous media yield steeper i-q curves with respect to the more uniformly-graded reference case (see Figure 7). This most likely follows from the increased amount of finer material present in case of the more well-graded porous media as can be seen in the smaller grain sizes for d_5 and d_{10}. The higher values for d_{90} and d_{95} do not seem to compensate for the elevated presence of finer material. This is proven by gap-graded composite porous media N-U3 (see Figure 7), for which fine material (U 0.2-0.63 [mm]) and coarse material (U 1.7-2.5 [mm]) are mixed in equal amounts resulting in a d_{50} similar to that of U 0.4-0.8 [mm]. The i-q curve is severely steeper with respect to the reference case, the Forchheimer coefficients a and b increasing with 160.2 [%] and 200.8 [%], respectively (see Table 6). No compensation for the increased flow resistance is offered by the course material. It seems that the presence of fine material has the overhand in determining the flow resistance and non-linear flow behavior in porous media.

Table 5: This table shows the statistical properties for porous media U 0.4-0.8 [mm], N-U1, N-U2, and N-U3 as also given in section 3.2. Results of the experiments for these porous media are given in terms of the coefficients of the fitted Forchheimer equations, the goodness of the fits, the d_{50} of the porous media, the minimum and maximum Reynolds number encountered during the experiments and the Reynolds numbers indicating the transition from the Darcy regime to the Forchheimer regime according to the various definitions explained in section 3.4, $Re_{F,1}$, $Re_{F,5}$, and $Re_{F,10}$. In case the Reynolds numbers are underlined, they fall within the range of measured Reynolds numbers.

Porous Medium	d_5 [mm]	d_{10} [mm]	d_{20} [mm]	d_{30} [mm]	d_{40}[mm]	d_{50} [mm]	d_{60} [mm]	d_{70} [mm]	d_{80} [mm]	d_{90} [mm]	d_{95} [mm]
U 0.4-0.8 [mm]	0,435	0,47	0,515	0,547	0,58	0,612	0,644	0,678	0,713	0,767	0,794
N-U1	0,341	0,404	0,478	0,53	0,575	0,617	0,659	0,702	0,756	0,826	0,889
N-U2	0,304	0,347	0,413	0,474	0,532	0,586	0,639	0,692	0,754	0,834	0,896
N-U3	0,275	0,316	0,366	0,408	0,46	0,619	1,862	2,046	2,18	2,318	2,407

Porous Medium	d_m [mm]	σ^2 [mm^2]	σ [mm]	$d_{m3}\sigma^{-3}$	C_C	C_U
U 0.4-0.8 [mm]	0,6148	0,0131	0,1145	0,05	0,99	1,37
N-U1	0,6186	0,0282	0,1680	0,34	1,06	1,63
N-U2	0,5901	0,0357	0,1888	0,41	1,01	1,84
N-U3	1,2314	0,7634	0,8737	0,14	0,28	5,89

Porous Medium	a [daym^{-1}]	b [day^{2}m^{-2}]	R^2 [-]	k [m^2]	n [-]	Re_{min} [-]	Re_{max} [-]	$Re_{F,1}$ [-]	$Re_{F,5}$ [-]	$Re_{F,10}$ [-]
U 0.4-0.8 [mm]	7,4570E-03	9,8748E-07	0,99994	1,5822E-10	0,3314	1,21	34,59	0,53	2,67	5,35
N-U1	8,6183E-03	1,1073E-06	0,99983	1,3690E-10	0,3340	0,97	32,38	0,56	2,78	5,56
N-U2	1,0476E-02	1,3252E-06	0,99992	1,1262E-10	0,3305	0,80	26,78	0,54	2,68	5,36
N-U3	1,9401E-02	2,9704E-06	0,99978	6,0813E-11	0,2683	0,41	17,07	0,47	2,34	4,68

Table 6: Relative error of Forchheimer equation coefficients a and b resulting from the experiments with composite porous media N-U1, N-U2, and N-U3 with respect to the Forchheimer equation coefficients a and b resulting from the experiments with reference porous medium U 0.4-0.8 [mm].

Porous Medium	Rel Error a [-]	Rel Error b [-]
U 0.4-0.8 [mm]	0,000	0,000
N-U1	0,156	0,121
N-U2	0,405	0,342
N-U3	1,602	2,008

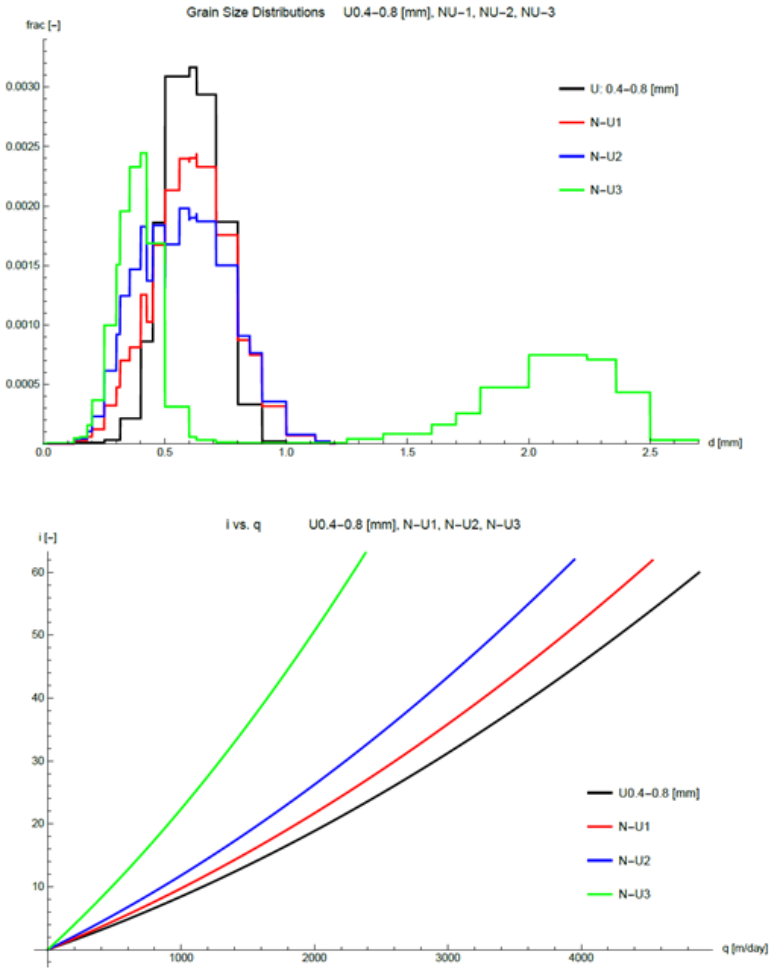

Figure 7: Grain size distributions and i-q curves shown for U 0.4-0.8 [mm], N-U1, N-U2, and N-U3.

4.2.2. Comparison with U 0.71-1.25 [mm]

The dominant role of the presence of finer material is further proven comparing composite porous media N-U7, N-U8, N-U9, and N-U10. As can be seen in Figure 8, the flow resistance (steepness of the i-q curves) increases with increasing amount of fine material present in the grain size distributions/porous media. The Forchheimer coefficients change accordingly (see Table 7). In case of the right-skewed grain size distribution (for composite porous medium N-U9), relatively little extra fine material is added with respect to the reference case, whilst a great amount of courser material is added. Although the i-q curve is similar to the reference case (see Table 7; Figure 8), the curve still is slightly steeper than the reference case, despite the amount of extra course material. For the gap-graded composite porous medium N-U10, similar results can be retrieved as in case of N-U3: as in this case the largest amount of fine material is added with respect to the reference case, the flow resistance becomes highest resulting in a 68.0 [%] and 44.5 [%] increase in Forchheimer coefficients a and b, respectively (see Table 8).

Table 7: This table shows the statistical properties for porous media U 0.71-1.25 [mm], N-U7, N-U8, N-U9, and N-U10 as also given in section 3.2. Results of the experiments for these porous media are given in terms of the coefficients of the fitted Forchheimer equations, the goodness of the fits, the d_{50} of the porous media, the minimum and maximum Reynolds number encountered during the experiments and the Reynolds numbers indicating the transition from the Darcy regime to the Forchheimer regime according to the various definitions explained in section 3.4, $Re_{F,1}$, $Re_{F,5}$, and $Re_{F,10}$. In case the Reynolds numbers are underlined, they fall within the range of measured Reynolds numbers.

Porous Medium	d_5 [mm]	d_{10} [mm]	d_{20} [mm]	d_{30} [mm]	d_{40}[mm]	d_{50} [mm]	d_{60} [mm]	d_{70} [mm]	d_{80} [mm]	d_{90} [mm]	d_{95} [mm]
U 0.71-1.25 [mm]	0,727	0,795	0,862	0,909	0,948	0,988	1,030	1,073	1,116	1,174	1,224
N-U7	0,479	0,606	0,755	0,847	0,919	0,993	1,081	1,177	1,323	1,516	1,647
N-U8	0,558	0,681	0,816	0,889	0,940	0,988	1,032	1,076	1,119	1,178	1,229
N-U9	0,658	0,740	0,828	0,885	0,938	0,990	1,049	1,110	1,186	1,344	1,477
N-U10	0,445	0,529	0,640	0,738	0,839	1,006	1,225	1,327	1,427	1,541	1,598

Porous Medium	d_m [mm]	σ^2 [mm^2]	σ [mm]	$d_{m3}\sigma^{-3}$ [-]	C_C	C_U
U 0.71-1.25 [mm]	0,9848	0,0280	0,1673	-0,39	1,01	1,30
N-U7	1,0323	0,1224	0,3498	0,40	1,10	1,78
N-U8	0,9607	0,0434	0,2084	-0,40	1,12	1,52
N-U9	1,0141	0,0579	0,2406	0,39	1,01	1,42
N-U10	1,0328	0,1574	0,3967	0,06	0,84	2,32

Porous Medium	a [daym^{-1}]	b [day^{2}m^{-2}]	R^2 [-]	k [m^2]	n [-]	Re_{min} [-]	Re_{max} [-]	$Re_{F,1}$ [-]	$Re_{F,5}$ [-]	$Re_{F,10}$ [-]
U 0.71-1.25 [mm]	2,8612E-03	5,9233E-07	0,99953	4,1235E-10	0,3459	5,02	87,29	0,55	2,76	5,52
N-U7	4,2186E-03	7,4928E-07	0,99977	2,7967E-10	0,3302	3,36	73,71	0,65	3,24	6,47
N-U8	3,7990E-03	6,9813E-07	0,99969	3,1056E-10	0,3436	3,86	77,58	0,62	3,11	6,22
N-U9	2,9901E-03	5,9019E-07	0,99963	3,9458E-10	0,3480	5,51	86,67	0,58	2,90	5,81
N-U10	4,8055E-03	8,5582E-07	0,99971	2,4552E-10	0,3320	3,08	70,14	0,65	3,27	6,54

Table 8: Relative error of Forchheimer equation coefficients a and b resulting from the experiments with the composite porous media N-U7, N-U8, N-U9 and N-U10 with respect to the Forchheimer equation coefficients a and b resulting from the experiments with reference porous medium U 0.71-1.25 [mm].

Porous Medium	Rel Error a [-]	Rel Error b [-]
U 0.71-1.25 [mm]	0,000	0,000
N-U7	0,474	0,265
N-U8	0,328	0,179
N-U9	0,045	-0,004
N-U10	0,680	0,445

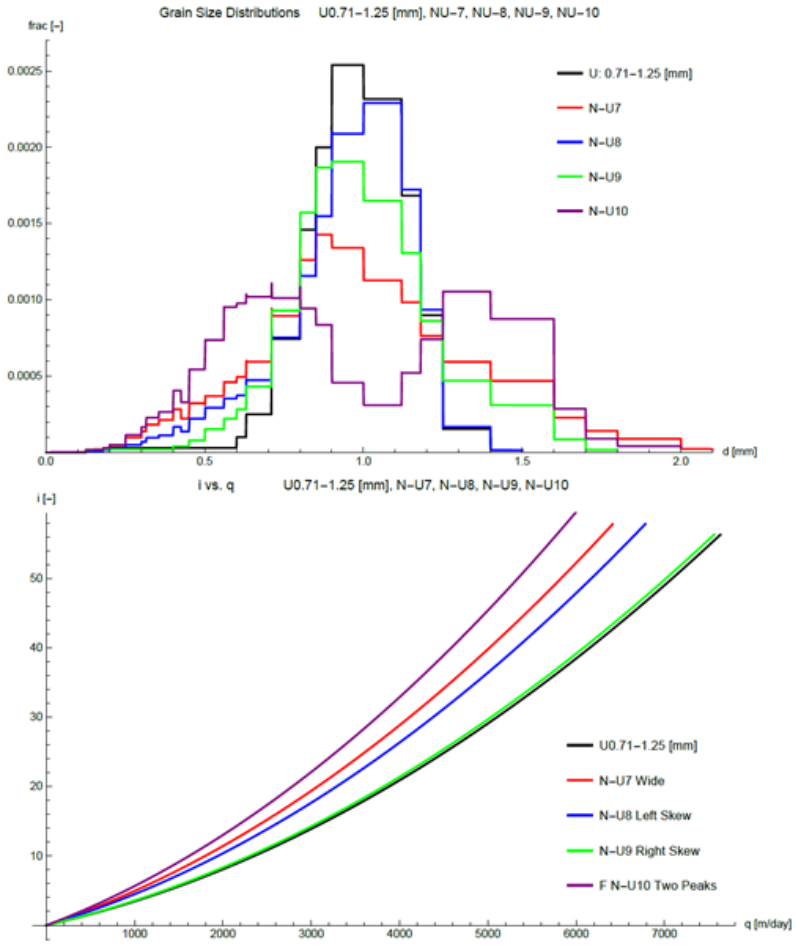

Figure 8: Grain size distributions and i-q curves shown for U 0.71-1.25[mm], N-U7, N-U8, N-U9, N-U10.

4.2.3. Other Comparisons

The comparison of the composite porous media with their respective reference counterpart, yield similar results as found in the previous subsections (see Figure 9 and Table 9): an elevated amount of finer material increases the flow resistance (increase of Forchheimer coefficients a and b). Again, elevated amounts of course material do not seems to compensate for this. An extreme case is the comparison of N-U5 with U 0.5-1.0 [mm]. Porous medium N-U5 is gap-graded and its grain size distribution has three distinct peaks. With respect to reference porous medium U 0.5-1.0 [mm] the Forchheimer coefficients a and b increase with 93.5 and 96.6 [%] respectively, thereby significantly increasing the flow resistance (see Table 10).

Table 9: This table shows the statistical properties for porous media U 0.5-1.0 [mm], U 0.63-1.0 [mm], U 0.8-1.25 [mm], U 1.0-1.6 [mm], N-U4, N-U5, N-U6, N-U11, N-U12 and N-U13 as also given in section 3.2. Results of the experiments for these porous media are given in terms of the coefficients of the fitted Forchheimer equations, the goodness of the fits, the d_{50} of the porous media, the minimum and maximum Reynolds number encountered during the experiments and the Reynolds numbers indicating the transition from the Darcy regime to the Forchheimer regime according to the various definitions explained in section 3.4, $Re_{F,1}$, $Re_{F,5}$, and $Re_{F,10}$. In case the Reynolds numbers are underlined, they fall within the range of measured Reynolds numbers. a this porosity is not directly determined from the porous medium with which the non-linear flow experiment is performed through disturbance of the weighing process. The porosity of a porous medium with the same mixture is used instead.

Porous Medium	d_5 [mm]	d_{10} [mm]	d_{20} [mm]	d_{30} [mm]	d_{40}[mm]	d_{50} [mm]	d_{60} [mm]	d_{70} [mm]	d_{80} [mm]	d_{90} [mm]	d_{95} [mm]
U 0.5-1.0 [mm]	0,494	0,532	0,588	0,632	0,673	0,714	0,757	0,8	0,849	0,917	0,975
N-U4	0,373	0,444	0,532	0,597	0,656	0,713	0,772	0,833	0,899	1,001	1,098
N-U5	0,299	0,341	0,407	0,48	0,596	0,718	0,854	1,754	2,054	2,252	2,356
U 0.63-1.0 [mm]	0,684	0,722	0,76	0,797	0,819	0,84	0,861	0,882	0,908	0,958	0,983
N-U6	0,511	0,569	0,658	0,731	0,791	0,841	0,887	0,944	1,007	1,103	1,164
U 0.8-1.25 [mm]	0,846	0,893	0,938	0,98	1,016	1,048	1,08	1,112	1,152	1,205	1,244
N-U11	0,564	0,689	0,823	0,904	0,975	1,045	1,116	1,203	1,333	1,507	1,611
N-U12	0,579	0,705	0,833	0,912	0,981	1,048	1,115	1,197	1,323	1,495	1,595
U 1.0-1.6 [mm]	1,03	1,125	1,209	1,268	1,315	1,361	1,409	1,466	1,522	1,579	1,626
N-U13	0,679	0,811	0,975	1,116	1,241	1,363	1,49	1,623	1,784	1,992	2,184

Porous Medium	d_m [mm]	σ^2 [mm^2]	σ [mm]	$d_{m3}\sigma^{-3}$	C_C	C_U
U 0.5-1.0 [mm]	0,7227	0,0252	0,1588	0,80	0,99	1,42
N-U4	0,7215	0,0477	0,2184	0,29	1,04	1,74
N-U5	1,0720	0,5803	0,7618	0,67	0,79	2,50
U 0.63-1.0 [mm]	0,8373	0,0090	0,0948	-0,34	1,02	1,19
N-U6	0,8384	0,0412	0,2030	0,12	1,06	1,56
U 0.8-1.25 [mm]	1,0494	0,0202	0,1421	1,05	1,00	1,21
N-U11	1,0710	0,1025	0,3201	0,33	1,06	1,62
N-U12	1,0715	0,0966	0,3108	0,32	1,06	1,58
U 1.0-1.6 [mm]	1,3541	0,0380	0,1950	-0,84	1,01	1,25
N-U13	1,3860	0,2049	0,4527	0,21	1,03	1,84

Table 9 (continued).

Porous Medium	a [daym^{-1}]	b [day^{2}m^{-2}]	R^2 [-]	k [m^2]	n [-]	Re_{min} [-]	Re_{max} [-]	$Re_{F,1}$ [-]	$Re_{F,5}$ [-]	$Re_{F,10}$ [-]
U 0.5-1.0 [mm]	6,5458E-03	9,1361E-07	0,99991	1,8024E-10	0,3400	1,58	43,72	0,59	2,96	5,92
N-U4	7,2597E-03	1,0562E-06	0,99985	1,6252E-10	0,3318	1,44	40,29	0,57	2,84	5,67
N-U5	1,2663E-02	1,7965E-06	0,99992	9,3171E-11	0,2894[a]	0,74	27,85	0,59	2,93	5,86
U 0.63-1.0 [mm]	4,2400E-03	7,6666E-07	0,99974	2,7826E-10	0,3327	3,28	62,07	0,54	2,69	5,38
N-U6	4,8707E-03	8,5555E-07	0,99979	2,4223E-10	0,3369	2,46	58,25	0,55	2,77	5,54
U 0.8-1.25 [mm]	2,8787E-03	5,2293E-07	0,99972	4,0985E-10	0,3477	5,51	96,28	0,67	3,34	6,68
N-U11	3,3014E-03	6,6897E-07	0,99977	3,5737E-10	0,3417	4,77	86,34	0,60	2,98	5,97
N-U12	3,5508E-03	6,7410E-07	0,99979	3,3227E-10	0,3372	4,44	84,89	0,64	3,19	6,39
U 1.0-1.6 [mm]	1,6373E-03	4,1821E-07	0,99973	7,2059E-10	0,3547	11,78	147,06	0,62	3,08	6,17
N-U13	1,9599E-03	4,7419E-07	0,99973	6,0198E-10	0,3454	10,16	138,27	0,65	3,26	6,52

Table 10: Relative error of Forchheimer equation coefficients a and b resulting from the experiments with the composite porous media N-U4, N-U5, N-U6, N-U11, N-U12, and N-U13 with respect to the Forchheimer equation coefficients a and b resulting from the associated experiments (similar median grain size) with reference porous media U 0.5-1.0 [mm], U 0.63-1.0 [mm], U 0.8-1.25 [mm], U 1.0-1.6 [mm].

Porous Medium	Rel Error a [-]	Rel Error b [-]
U 0.5-1.0 [mm]	0,0000	0,0000
N-U4	0,1091	0,1561
N-U5	0,9345	0,9664
U 0.63-1.0 [mm]	0,0000	0,0000
N-U6	0,1488	0,1159
U 0.8-1.25 [mm]	0,0000	0,0000
N-U11	0,1468	0,2793
N-U12	0,2335	0,2891
U 1.0-1.6 [mm]	0,0000	0,0000
N-U13	0,1970	0,1339

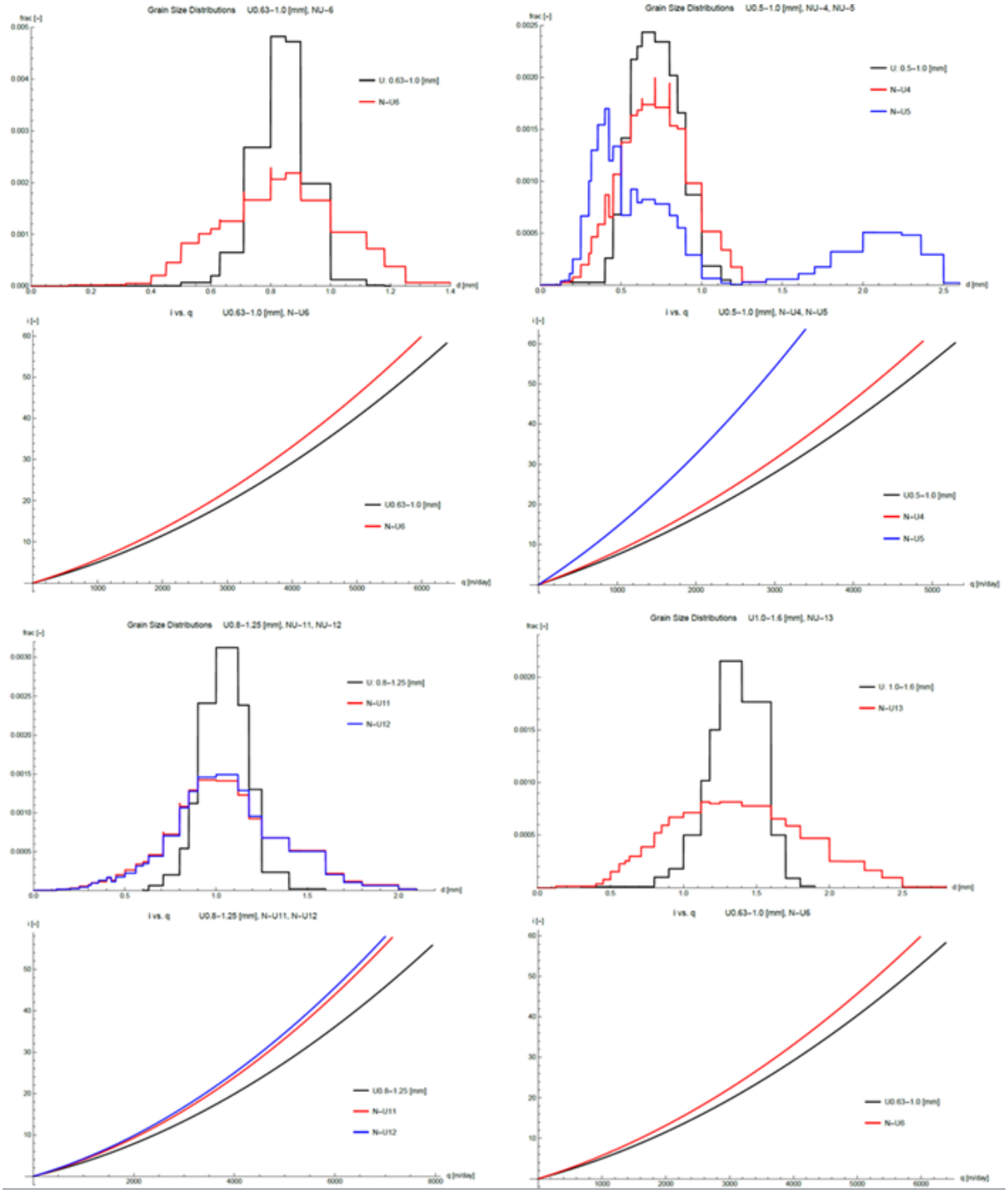

Figure 9: Grain size distributions and i-q curves shown for U 0.5-1.0 [mm], U 0.63-1.0 [mm], U 0.8-1.25 [mm], U 1.0-1.6 [mm], N-U4, N-U5, N-U6, N-U11, N-U12, and N-U13.

4.2.4. Relation Forchheimer Coefficients and Median Grain Size

In Figures 10 and 11, the relations between the median grain size and the Forchheimer equation coefficients a and b can be seen for both the reference and the composite porous media. On the data points for the reference porous media the same power functions as in Figures 5 and 6 are shown. For the data points for the composite porous media, a similar trend can be seen as for the reference porous media: a drastic increase of the Forchheimer coefficients with decreasing median grain size and, hence, increasing flow resistance. However, the data points of the composite porous media do in many cases deviate quite severely from the fit on the data of the reference porous media. This indicates that the median grain size, d_{50}, is not an appropriate indicator for the flow resistance encountered: various porous media with similar d_{50}'s show different values Forchheimer coefficients a and b and, hence, different values of flow resistance. As can be derived from Figures 10 and 11 the gap-graded composite porous media give the most deviating Forchheimer coefficients a and b with respect to the fit on the Forchheimer coefficients of the reference porous media.

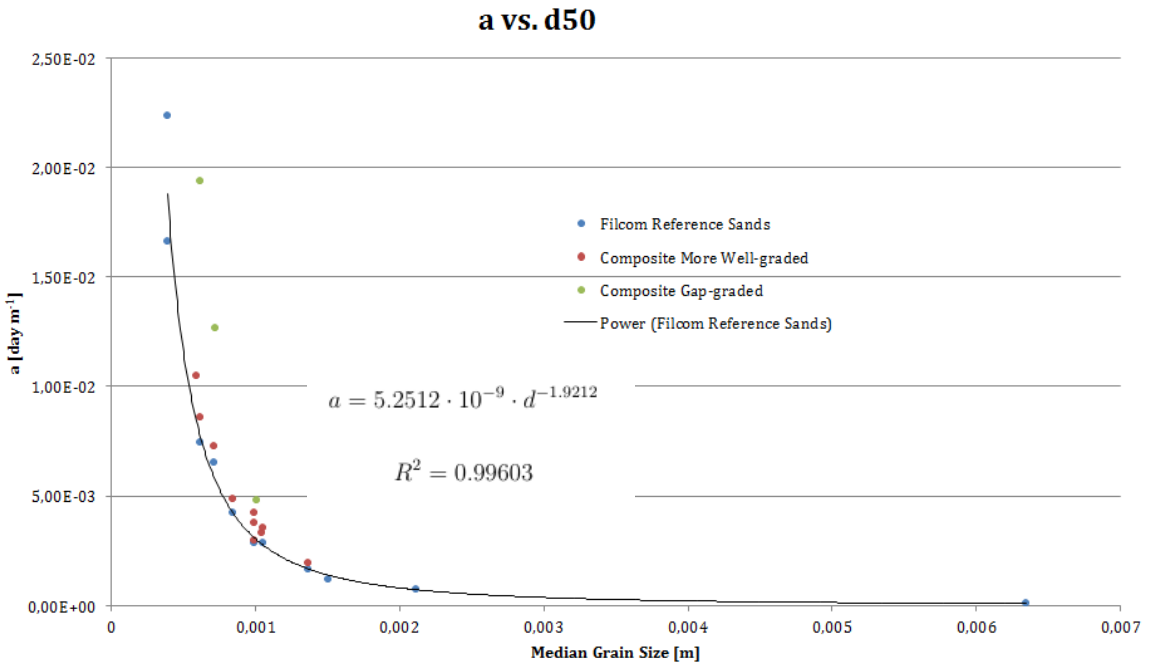

Figure 10: Fitted Forchheimer coefficients a [day m^{-1}] of the experimental data vs. the median grain size [m] for the reference porous media. A fit on the data is shown in the form of a power law. Also the Forchheimer coefficients a for the composite porous media are given. No fit is made on these values.

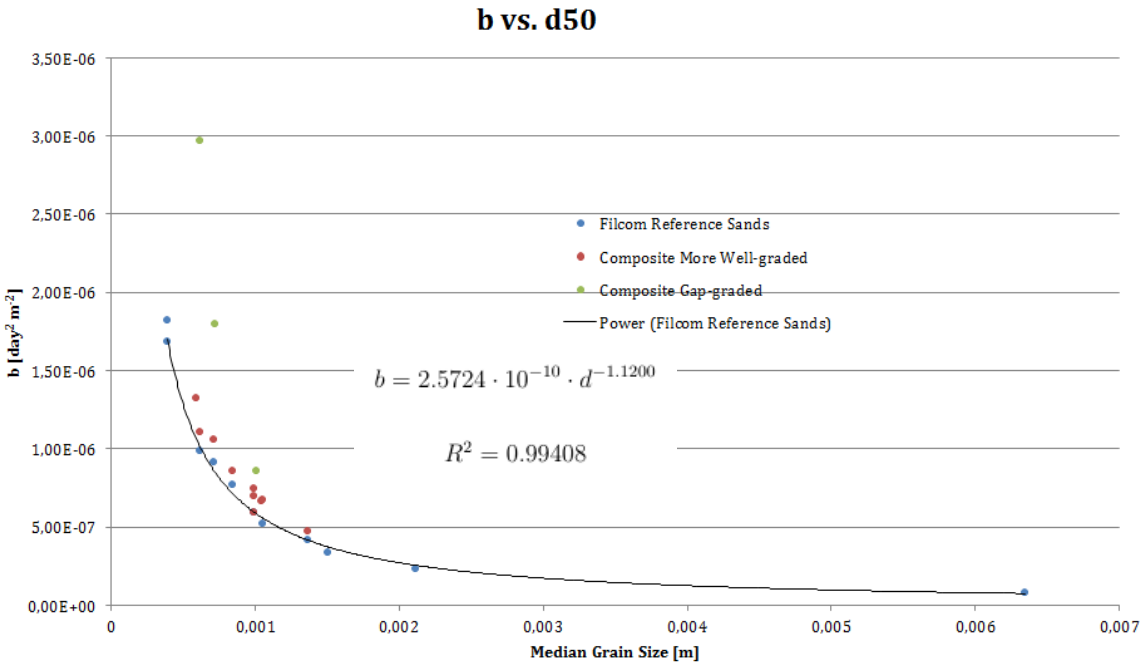

Figure 11: Fitted Forchheimer coefficients b [day^2 m^{-2}] of the experimental data vs. the median grain size [m] for the reference porous media. A fit on the data is shown in the form of a power law. Also the Forchheimer coefficients b for the composite porous media are given. No fit is made on these values.

4.2.5. The Effect of Porosity

The packing method employed in this research yields optimal compaction for every porous medium. Therefore, for a given grain size distribution, the porosity is different from that of another with a different grain size distribution. In the previous subsections, it is found that the shape grain size distribution has a significantly effect on non-linear flow in porous media. However, the grain size distribution also has an effect on porosity which subsequently also influences non-linear flow in porous media. This will be shown in the next section when the macroscopic porous medium parameters d_{50} and porosity are used for the empirical relations (similar d_{50}, different porosity).

4.3. Comparison of Experimental Data with Empirical i-q Relations

To compare the i-q curves based on the experimental data with the empirical relations provided in literature (see sections 2.3. and 3.6.), the NOF is used (see section 3.6.). The closer the value of NOF to 0, the better the ability of the empirical relation to describe the experimental data. In Figures 12 and 13, the comparison of the experimental data with the empirical relations is shown for reference porous media U 0.2-0.63 [mm] and U 5.0-8.0 [mm] as examples, the other comparisons can be found in Appendix A.5. Values for NOF are given in Table 11.

It appears that both the empirical expressions of Kovács (1981) and Macdonald et al. (1979) fit the data very well as can be seen from their low values for the NOF (see Table 11). Generally, for the uniform reference porous media, Kovács yields the best fit for the reference porous media with a d_{50} under ± 1[mm] and Macdonald et al. for the reference porous media with a d_{50} above ± 1[mm]. As follows from section 4.2., the elevated presence of fine material in the composite porous media increases the flow resistance. As the relation by Macdonald et al. overestimates the steepness of the i-q curve for the reference porous media, this relation provides a more accurate estimate for the composite porous media with a similar value for d_{50}. The empirical relations only use the median grain size in the determination of the relation for i-q, without taking into account the grain size distribution. Hence, the empirical i-q relation for the composite porous media is only altered by a different porosity and not a different d_{50} with respect to the empirical i-q relation for the reference porous media. The differences in porosity between the reference porous media are, generally, small. For the gap-graded porous media the difference is larger as very fine material tends to fill up empty void space well if combined with (very) coarse sand as is done in case of the gap-graded porous media.

The relations by Ergun (1952) and Du Plessis (1994) are moderately appropriate to model the experimental i-q data, considering the NOF. However, the Ergun and the Du Plessis relations do deliver approximately a fairly stable NOF (± 0.40) over the wide range of grain sizes. This in contrast to the relations by Macdonald et al., Ward, Schneebeli and Sidiropoulou et al.. The results for the Kovacs relation display the same level of consistency as the Ergun and Du Plessis relations. In case of the Ergun expression, it is known (see section 2.3.) that the relation is based on experiments with a big amount of porous media (640). Perhaps it is the amount of data on which the relation is based that determined its consistency in prediction of an i-q relation.

The performance of the empirical relation by Ward (1964) is poor. Ward used 20 different porous media for the construction of his relation (as cited in Sidiropoulou et al. (2007)). It is not known to the author which (type of) porous media are used by Ward, but it could be true that the expression is based on porous media not representative of the porous media used in the current work. Schneebeli's (1955) similar empirical expression gives a better fit than Ward's. Of Schneebeli's proposed relations, Eq. 13 and Eq. 14, Eq. 14 is used for the analysis. This relation is based on experiments using crushed granite (coarse) and was expected to be able to represent the experimental data better than his other relation based on experiments using glass spheres (Eq. 13). This indeed seems to be the case, but both generally severely underestimate the experimental i-q relation, Eq. 14 less than Eq. 13. In case of the reference porous media, the

ability of the Schneebeli relation (Eq. 14) to predict the i-q curve improves with increasing grain size. This might have to do with the fact that Schneebeli devised his equation based on coarse gravelly material. Perhaps the average d_{50} used in this research is not suitable for Schneebeli's relation.

The Sidiropoulou et al. (2007) relation is moderately appropriate in modeling the experimental results. As the Sidiropoulou relation is based on a large number of data from previous experimental studies on non-linear flow in porous media, it was expected that this relation would yield low values of NOF. It is true that the porous media used in this current research might not be representative of the porous media used by Sidiropoulou et al. (see Figures 14 and 15) as in the current research very large d_{50}'s, included in the data used by Sidiropoulou et al., are not used and focus lies mainly on the porous media with relatively small d_{50}'s.

In general, when comparing the values for NOF for the reference porous media and the associated (same d_{50}) composite porous media, it is noted that the ability of the empirical relations to represent the experimental results is poorer for the composite media than for the reference media. This comes as no surprise as all, but one (Macdonald et al.'s) empirical relations underestimate the experimental data. In case of the composite porous media, the flow resistance is even more elevated which, in case of a similar porosity and same d_{50}, leads to an even greater underestimation than for the reference cases.

Table 11: NOF values [-] for all investigated empirical expressions calculated relative to the Forchheimer equation fit on the experimental data. Shown for reference and composite porous media.

Porous Medium	Data	Ergun	Kovacs	Macdonald	Du Plessis	Ward	Schneebeli	Sidiropoulou
U 0.2-0.5 [mm]	0,00	0,78	0,72	0,20	0,73	4,05	1,23	1,39
U 0.2-0.63 [mm]	0,00	0,25	0,21	0,47	0,21	2,89	0,70	0,76
U 0.4-0.8 [mm]	0,00	0,26	0,16	0,39	0,20	2,28	0,61	0,48
U 0.5-1.0 [mm]	0,00	0,50	0,36	0,20	0,43	2,39	0,71	0,55
U 0.63-1.0 [mm]	0,00	0,31	0,18	0,29	0,25	2,00	0,55	0,37
U 0.7-1.25 [mm]	0,00	0,35	0,20	0,21	0,29	1,68	0,41	0,26
U 0.8-1.25 [mm]	0,00	0,38	0,22	0,18	0,32	1,67	0,42	0,27
U 1.0-1.6 [mm]	0,00	0,41	0,23	0,11	0,34	1,49	0,35	0,24
U 1.0-2.0 [mm]	0,00	0,33	0,15	0,15	0,26	1,28	0,24	0,15
U 1.7-2.5 [mm]	0,00	0,32	0,13	0,13	0,25	1,21	0,22	0,16
U 5.0-8.0 [mm]	0,00	0,32	0,12	0,08	0,25	1,07	0,17	0,31
Porous Medium	Data	Ergun	Kovacs	Macdonald	Du Plessis	Ward	Schneebeli	Sidiropoulou
N-U1	0,00	0,46	0,34	0,28	0,39	2,67	0,81	0,66
N-U2	0,00	0,55	0,44	0,25	0,48	3,10	1,00	0,85
N-U3	0,00	0,55	0,48	0,39	0,45	6,39	2,72	2,06
N-U4	0,00	0,53	0,40	0,20	0,46	2,71	0,88	0,68
N-U5	0,00	0,64	0,52	0,26	0,54	4,73	1,95	1,46
N-U6	0,00	0,49	0,34	0,18	0,42	2,28	0,70	0,51
N-U7	0,00	0,51	0,34	0,14	0,43	2,33	0,77	0,54
N-U8	0,00	0,56	0,38	0,09	0,48	2,12	0,65	0,47
N-U9	0,00	0,39	0,23	0,18	0,33	1,72	0,43	0,29
N-U10	0,00	0,71	0,52	0,02	0,62	2,68	0,96	0,72
N-U11	0,00	0,51	0,34	0,11	0,44	2,04	0,62	0,44
N-U12	0,00	0,51	0,34	0,12	0,43	2,13	0,67	0,47
N-U13	0,00	0,46	0,27	0,09	0,38	1,73	0,49	0,34

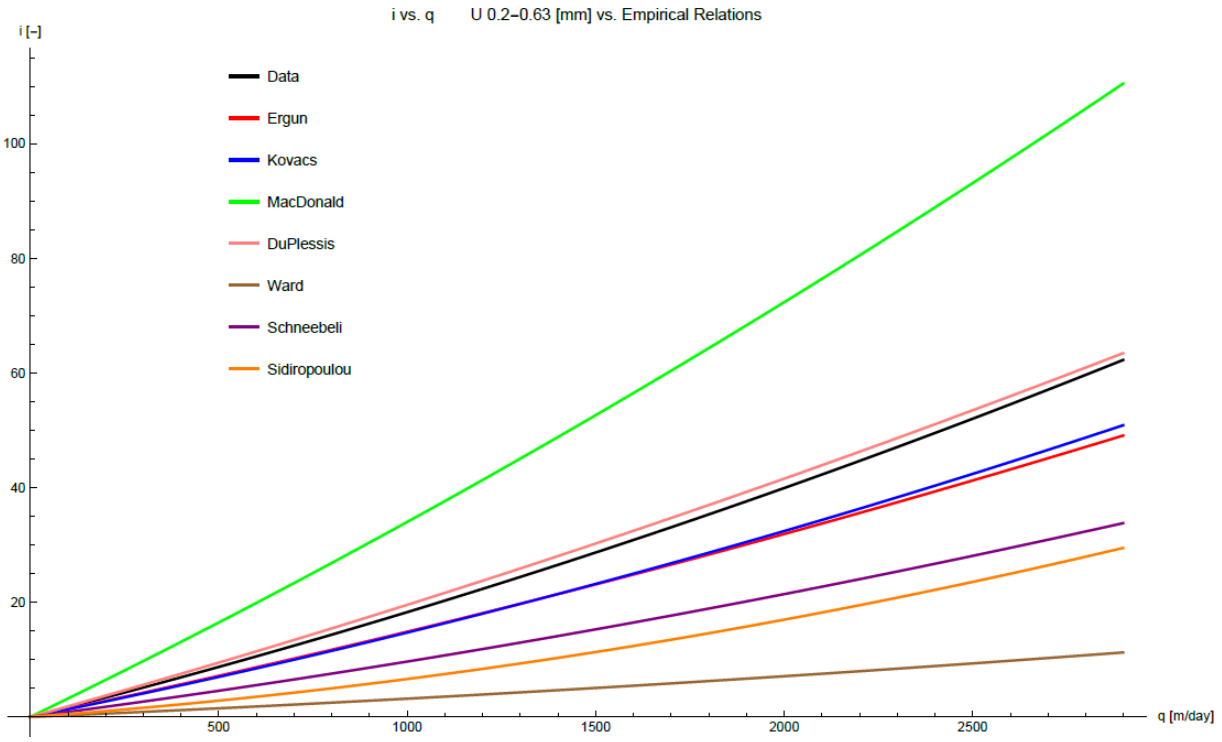

Figure 12: i-q curves shown for U 0.2-0.63 [mm], and the empirical relations using the same n, d_{50}, and ν as U 0.2-0.63 [mm].

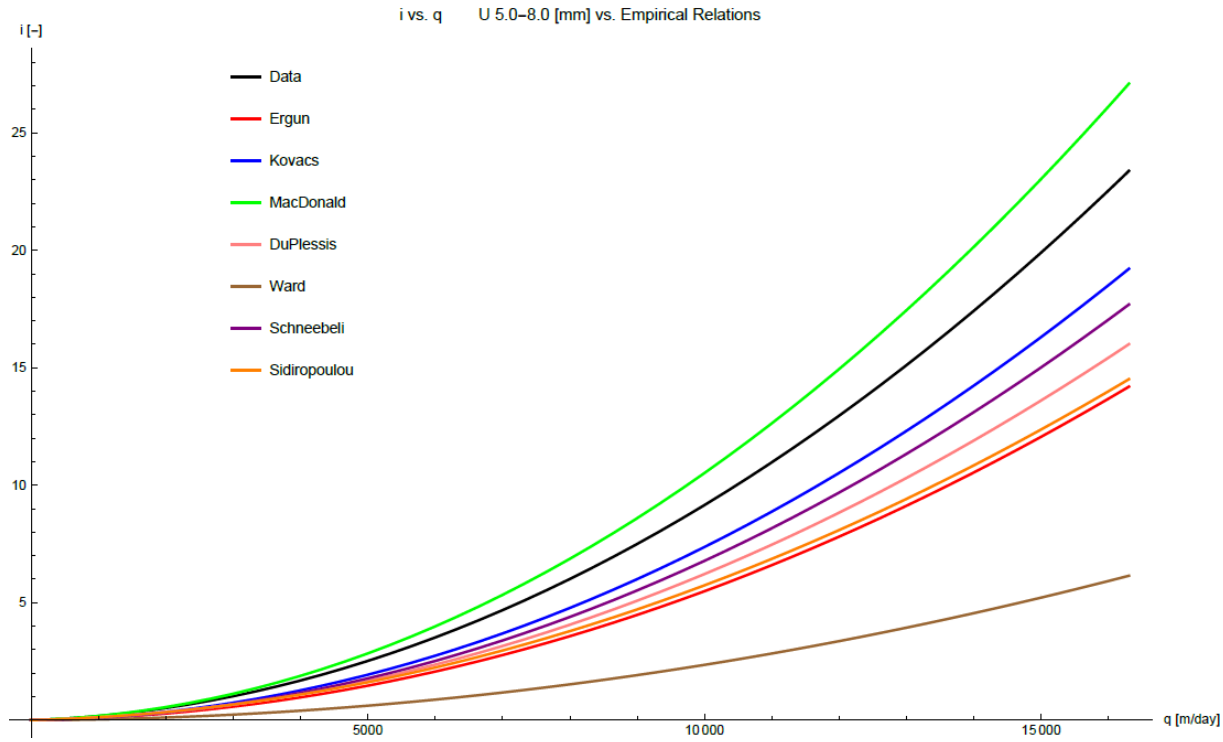

Figure 13: i-q curves shown for U 5.0-8.0 [mm], and the empirical relations using the same n, d_{50}, and ν as U 5.0-8.0 [mm].

5. Discussion

5.1. Comparison Experimental Results with Existing Literature

The data generated in this work contributes to the already existing database on post-Darcy non-linear flow in various porous media. Sidiropoulou et al. (2007) have summarized a large dataset of non-linear flow experiments in the form of Forchheimer coefficients versus median grain size plots with log-log scales to provide the opportunity to include experimental data for a large variety of grain sizes. Their summarizing plots are remade and shown in Figures 14 and 15 for Forchheimer coefficients a and b, respectively. Also their power function giving the best fit for the data is given. For comparison, the results of the current work are included in these figures as well as a separate fit on this data. As expected, the current work's data seems to shed light on non-linear flow in a region of median grain sizes relatively underrepresented in previous experimental works. Obviously, the figures by Sidiropoulou et al. (2007) do not include all data on the topic. However, it is expected that these figures particularly give a good representation of the data available in literature, as is also includes results for smaller median grain sizes. Outside of these figures, mainly course granular material is encountered (e.g. Huang et al., 2013; Bağci et al., 2014; Sedghi-Asl et al., 2014). The fit on this work's experimental data deviates slightly from the fit by Sidiropoulou et al.. This is expected, however, as this work's data is not representative of the summarizing dataset by Sidiropoulou et al., partially because of the sample size, partially because of the excessive representation of small grain sizes in this work.

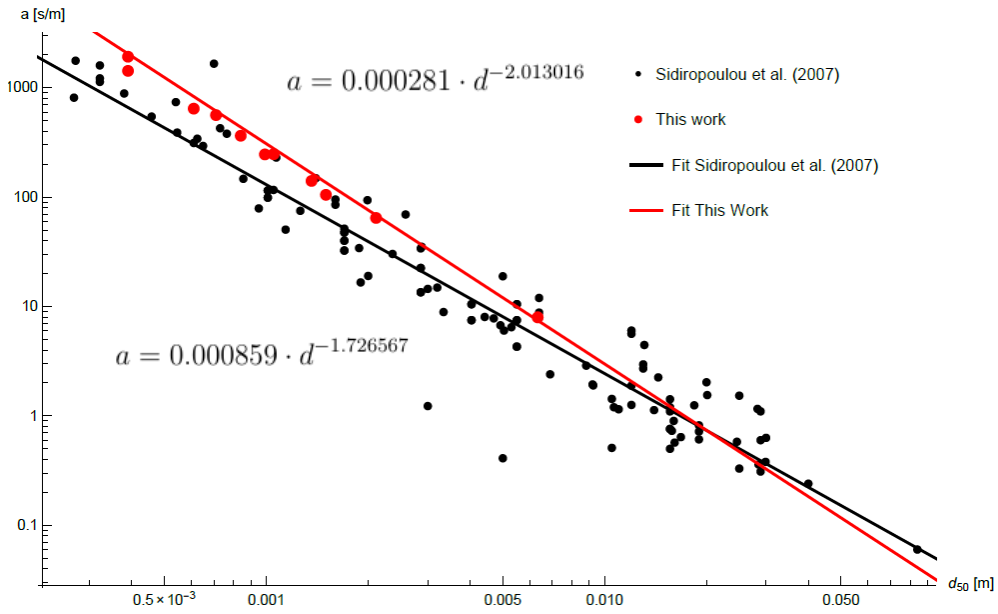

Figure 14: Forchheimer coefficient a [sm^{-1}] versus the median grain size, d_{50} [m]. Data from Sidiropoulou et al. (2007), who summarized various datasets from previous studies, as well as this work's data are given. Power law fits are given for both datasets.

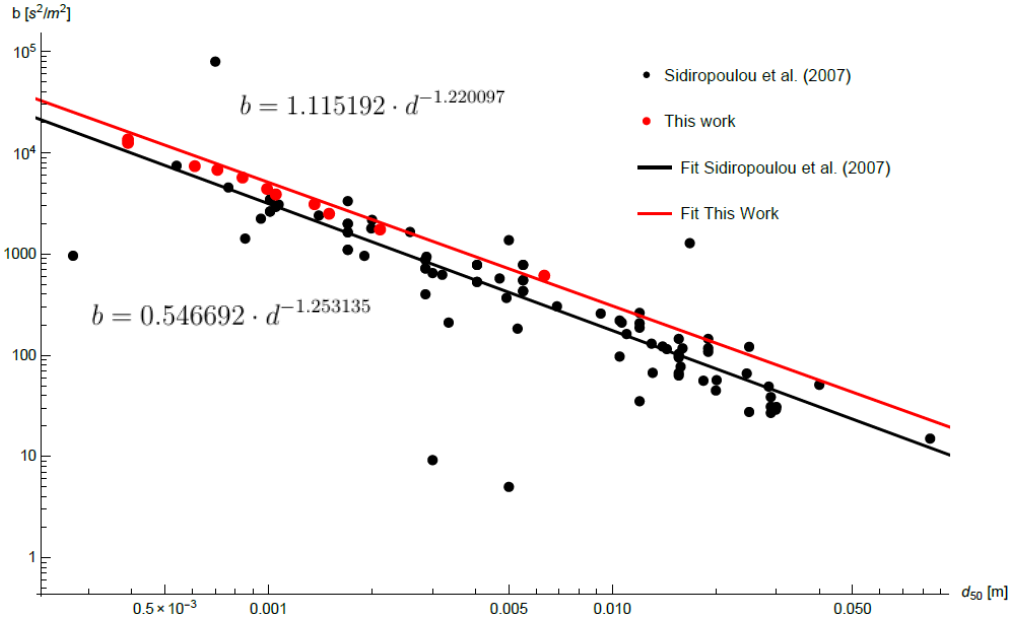

Figure 15: Forchheimer coefficient b [s^2m^{-2}] versus the median grain size, d_{50} [m]. Data from Sidiropoulou et al. (2007), who summarized various datasets from previous studies, as well as this work's data are given. Power law fits are given for both datasets.

5.2. Effect of the Grain Size Distribution on Non-linear Flow in Porous Media

5.2.1. Fraction of Fine Material

As is evident from the previous chapter, the grain size distribution has a significant effect on non-linear flow in porous media. It appears that the presence of fine material is the dominant factor in determining the flow resistance and hence the steepness of the i-q curve and the value of the coefficients a and b of the Forchheimer fit. In case of porous media U 0.7-1.25, N-U7, N-U8, N-U9, and N-U10, the more fine granular material present in the porous media, the higher the flow resistance, the steeper the i-q curve, and the higher the Forchheimer coefficients a and b (see Figure 8; Tables 7 and 8). Similar trends are seen for the other porous media.

The effect of the shape of the grain size distribution on non-linear flow in porous media has not been touched upon extensively in literature. Keyser et al. (2006), based on an earlier experimental study by Conradie and Keyser (2002), point out that experiments with porous media (coal) with wider grain size distributions result in steeper i-q curves than in case the experiments are performed with porous media with narrow grain size distributions. They obtained these results comparing porous media with the same representative linear parameter, porosity, and particle sphericity. These results are similar to this work's results.

5.2.2. Grain Size Distribution versus Porosity for a Given Compaction

An important question to consider is what causes the steeper i-q relation for wider grain size distributions including an increased amount of fine granular material. Eastwood et al. and Hoffman and Finkers (as cited in Koekemoer and Luckos (2015)), point out that a wide grain size distribution enhances the filling of empty void space in the porous media which reduces the

porosity. According to Koekemoer and Luckos (2015), this result in a steeper i-q curve. The results for the gap-graded porous media are certainly in agreement with these statements. Mott and Eastwood et al. (as cited in Koekemoer and Luckos (2015)), emphasize that in the presence of smaller grain sizes, friction between individual grains in the porous medium increases through enhanced grain surface area for a particular volume of porous medium, which increases the flow resistance. This could be an explanation why the presence of fine material, even when combined with an increase in coarser material, still increases the flow resistance. Mott and Eastwood et al. (as cited in Koekemoer and Luckos, 2015) generally point out that flow resistance increases for decreasing grain size, a statement in agreement with the series of experiments with the reference porous media (see Table 4; Figure A-6).

To determine the effect of the shape of the grain size distribution on non-linear flow in porous media solely, the porosity of the compared porous media should be exactly the same. However, in reality, especially when working with natural porous media, this is not feasible.

5.3. Uncertainty in the Experimental Data

As can be derived from Tables 4, 5, 7, and 9, and from Figure 4 and the figures in Appendix A-4, in case of some porous media, relatively few measurements are taken in the Darcy regime or the Forchheimer regime. For example, no measurements in the Darcy regime are taken in case of porous medium U 5.0-8.0 [mm]. Van Dooren (2015) has pointed out the effect of the amount of measurement in each regime on the Forchheimer coefficients a and b for porous media U 0.2-0.63 [mm], U 0.4-0.8 [mm], and U 0.63-1.0 [mm]. It appeared that excluding measurements can have a significant effect on the Forchheimer coefficients, especially when measurements for the higher gradients are excluded. For future research, it is recommended that the experimental setup is altered such that a wider range of hydraulic gradients can be applied onto the porous medium such that measurements can be made in the Darcy regime also for coarser porous media and also more measurements can be made for the Forchheimer regime in case of the fine porous media (e.g. see results for U 0.2-0.5 [mm]).

5.4. Use of Empirical Relations

5.4.1. Fit of the Empirical Relation on the Data

In case of our experimental data, the expression by Kovács (1981) yields the best fit in case of the fairly uniformly-distributed reference porous media if the median grain size is smaller than approximately 1 [mm]. In case the median grain size exceeds this value, the expression by Macdonald et al. (1979) yields the best fit. In case of the composite porous media, Macdonald et al. (1979) gives the best fit. The relative good fit by Kovács (1981) for the uniformly distributed reference porous media could be due to the fact that Kovács derived his expression using/for homodisperse porous media. For the derivation of the equation by Macdonald et al. non-spherical particles are taken into account (Macdonald et al., 1979; Nemec and Levec, 2005). In their study they also derived another expression, changing Ergun constant B from 1.8 to 4.0 to use in case of the most rough particles. It seems, however, that the expression for smooth particles

gives the best fit on our data (smallest overestimation). The particles used in our research are relatively smooth. Regarding the fit of the other empirical relations, the reader is referred to section 4.3..

5.4.2. Definition of the Length Parameter d

Another major uncertainty stems from the definition of the particle diameter used in the relations. For instance, Ergun's definition of this parameter is based on the volume and surface area of the particle (e.g. as cited in Allen et al., 2013). Within the experimental framework of this research, it was not possible to determine the volume and the surface of the particle, but the median grain size of the grain size distribution was used. In studies with porous media with non-uniform grain sizes, the Sauter diameter is used to obtain a better fit of the empirical relation on the experimental data (e.g. Leva as cited in Keyser et al. (2006); Koekemoer and Luckos, 2015). As in this research no perfectly uniform porous media are used (even the reference porous media are slightly non-uniform), it would have been beneficial to use the Sauter mean for this reason.

5.4.3. Effect of Shape and Roughness of Grains

As pointed out by Allen et al. (2013) and many others, there are many factors influencing the flow resistance such as the exact arrangement of grains in the porous medium and the shape and roughness of the particles. Other studies point out that also the sphericity of the particles should be taken into account (e.g. Chhabra and Scrinivas, 1991). Allen et al. (2013) even recommend not to use Ergun's relation in case of non-spherical grains. They argue that, in case of porous media with a non-uniform shape, an empirical relation needs to be determined in advance for the same type of particles and same orientation of particles, before an estimate using this empirical relation is of value. Within the scope of this research it was not possible to account for these factors.

5.5. Future Work

5.5.1. Account for the Effect of Grain Size Distribution

This study has shown that the grain size distribution is of great importance in the determination of the non-linear flow behavior in porous media. It seems that characterization of the non-linear flow based on solely the median grain size (d_{50}) and the porosity is insufficient and also other factors, as the amount of fine material, need to be taken into account.

In order to use empirical relations to describe non-linear flow in porous media, the existing empirical relations will need to be modified to account for non-uniformity of the grain size distribution. The inapplicability of (most of) the existing equations is expresses before in literature. In some works it is argued that the Ergun equation cannot be applied to porous media with a wide grain size distribution (e.g. Keyser et al., 2006). Empirical relations based on, for instance, d_{10} or d_{20}, in addition to d_{50}, would provide the possibility to account for some of the non-uniformity in the empirical relation.

5.5.2. FHVI and Non-linear Flow Behavior

One of the goals in this research is to obtain information on non-linear flow behavior as a first step to characterize non-linear flow around a FHVI-well. Within this research, a large database is created describing non-linear flow in a variety of porous media in terms of Forchheimer equation coefficients a and b. Also much information is obtained on the macroscopic porous media characteristics influencing non-linear flow. Further numerical modelling using the obtained experimental data is necessary to further explore the scientific base of FHVI.

6. Conclusions

In this study, non-linear Forchheimer flow in unconsolidated sandy porous media was investigated by means of column experiments which allowed relating hydraulic head to superficial velocity for a variety of porous media. This research was partially conducted to provide experimental input for a model describing a novel subsurface infiltration method, FHVI, and partially to add experimental data to the existing literature on non-linear flow in porous media and to investigate the effect of the grain size distribution on non-linear flow. The result of this research is an extensive database on non-linear flow experiments for a variety of uniformly-graded reference porous media as well as more well-graded or gap-graded composite porous media.

First, the fairly uniformly distributed reference porous media were considered. The highest values for Forchheimer coefficients a and b (highest flow resistance) were obtained for the porous medium with the smallest median grain size, U 0.2-0.5 [mm]. The a and b coefficients amounted to $2.2369 \cdot 10^{-2}$ [day m^{-1}] and $1.8249 \cdot 10^{-6}$ [day^2 m^{-2}], respectively. The lowest values for Forchheimer coefficients a and b (lowest flow resistance) were obtained for the porous medium with the largest grain size, U 5.0-8.0 [mm], being equal to $9.268 \cdot 10^{-5}$ [day m^{-1}] and $8.2308 \cdot 10^{-8}$ [day^2 m^{-2}], respectively. It was found that flow resistance increased with decreasing median grain size.

Secondly, the effect of the shape of the grain size distribution on non-linear flow in porous media was analyzed. It appeared that the fraction of fine material present in the porous medium is the most important determinant of the Forchheimer coefficients a and b and therefore of the flow resistance. For a given median grain size (d_{50}), it found that the more well-graded the distribution (higher σ and C_U) the higher the flow resistance. The most significant results were obtained in case of analysis of gap-graded porous media. For gap-graded porous medium N-U3, the Forchheimer coefficients a and b increased with 160.2 [%] and 200.8 [%], respectively, with respect to the fairly uniformly distributed reference porous medium U 0.4-0.8 [mm].

Furthermore, it was investigated if frequently-used empirical relations were adequate in describing non-linear flow in case of this work's experimental results. In case of the reference porous media, the expressions by Kovács (1981) and Macdonald et al (1979) yielded the best fit for porous media with median grain sizes lower than ± 1[mm] and higher than ± 1[mm], respectively. It is recommended that in case of non-uniform grain size distributions, modifications are made of the existing empirical relations to account for the shape of the grain size distribution.

Within the context of FHVI, great insight is obtained on possible non-linear flow behavior around a FHVI-well for a variety of porous media. The next step will be implementing the experimental data into a numerical model.

References

Allen, K. G., Von Backström, T. W., & Kröger, D. G. (2013). Packed bed pressure drop dependence onn particle shape, size distribution, packing arrangement and roughness. *Powder Technology, 246*, 590-600.

Asano, T. (1985). *Artificial Recharge of Groundwater*. Asano, T. (Ed.). Stoncham, MA: Butterworth Publishers.

ASTM International (2006). *Standard Practice for Classification of Soils for Engineering Purposes (Unified Soil Classification System)* (ASTM D2487 – 06). West Conshohocken, PA: ASTM International.

Bağci, Ö, Dukhan, N., & Özdemir, M. (2014). Flow regimes in packed beds of spheres from pre-Darcy to turbulent. *Transport in Porous Media, 104*, 501-520.

Basak, P. (1977a). Non-Darcy flow and its implications to seepage problems. *Journal of Irrigation and Drainage Engineering (ASCE), 103* (4), 459-473.

Basak, P. (1977b). Non-penetrating well in a semi-infinite medium with non-linear flow. *Journal of Hydrology, 33*, 375-382.

Bear, J. (1988). *Dynamics of fluids in porous media*. Mineola, NY: Dover Publications, Inc. (Original work published in 1972).

Bordier, C., & Zimmer, D. (2000). Drainage equations and non-Darcian modelling in coarse porous media or geosynthetic materials. *Journal of Hydrology, 228*, 174-187.

Brusseau, M. L., Nelson, N. T., Zhang, Z., Blue, J. E., Rohrer, J., & Allen, T. (2007). Source-zone characterization of a chlorinated-solvent contaminated Superfund site in Tucson, AZ. *Journal of Contaminant Hydrology, 90*(1-2), 21-40.

Cao, L., Zhang, Y., & Shi, Y. (2011). Climate change effect on hydrological processes over the Yangtze River basin. *Quaternary International, 244*, 202-210.

Carman, P. C. (1937). Fluid flow through a granular bed. *Transaction of the Institution of Chemical Engineers London, 15*, 150-156.

Cashman, P. M., & Preene, M. (2013). *Groundwater Lowering in Construction* (2nd ed.). Boca Raton, FL: CRC Press.

Chapuis, R. P., & Aubertin, M. (2003). On the use of the Kozeny-Carman equation to predict the hydraulic conductivity of soils. *Canadian Geotechnical Journal, 40*, 616-628.

Chauveteau, G., & Thirriot, C. L. (1967). Régimes d'écoulement en milieu poreux et limite de la loi de Darcy. *La Houille Blanche, 2*, 141-148.

Chen, Z., Lyons, S., & Qin, G. (2001). Derivation of the Forchheimer Law via homogenization. *Transport in Porous Media, 44*, 325-335.

Chhabra, R. P., Comiti, J., & Machač, I. (2001). Flow of non-Newtonian fluid in fixed and fluidised beds. *Chemical Engineering Science, 56*, 1-27.

Conradie, M., & Keyser, M. J. (2002). Pressure drop over coal beds, char beds and full-scale fixed bed sasol-lurgi gasifiers. Presented at coal indaba 2002: *8th coal science and technology conference of the fossil fuel foundation, Secunda, Douth Africa, 15-17 October, 2002.*

Darcy, H. (1856). *Les fontaines publiques de la Ville de Dijon.* Paris: Victor Dalmont. [in French].

Dillon, P., Pavelic, P., Toze, S., Rinck-Pfeiffer, S., Martin, R., Knapton, A., & Pidsley, D. (2006). Role of aquifer storage in water reuse. *Desalinisation, 188*(1-3), 123-134.

Dufour, A., Ouartassi, B., Bounaceur, R., & Zoulalian, A. (2011). Modelling intra-particle phenomena of biomass pyrolysis. *Chemical Engineering Research and Design, 89*, 2136-2146.

Dukhan, N., Bağci, Ö, & Özdemir, M. (2014). Metal foam hydrodynamics: Flow regimes from pre-Darcy to turbulent. *International Journal of Heat and Mass Transfer, 77*, 114-123.

Dullien, F. A. L. (1979). *Porous Media – Fluid Transport and Pore Structure.* New York, NY: Academic Press, Inc.

Du Plessis, J. P. (1994). Analytical quantification of coefficient in the Ergun equation for fluid friction in packed beds. *Transport in Porous Media, 16*, 189-207.

Hölscher Wasserbau GmbH (2010). *Groundwaterpreservation using DSI©-Infiltration – A new approach for pipeline dewatering campains.* Werder: S. Ebneth.

Ergun, S. (1952). Fluid flow through packed columns. *Chemical Engineering Progress 48*, 89-94.

Ergun, S., & Orning, A. A. (1949). Fluid flow through randomly packed columns and fluidized beds. *Industrial and Engineering Chemistry, 41*(6), 1179-1184.

Fancher, G. H., Lewis, J. A., & Barnes, K. B. (1933). Some physical characteristics of oil sand. *Pennsylvania State College Mineral Industries Experiment Station Bulletin, 12*, 65-167.

Fand, R. M., Kim, B. Y. Y., Lam A. C. C., & Phan, R. T. (1987). Resistance to the flow of fluids through simple and complex porous media whose matrices are composed of randomly packed spheres. *Journal of Fluids Engineering, 109*, 268-273.

Fitts, C. R. (2013). *Groundwater Science* (2nd ed.). Waltham, MA: Academic Press.

Forchheimer, P. H. (1901). Wasserbewegung durch Boden. *Zeitschrift des Vereines Deutscher Ingenieure, 50*, 1781-1788.

Fourar, M., Radilla, G., Lenormand, R., & Moyne, C. (2004). On the non-linear behavior of a laminar single-phase flow through two and three-dimensional porous media. *Advances in Water Resources, 27*, 669-677.

Fugro GeoServices B.V. (2012). *DSI-bemalingsproef Gasunie A/D Ganzenweg 10 te Ravenstein.* Leidschendam: B.I.Y.A. Snacken.

Giorgi, T. (1997). Derivation of the Forchheimer Law via matched asymptotic expansions. *Transport in Porous Media, 29*, 191-206.

Gray, W. G., & O'Neill, K. (1976). On the general equations for flow in porous media and their reduction to Darcy's law. *Water Resources Research, 12* (2), 148-154.

Green, L. Jr., & Duwez, P. (1951). Fluid flow through porous metals. *Journal of Applied Mechanics, 18*(1), 39-45.

Hagen, G. H. L. (1839). Über die Bewegung des Wassers in engen zylindrischen Röhren. *Poggendorffs Annalen, 46*, 423-442. [in German].

Hassanizadeh, S. M., & Gray, W. G. (1987). High velocity flow in porous media. *Transport in Porous Media, 2*, 521-531.

Hlushkou, D., & Tallarek, U. (2006). Transition from creeping via viscous-inertial to turbulent flow in fixed beds. *Journal of Chromatography A, 1126*, 70-85.

Huang, K., Wan, J. W., Chen, C. X., He, L. Q., Mei, W. B., & Zhang, M. Y. (2013). Experimental investigation on water flow in cubic arrays of spheres. *Journal of Hydrology, 492*, 61-68.

Irmay, S. (1964). Modèles théoriques d'écoulement dans les corps poreux. *Bulletin Rilem, 29*, 37-43.

Kanarek, A., & Michail, M. Groundwater recharge with municipal effluent: Dan Region Reclamation Project, Israel. *Water Science and Technology, 34*(11), 227-233.

Keyser, M. J., Conradie, M., Coertzen, M., & Van Dyk, J. C. (2006). Effect of coal particle size distribution on packed bed pressure drop and gas flow distribution. *Fuel, 85*, 1439-1445.

King, F. H. (1899). *Principles and conditions of the movements of ground water*. Washington, D.C.: Washington, D.C.

Koekemoer, A., Luckos, A. (2015). Effect of material type and particle size distribution on pressure drop in packed beds of large particles: Extending the Ergun equation. *Fuel, 158*, 232-238.

Kovács, G. (1981). *Seepage Hydraulics*. Amsterdam: Elsevier Scientific Publishing Company.

Kozeny, J. (1927). Über kapillare Leitung des Wassers im Boden. *Sitzungsberichte Akademies der Wissenschaften Wien, 136*(2a), 271-306

Li, L., Ma, W. (2011). Experimental study on the effective particle diameter of a packed bed with non-spherical particles. *Transport in Porous Media, 89*, 35-48.

Loaiciga, H. A., Valdes, J. B., Vogel, R., Garvey, J., & Schwarz, H. (1996). Global warming and the hydrologic cycle. *Journal of Hydrology, 174*, 83-127.

Macdonald, I. F., El-Sayed, M. S., Mow, K., & Dullien, F. A. L. (1979). Flow through porous media – the Ergun equation revisited. *Industrial & Engineering Chemistry Fundamentals, 18*(3), 199-208.

Marryott, R. A., Dougherty, D. E., & Stollar, R. L. (1993). Optimal groundwater management .2. Application of simulated annealing to a field-scale contamination site. *Water Resources Research, 29*(4), 847-860.

Mathias, S. A., Butler, A. P., & Zhan, H. (2008). Approximate solutions for Forchheimer flow to a well. *Journal of Hydraulic Engineering, 134*(9), 1318-1325.

Mitchell, J. K., Chatoian, J. M., & Carpenter, G. C. (1976). *The influences of sand fabric in liquefaction behavior*. (Report note 76-1, Report No. S-76-5.). Berkeley, CA: US Army Engineer Waterways Experiment Station, University of California.

Moutsopoulos, K. N., Papaspyros, I. N. E., & Tsihrintzis, V. A. (2009). Experimental investigation of inertial flow processes in porous media. *Journal of Hydrology, 374*, 242-254.

Muljadi, B. P., Blunt, M. J., Raeini, A . Q., & Bijeljic, B. (2015). The impact of porous media heterogeneity on non-Darcy flow behavior from pore-scale simulation. *Advances in Water Resources*, doi: 10.1016/j.advwatres.2015.05.019

Nemec, D., & Levec, J. (2005). Flow through packed bed reactors: 1. Single-phase flow. *Chemical Engineering Science, 60*, 6947-6957.

Neuman, S. P. (1977). Theoretical derivation of Darcy's law. *Acta Mechanica, 25*, 153-170.

Nield, D. A., & Bejan, A. (2013). *Convection in Porous Media* (4th ed.). New York, NY: Springer.

Oude Essink, G. H. P. (2001a). Salt water intrusion in a three-dimensional groundwater system in The Netherlands: a numerical study. *Transport in Porous Media, 43*, 137-158.

Oude Essink, G. H. P. (2001b). Improving fresh groundwater supply – problems and solutions. *Ocean & Coastal Management, 44*, 429-449.

Ozahi, E., Gundogdu, M. Y., Carpinlioglu, M. Ö. (2008). A modification on Ergun's correlation for use in cylindrical packed beds with non-spherical particles. *Advanced Powder Technology, 19*, 369-381.

Palmer, C. D., Blowes, D. W., Frind, E. O., & Molson, J. W. (1992). Thermal-energy storage in an unconfined aquifer .1. Field injection experiment. *Water Resources Research 28*(10), 2845-2856.

Patel, A. S., & Shah, D. L. (2009). *Water Management – Conservation, Harvesting and Artificial Recharge*. New Delhi: New Age international (P) Ltd., Publishers.

Poesen, J. W. A., & Hooke, J. M. (1997). Erosion, flooding and channel management in Mediterranean environments of southern Europe. *Progress in Physical Geography 21*(2), 157-199.

Poiseuille, J. L. M. (1840). Récherches expérimentales sur le mouvement des liquides dans les tubes de très petits diamètres. Compte Rendu, 11, 961-967, 1041-1048. [in French].

Powers, J. P., Corwin, A. B. Schmall, P. C., & Kaeck, W. E. (2007). *Construction dewatering and groundwater control* (3rd ed.). Hoboken, NJ: John Wiley & Sons, Inc.

Rietdijk, J., Schenkeveld, F. M., Schaminée, P. E. L., & Bezuijen, A. (2010). The drizzle method for sand sample preparation. In S. Springman, J. Laue, & L. Seward (Eds.), Physical Modelling in Geotechnics, Two Volume Set: Proceedings of the 7th International Conference on Physical Modelling in Geotechnics (ICPMG 2010), 28th June-1st July, Zurich, Switzerland. (Vol. 1). Boca Raton, FL: CRC Group.

Sabiri, N.- E., & Comiti, J. (1995). Pressure drop in non-Newtonian purely viscous fluid flow through porous media. *Chemical Engineering Science, 50*(7), 1193-1201.

Santos, J. E., & Sheen, D. (2008). Derivation of a Darcy's law for a porous medium composed of two solid phases saturated by a single-phase fluid: A homogenization approach. *Transport in Porous Media, 74*, 349-368.

Scanlon, B. R., Faunt, C. C., Longuevergne, L., Reedy, R. C., Alley, W. M., McGuire, V. L., & McMahon, P. B. (2012). Groundwater depletion and sustainability of irrigation in the US High Plains and Central Valley. *Proceedings of the National Academy of Sciences of the United States of America, 109*(24), 9320-9325.

Schneebeli, G. (1955). Expériences sur la limite de validité de la loi de Darcy et l'apparition de la turbulence dans un écoulement de filtration. *La Houille Blanche, 141*, 141-149. [in French].

Sedghi-Asl, M., Rahimi, H., & Salehi, R. (2014). Non-Darcy flow of water through a packed column test. *Transport in Porous Media, 101*, 215-227.

Seguin, D., Montillet, A., & Comiti, J. (1998). Experimental characterization of flow regimes in various porous media – I: Limit of laminar fow regime. *Chemical Engineering Science, 53*(21), 3751-3761.

Sidiropoulou, M. G., Moutsopoulos, K. N., & Tsihrintzis, V. A. (2007). Determination of Forchheimer equation coefficients a and b. *Hydrological Processes, 21*, 534-554.

Simmons, G. T. (2008). Henry Darcy (1809-1858): Immortalised by his scientific legacy. *Hydrogeology Journal, 16*, 1023-1038.

Singh, P. P., Cushman, J. H., & Maier, D. E. (2003). Multiscale fluid transport theory for swelling biopolymers. *Chemical Engineering Science, 58*. 2409-2419.

Skjetne, E., & Auriault, J. L. (1999). New insights on steady, non-linear flow in porous media. *European Journal of Mechanics – B/Fluids, 18*(1), 131-145.

Soni, J. P., Islam, N., & Basak, P. (1978). An experimental evaluation of non-darcian flow in porous media. *Journal of Hydrology, 38*, 231-241.

Stichting Technologie en Wetenschap (STW) (April, 2014). *Extreme neerslag vereist een snelle injectie van zoet water*. Retrieved from Stichting Technologie en Wetenschap: http://stwstichtingvoo.m5.mailplus.nl/archief/mailing-325422.html

Theo van Velzen BV (2013). *ISA Amsteveel DSI© pompproef*. Alkmaar: D. Van Gaalen.

Tipler, P. A., & Mosca, G. (2008). *Physics for Scientists and Engineers* (6th ed.). New York, NY: W. H. Freeman and Company.

Tsanis, I. K., Koutroulis, A. G., Daliakopoulos, I. N., & Jacob, D. (2011). Severe climate-induced water shortage and extremes in Crete. *Climate Change, 106*, 667-677.

Vandenbohede, A., Hermans, T., Nguyen, F., & Lebbe, L. (2011). Shallow heat injection and storage experiment: Heat transport simulation and sensitivity analysis. *Journal of Hydrology*, doi:10.1016/j.jhydrol.2011.08.024.

Van Dooren, T.C.G.W. (2015). *Investigation of various sand column preparation procedures for non-Darcy groundwater flow experiments* (Unpublished bachelor's thesis). Utrecht University, Utrecht, The Netherlands.

Vanoni, V. (2006). *Sedimentation Engineering: Classic Edition – Appendix II. Density and viscosity of water 0°C-40°C*, 407-409.

Wada, Y., Van Beek, L. P. H., Van Kempen, C. M., Reckman, J. W. T. M., Vasak, S., & Bierkens, F. P. (2010). Global depletion of groundwater resources. *Geophysical Research Letter, 37*(20), L20402, 1-5.

Wahyudi, I., Montillet, A., & Khalifa, A. O. A. (2002). Darcy and post-Darcy flows within different sands. *Journal of Hydraulic Research, 40*(2), 519-525.

Walton, W. C. (2007). *Aquifer Test Modeling.* Boca Raton, FL: CRC Press.

Ward, J. C. (1964). Turbulent flow in porous media. *Journal of Hydraulic Division, ASCE, 90*(5), 1-12.

Werner, A. D., Bakker, M., Post, V. E. A., Vandenbohede, A., Lu, C., Ataie-Ashtiani, B., Simmons, C. T., et al. (2013). Seawater intrusion processes, investigation and management: Recent advances and future challenges. *Advances in Water Resources, 51*, 3-26.

Whitaker, S. (1986). Flow in porous media I: A theoretical derivation of Darcy's law. *Transport in Porous Media, 1*, 3-25.

Wilby, R. L., & Keenan, R. (2012). Adapting to flood risk under climate change. *Progress in Physical Geography, 36*(3), 348-378.

Wu, Y.-S. (2005). Non-Darcy flow behavior near high-flux injection wells in porous and fractured formations. In C.-F. Tsang & J. A. Apps. *Underground Injection Science and Technology* (221-242). Amsterdam: Elsevier B.V..

Yu, Z., & Lerche, I. (1995). Three-phase fluid migration with solubilities in a two- dimensional basin simulation model. *Marine and Petroleum Geology, 12*, 3-16.

Zeng, B., Cheng, L., & Li, C. (2012). Low velocity non-linear flow in ultra-low permeability reservoir. *Journal of Petroleum Science and Engineering, 80*, 1-6.

Zeng, Z., & Grigg, R. (2006). A criterion for non-Darcy flow in porous media. *Transport in Porous Media, 63*, 57-69.

Zenner, M. A. (2009). Near-well nonlinear flow identified by various displacement well response testing. *Groundwater, 47*(4), 526-535.

Appendix

Appendix A.1 – Various aspects/details of the experimental setup

In this Appendix section, images and additional information on the experimental setup are provided. Figure A-1 shows the column in which the porous media are packed. As one can see, a system of valves and tubes allows for the determination of the pressure at 0.1275 [m], 0.2550 [m] and 0.3825 [m] of the porous medium, measured with respect to the left side of the porous medium. These pressure measurements can be taken in addition to the regular pressure measurement left of the porous medium. Note that the latter pressure is used for the analysis and the three pressure measurements of the course of the porous medium are not considered within the scope of this work. On the left pressure 'outlet', a pressure transmitter can be mounted, which (via the valves/a degasser/tubing) can measure the pressure at the three locations over the extent of the porous medium and the pressure left of the porous medium.

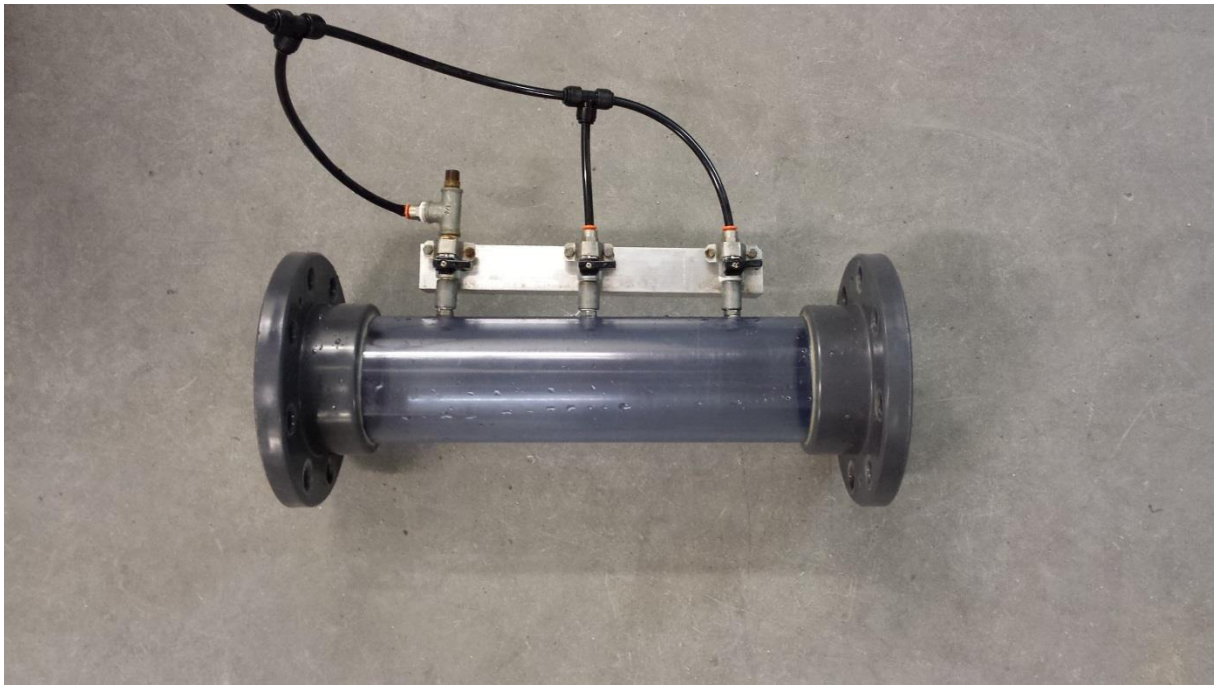

Figure A-1: Column holding the porous media.

The entire sealing system of the column holding the porous medium is shown in Figure A-1. Part D is the fibrous polyester filter (Enkadrain B10), which is a combination of two single fibrous sheets, attached with polypropylene wiring. Part C denotes a metal filter that keeps the fibrous filter in place. Part B is an air-/water-tight rubber band. Part A is the most outer segment of the column which can be attached to the rest of the column with two screws and holds parts B, C, D in place. Over the entire process, parts A, B, C, and D are mounted onto both ends of the column.

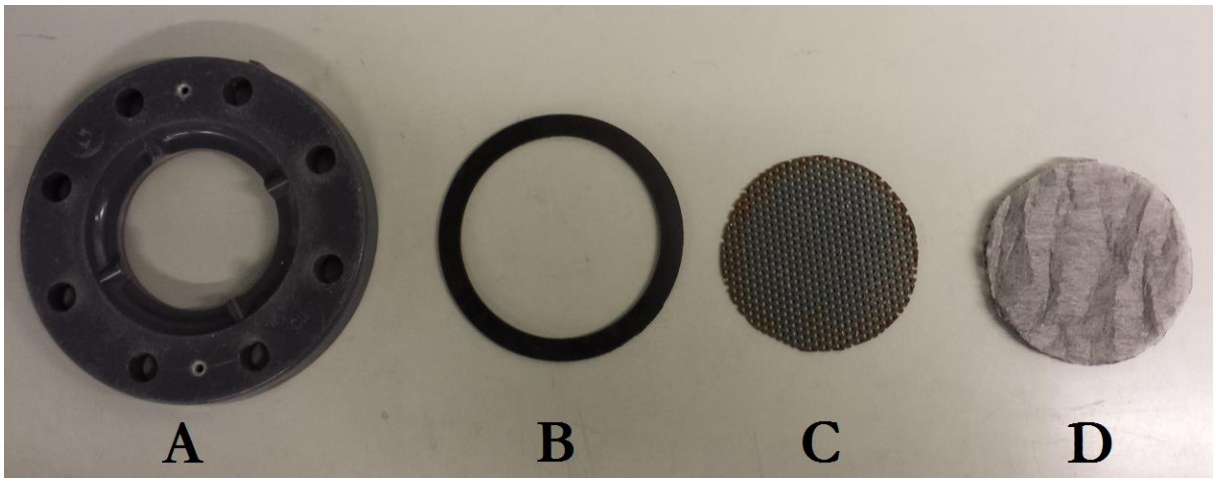

Figure A-2: Sealing system of the column holding the porous media. Parts A, B, C, and D are installed onto both outer ends of the column in the following order: D, C, B, A.

The porous medium is packed under saturated conditions. To ensure full saturation, the column is packed under water in a large reservoir (see Figure A-3). Also, the column is mounted to the rest of the setup under water in this reservoir to avoid any contact with air.

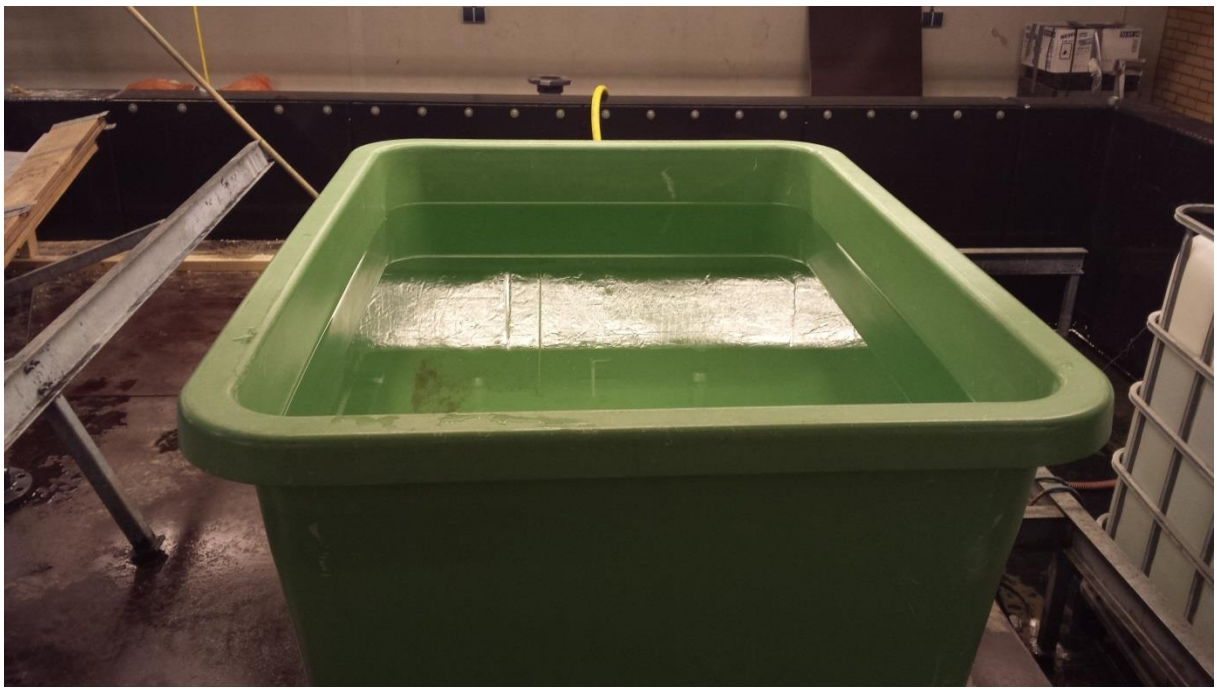

Figure A-3: Reservoir in which the porous medium is packed and installed into the setup.

Figure A-4 offers a view of the reservoir that is part of the experimental setup.

Figure A-4: Reservoir which is parts of the setup. Supplies water to the rest of the setup and functions as water catchment for the water leaving the setup.

Appendix A.2 – Grain size distributions of the porous media

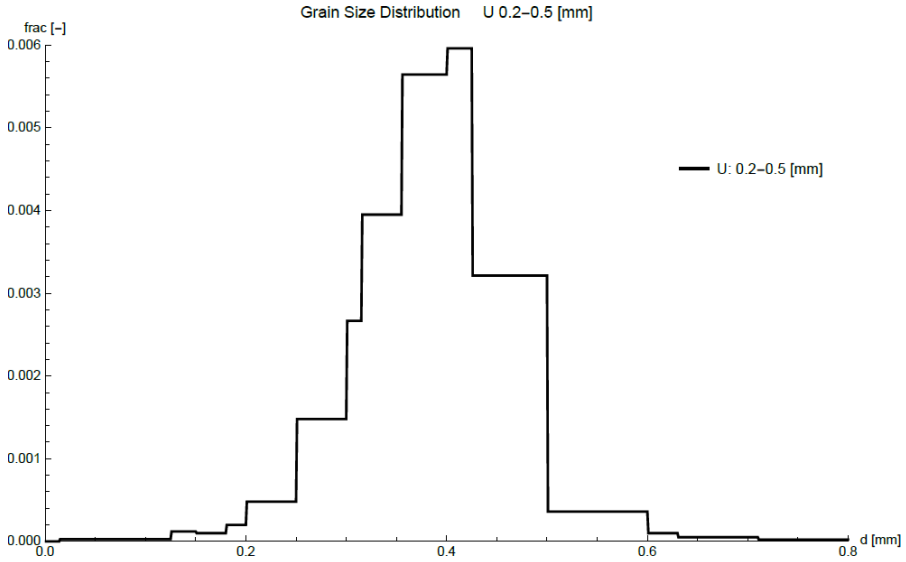

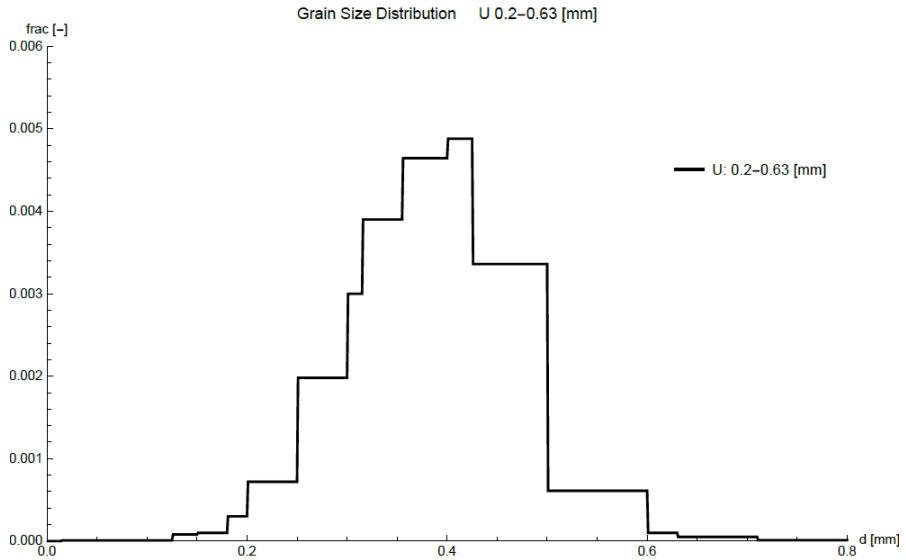

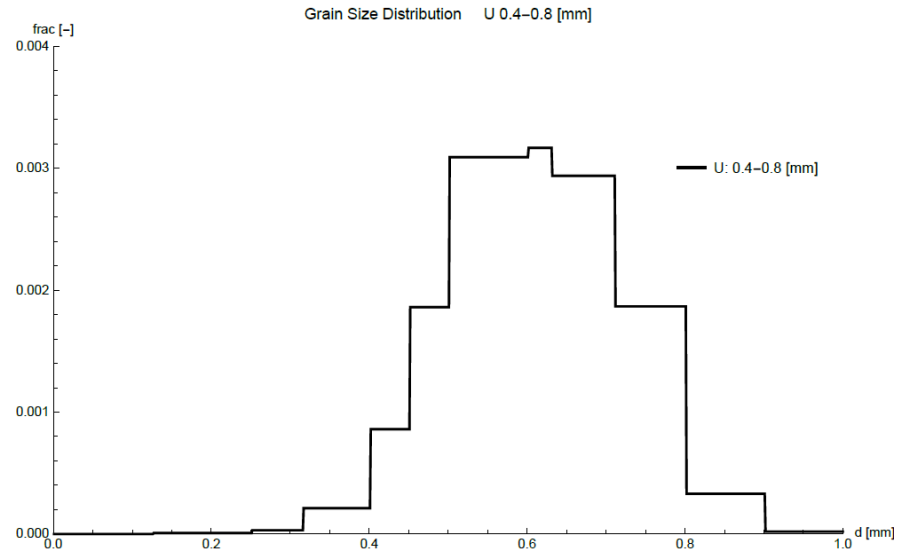

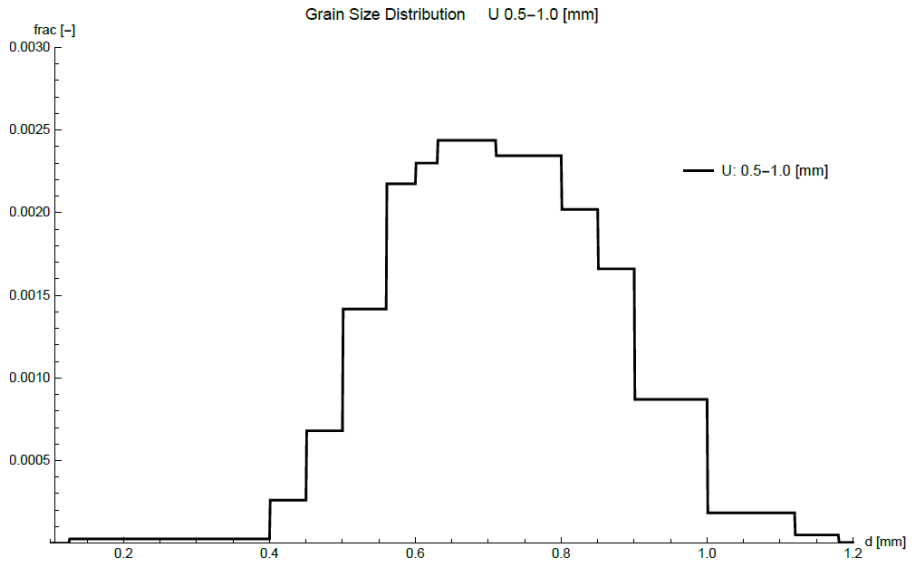
Grain Size Distribution U 0.5–1.0 [mm]
frac [–]
0.0030
0.0025
0.0020
0.0015
0.0010
0.0005
U: 0.5–1.0 [mm]
0.2
0.4
0.6
0.8
1.0
1.2
d [mm]

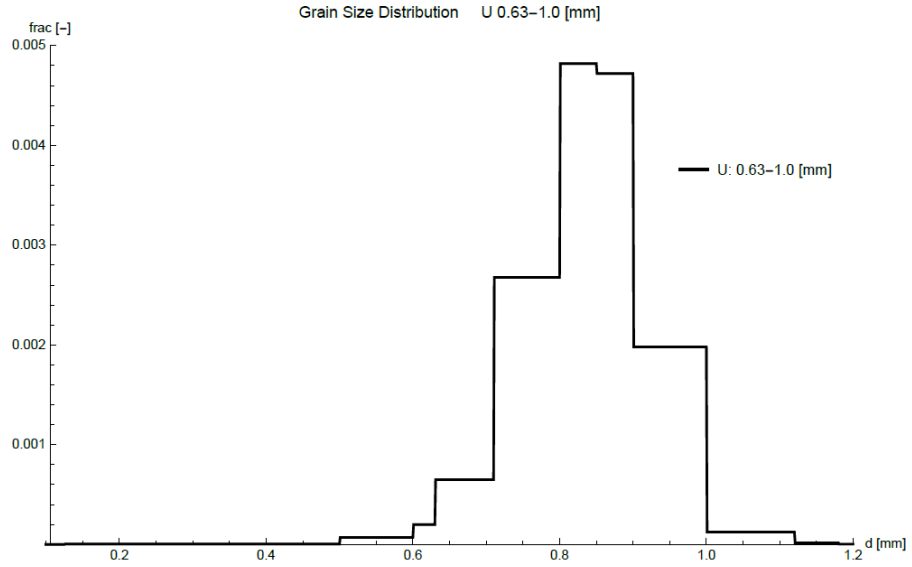
Grain Size Distribution U 0.63–1.0 [mm]
frac [–]
0.005
0.004
0.003
0.002
0.001
U: 0.63–1.0 [mm]
0.2
0.4
0.6
0.8
1.0
1.2
d [mm]

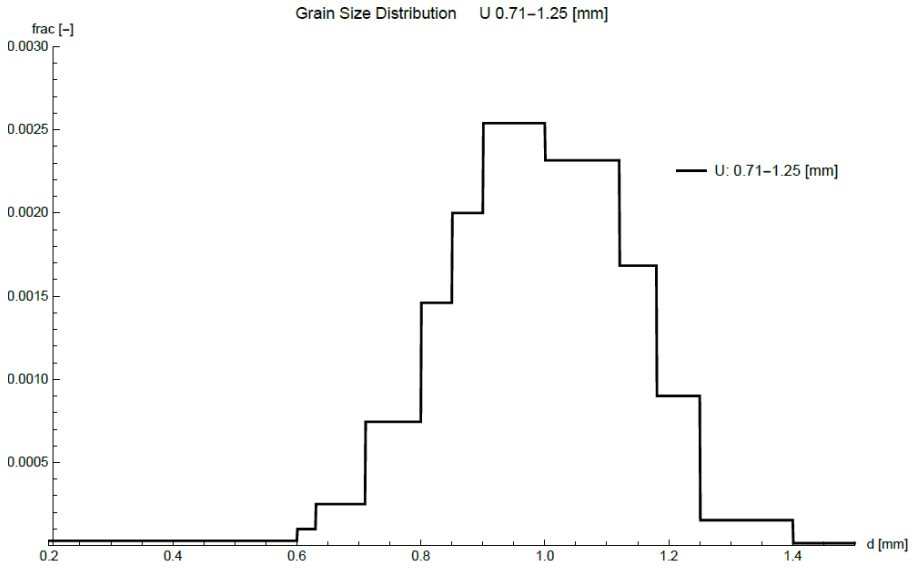
Grain Size Distribution U 0.71–1.25 [mm]
frac [–]
0.0030
0.0025
0.0020
0.0015
0.0010
0.0005
U: 0.71–1.25 [mm]
0.2
0.4
0.6
0.8
1.0
1.2
1.4
d [mm]

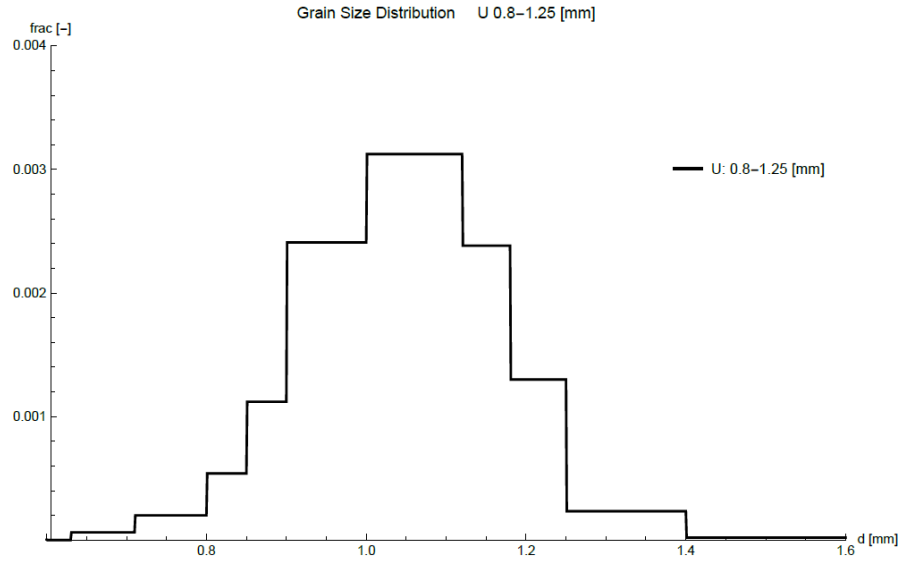
Grain Size Distribution U 0.8–1.25 [mm]
frac [–]
0.004
0.003
0.002
0.001
U: 0.8–1.25 [mm]
0.8
1.0
1.2
1.4
1.6
d [mm]

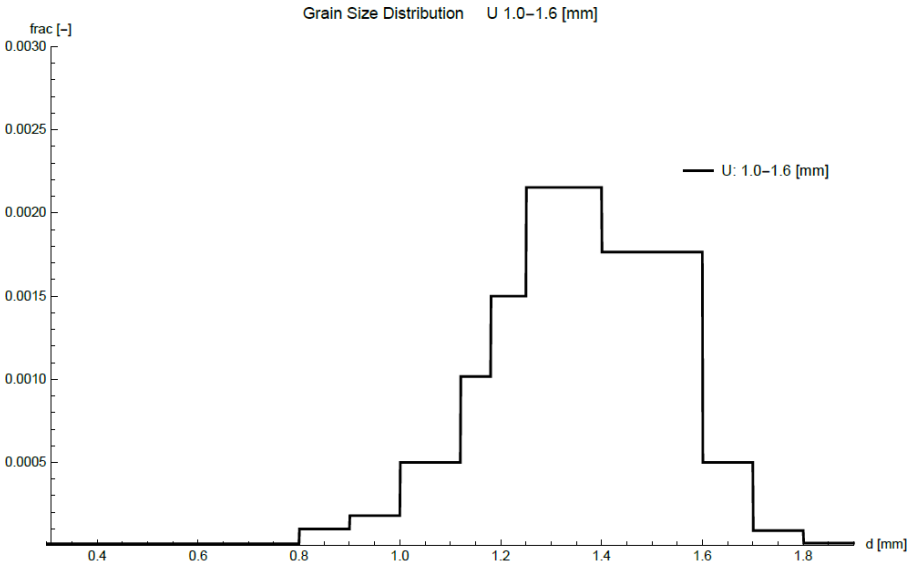
Grain Size Distribution U 1.0–1.6 [mm]
frac [–]
0.0030
0.0025
0.0020
0.0015
0.0010
0.0005
U: 1.0–1.6 [mm]
0.4
0.6
0.8
1.0
1.2
1.4
1.6
1.8
d [mm]

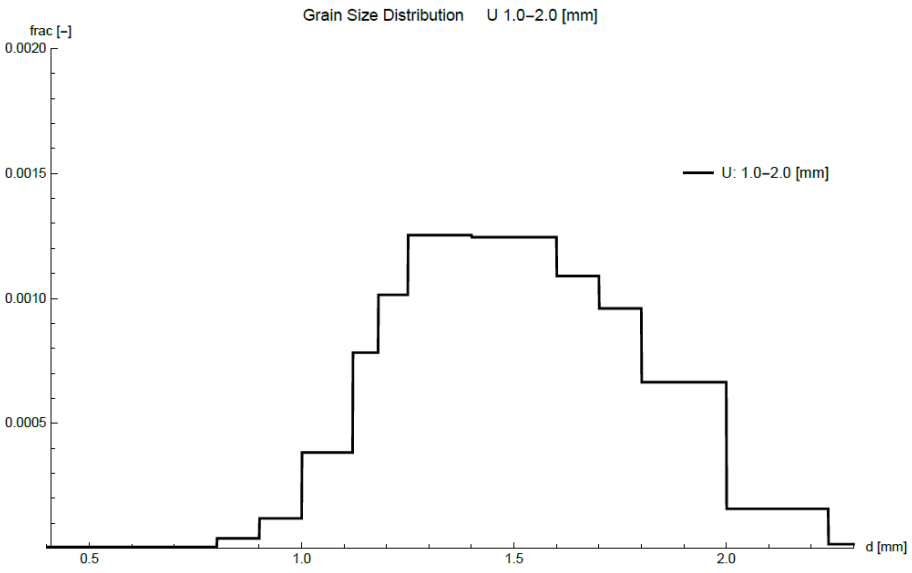
Grain Size Distribution U 1.0–2.0 [mm]
frac [–]
0.0020
0.0015
0.0010
0.0005
U: 1.0–2.0 [mm]
0.5
1.0
1.5
2.0
d [mm]

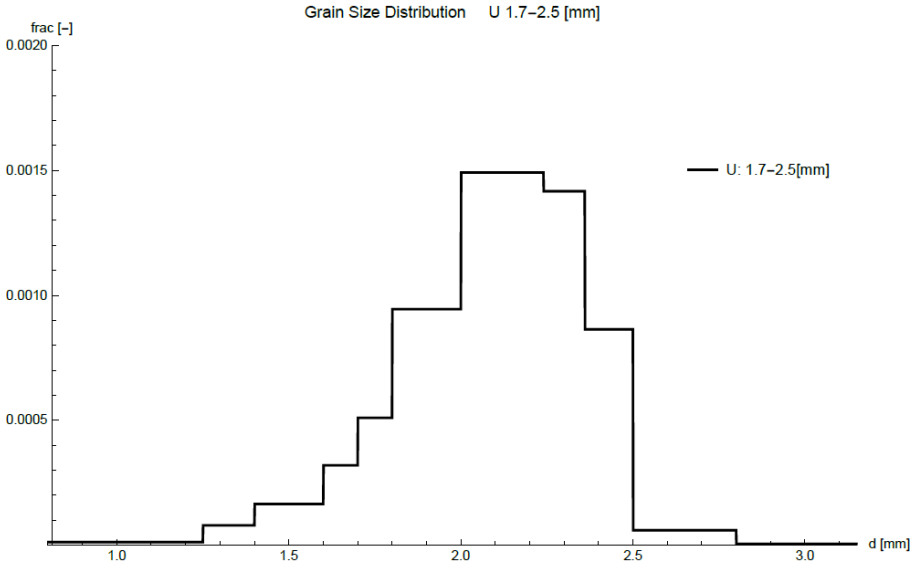
Grain Size Distribution U 1.7–2.5 [mm]
frac [–]
0.0020
0.0015
0.0010
0.0005
U: 1.7–2.5[mm]
1.0
1.5
2.0
2.5
3.0
d [mm]

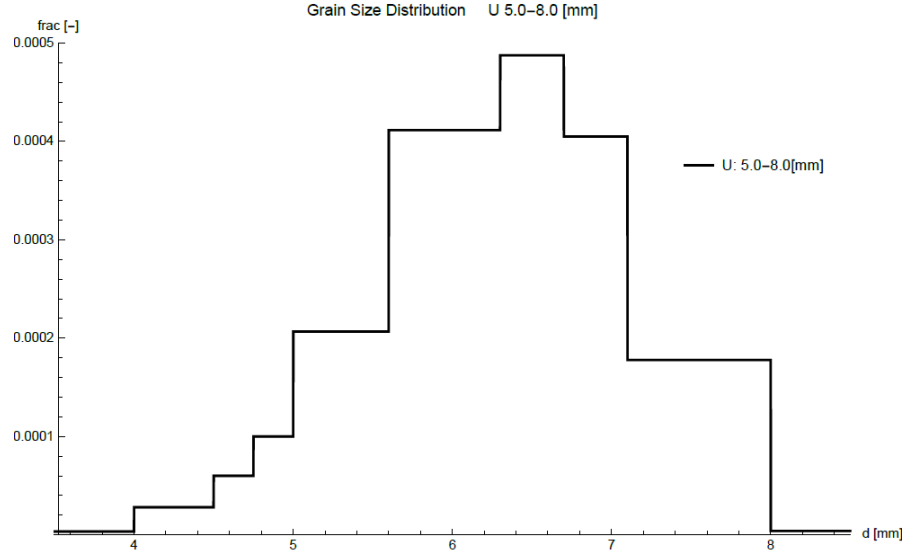
Grain Size Distribution U 5.0–8.0 [mm]
frac [–]
0.0005
0.0004
0.0003
0.0002
0.0001
U: 5.0–8.0[mm]
4
5
6
7
8
d [mm]

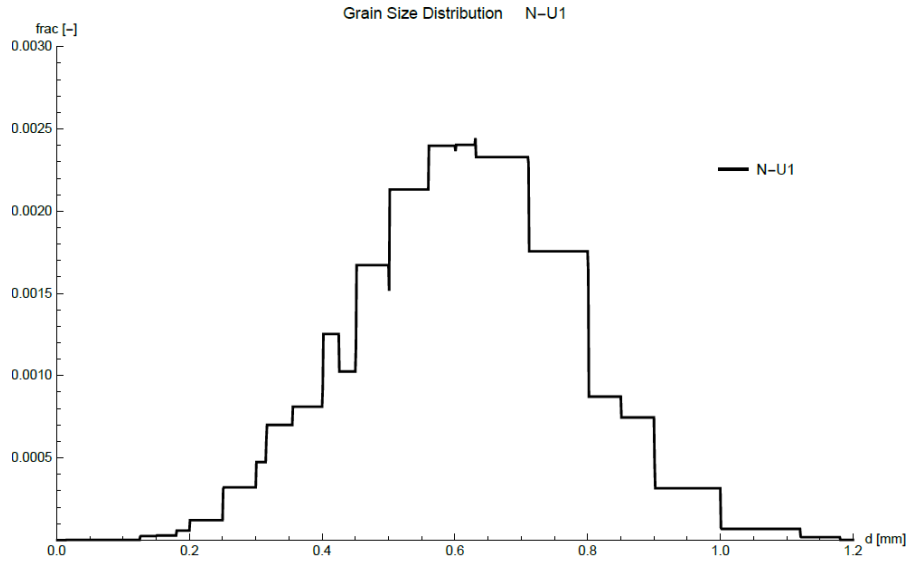
Grain Size Distribution N–U1
frac [–]
0.0030
0.0025
0.0020
0.0015
0.0010
0.0005
N–U1
0.0
0.2
0.4
0.6
0.8
1.0
1.2
d [mm]

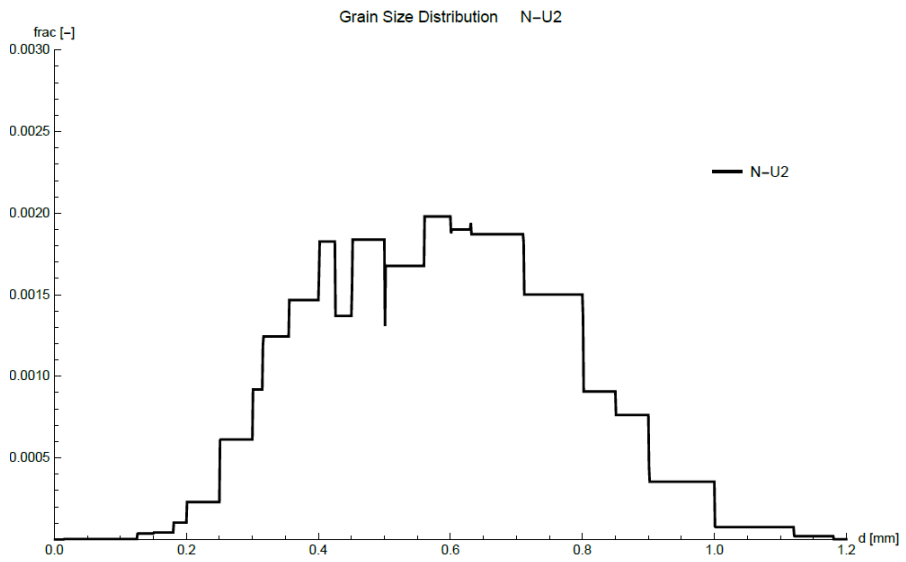
Grain Size Distribution N–U2
frac [–]
0.0030
0.0025
0.0020
0.0015
0.0010
0.0005
N–U2
0.0
0.2
0.4
0.6
0.8
1.0
1.2
d [mm]

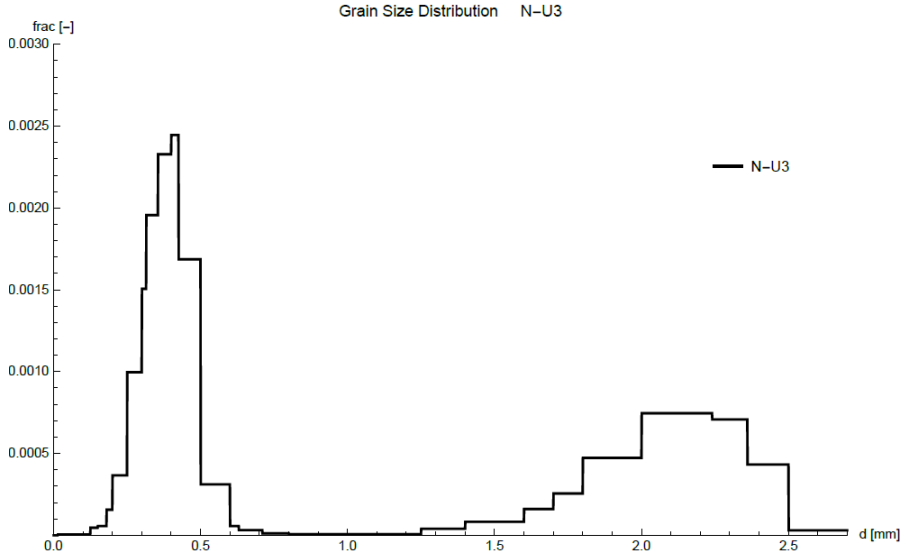
Grain Size Distribution N–U3
frac [–]
0.0030
0.0025
0.0020
0.0015
0.0010
0.0005
N–U3
0.0
0.5
1.0
1.5
2.0
2.5
d [mm]

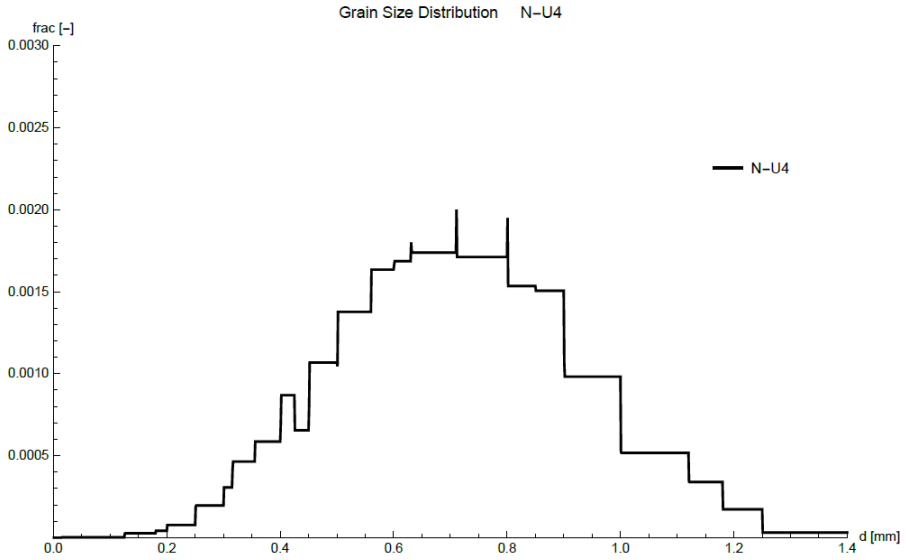
Grain Size Distribution N–U4
frac [–]
0.0030
0.0025
0.0020
0.0015
0.0010
0.0005
N–U4
0.0
0.2
0.4
0.6
0.8
1.0
1.2
1.4
d [mm]

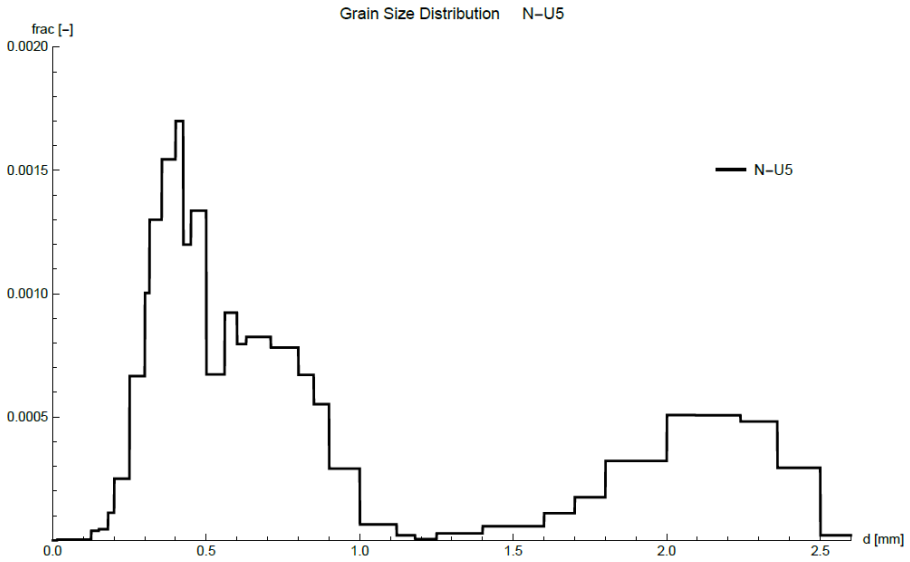
Grain Size Distribution N–U5
frac [–]
0.0020
0.0015
0.0010
0.0005
0.0
0.5
1.0
1.5
2.0
2.5
d [mm]
N–U5

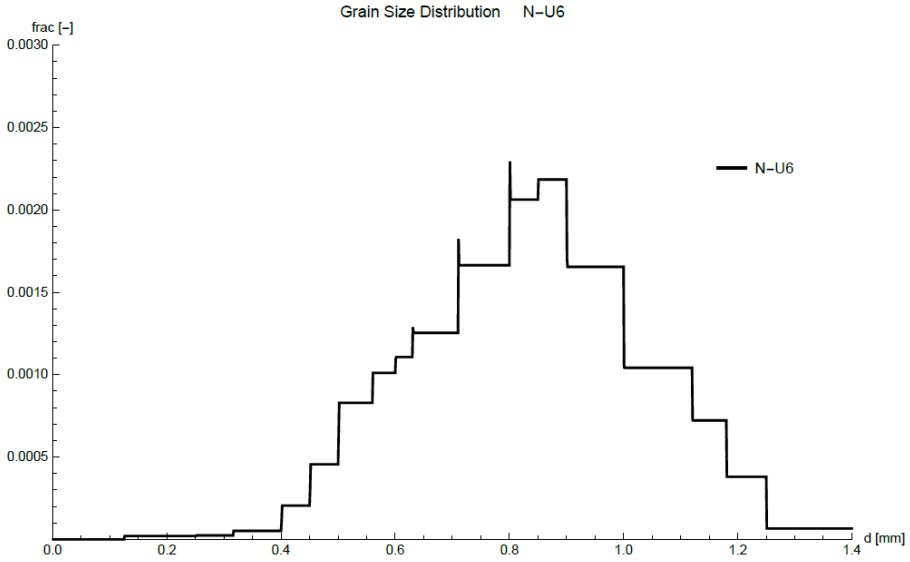
Grain Size Distribution N–U6
frac [–]
0.0030
0.0025
0.0020
0.0015
0.0010
0.0005
0.0
0.2
0.4
0.6
0.8
1.0
1.2
1.4
d [mm]
N–U6

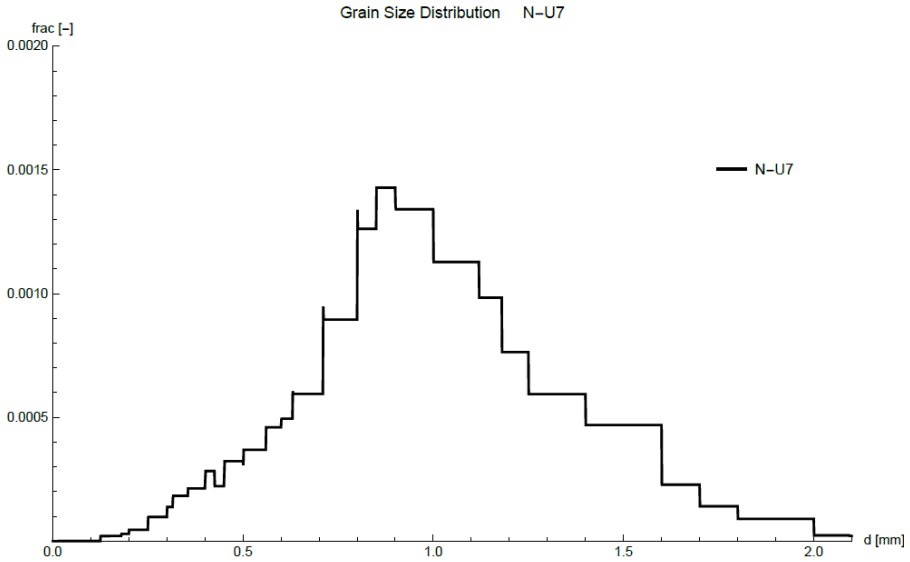
Grain Size Distribution N–U7
frac [–]
0.0020
0.0015
0.0010
0.0005
0.0
0.5
1.0
1.5
2.0
d [mm]
N–U7

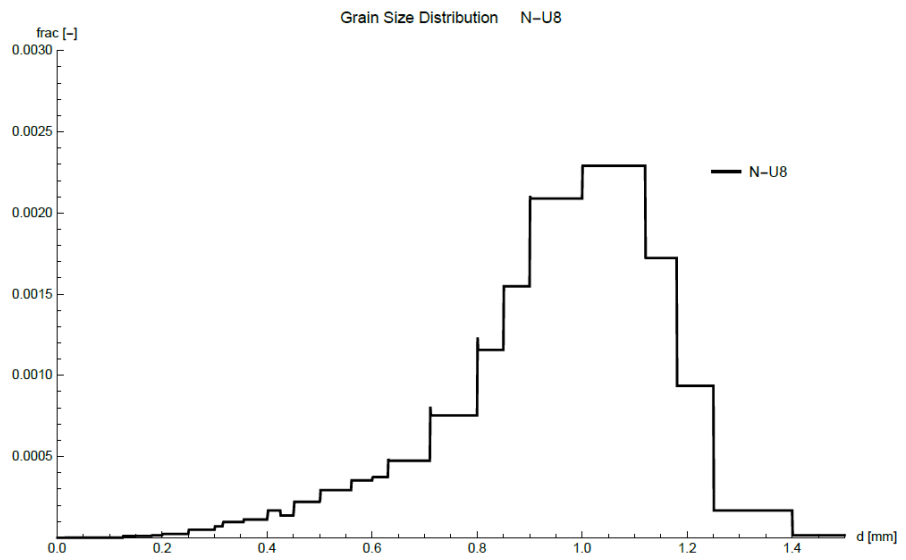
Grain Size Distribution N–U8
frac [–]
0.0030
0.0025
0.0020
0.0015
0.0010
0.0005
0.0
0.2
0.4
0.6
0.8
1.0
1.2
1.4
d [mm]
N–U8

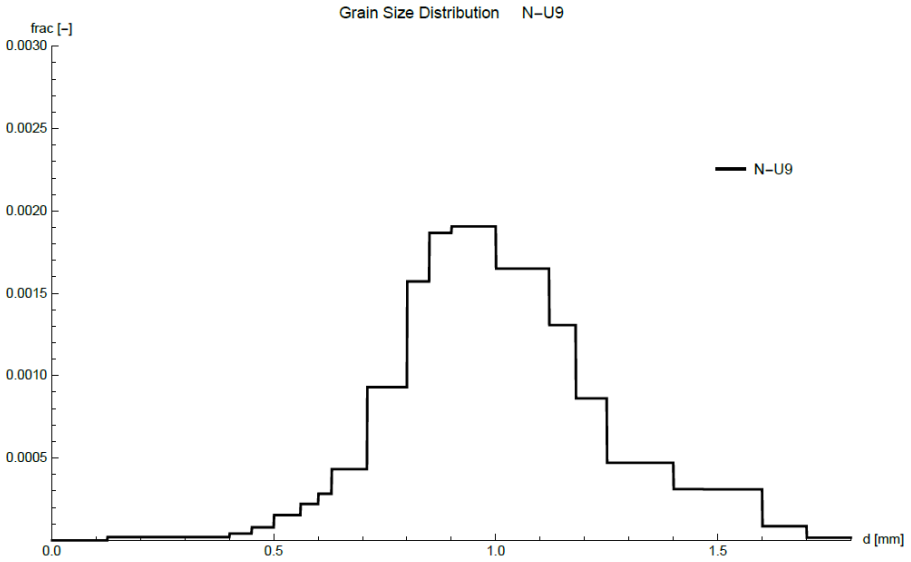
Grain Size Distribution N–U9
frac [–]
0.0030
0.0025
0.0020
0.0015
0.0010
0.0005
0.0
0.5
1.0
1.5
d [mm]
N–U9

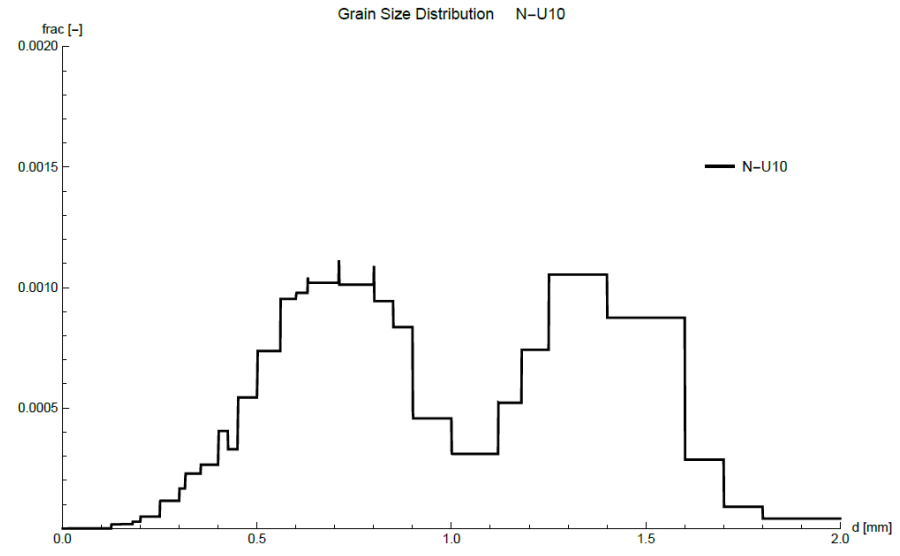
Grain Size Distribution N–U10
frac [–]
0.0020
0.0015
0.0010
0.0005
0.0
0.5
1.0
1.5
2.0
d [mm]
N–U10

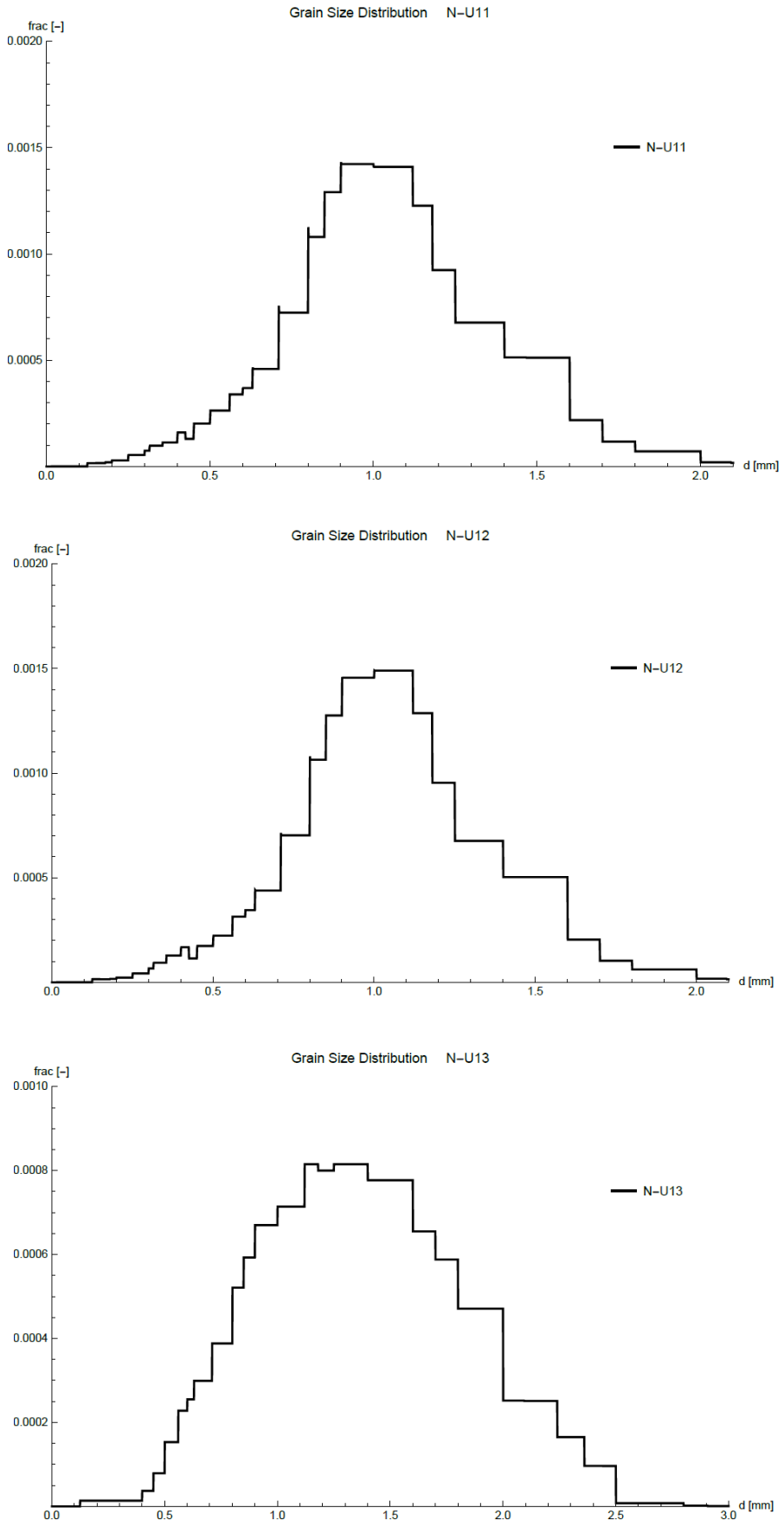

Figure A-5: Grain size distributions for all porous media used in this work.

A.3 – I-q curves for all reference porous media combined in one plot.

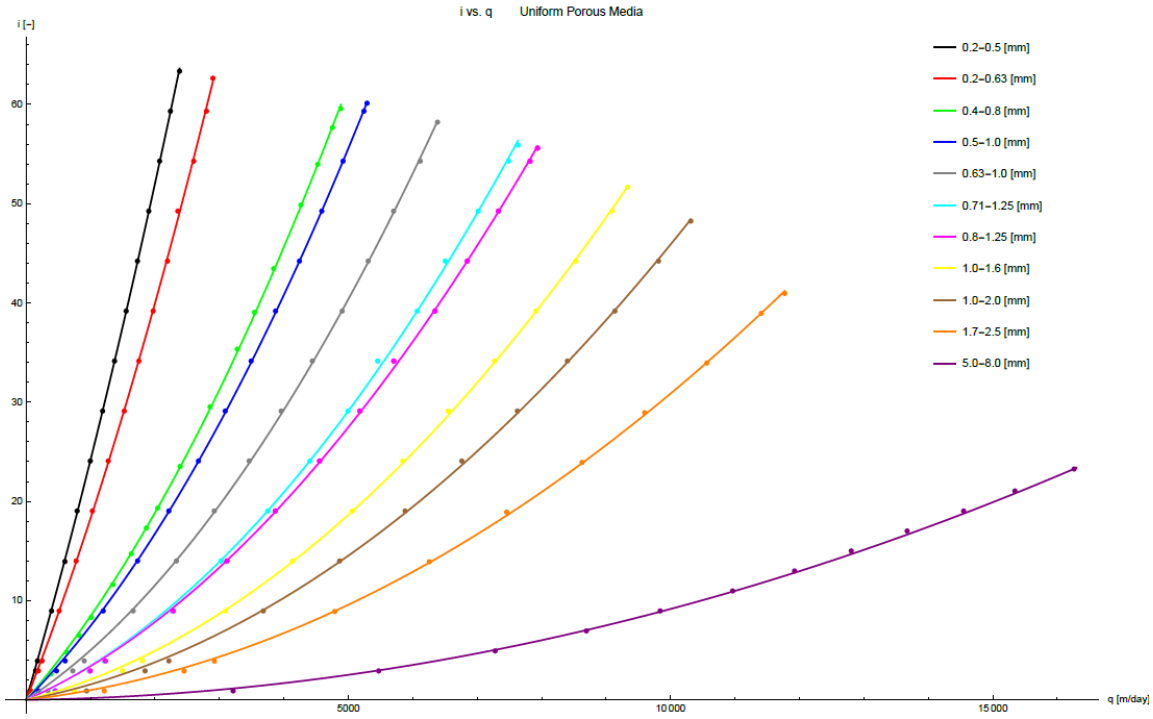

Figure A-6: All i-q relations for the reference porous media. Shown are the experimental data for i-q and the Forchheimer equation for each array of i-q pairs. Forchheimer equation coefficients a and b as well as the goodness of fit are given in Table 4.

Appendix A.4 – I-q curves for the composite porous media N-U1-13

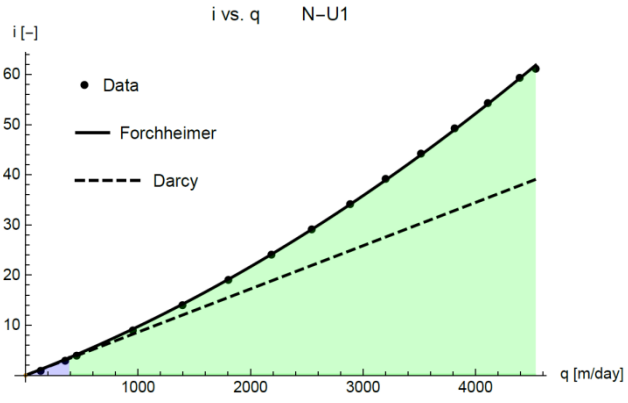

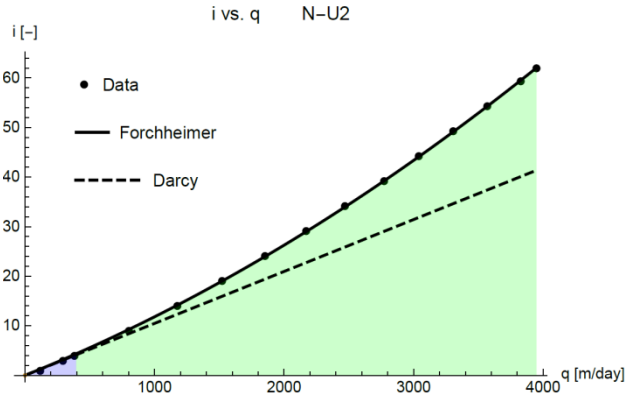

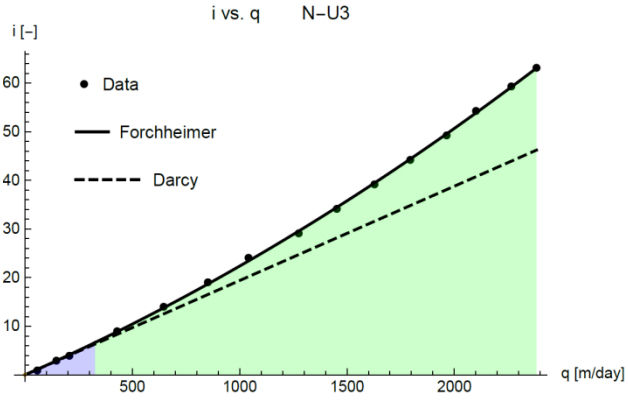

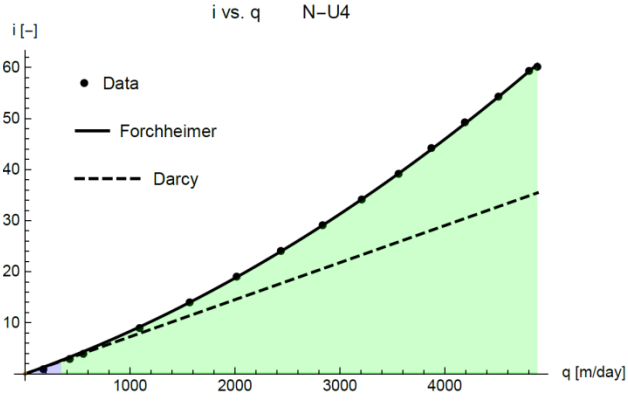

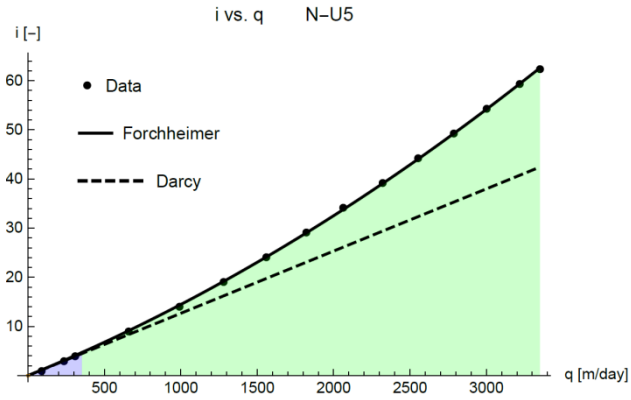

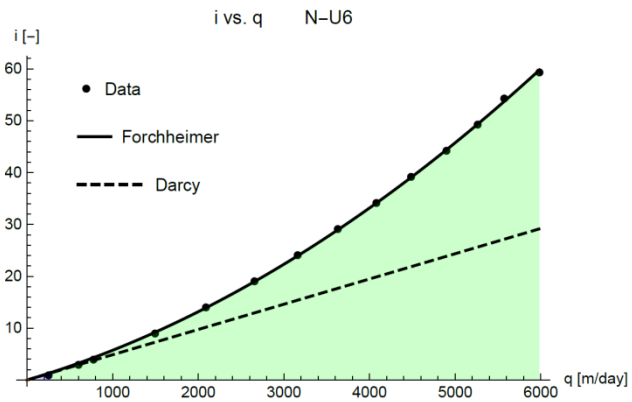

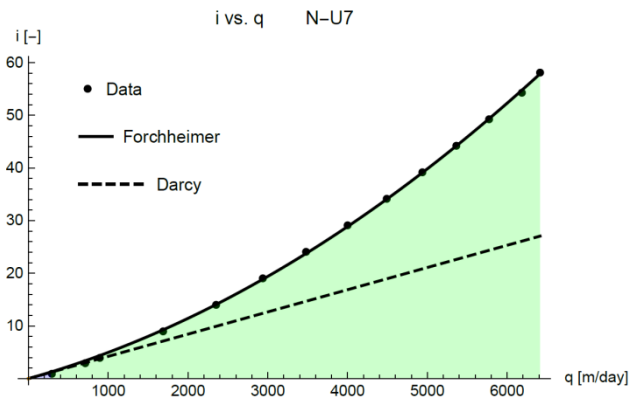

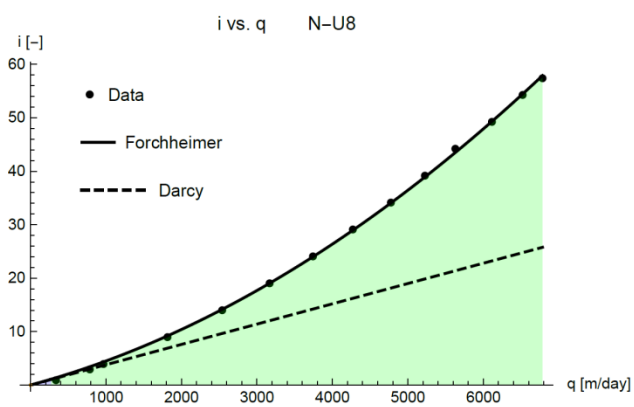

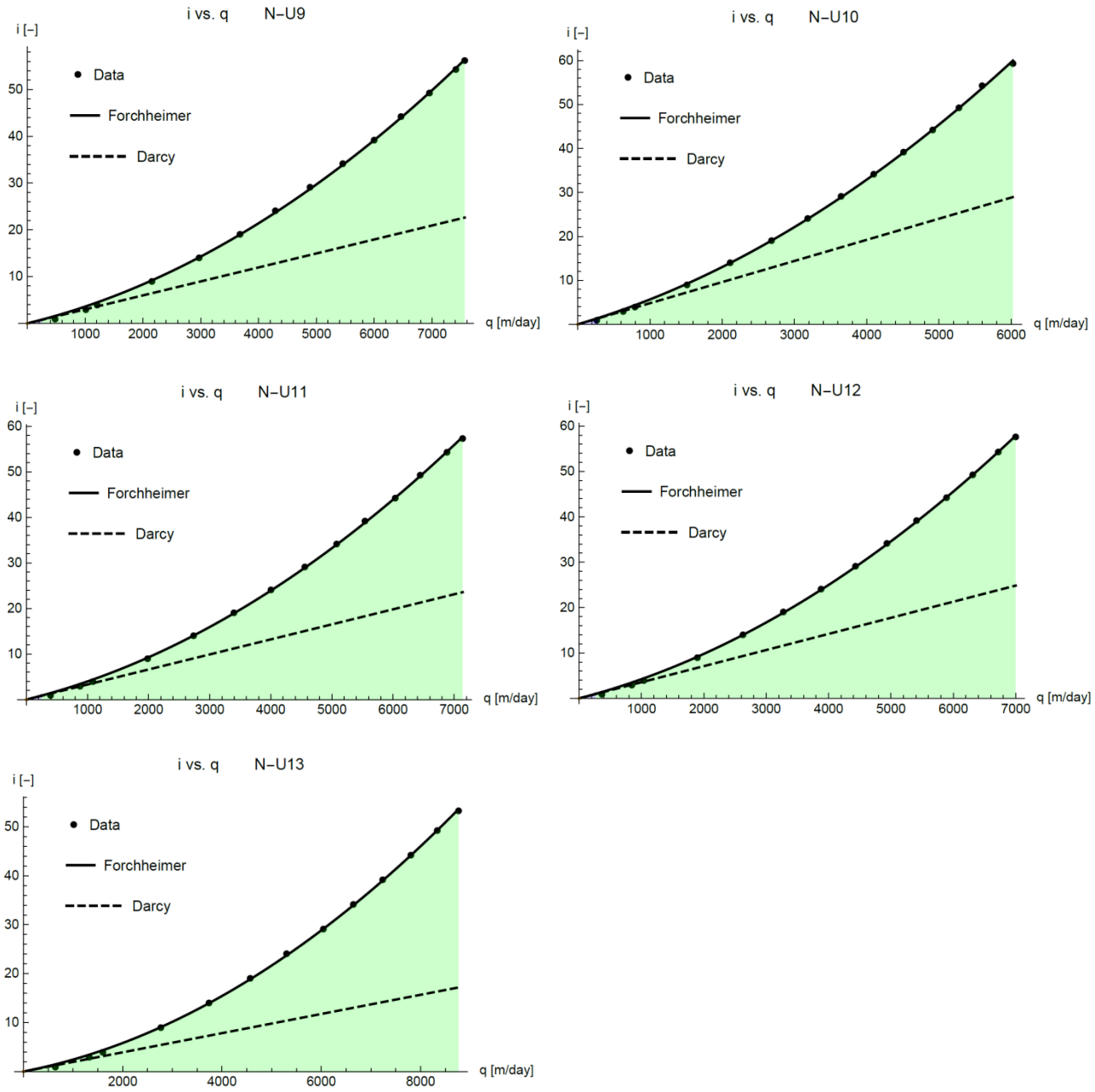

Figure A-7: i-q curves for all composite porous media.

Appendix A.5 – Comparison i-q curves all porous media with the empirical relations

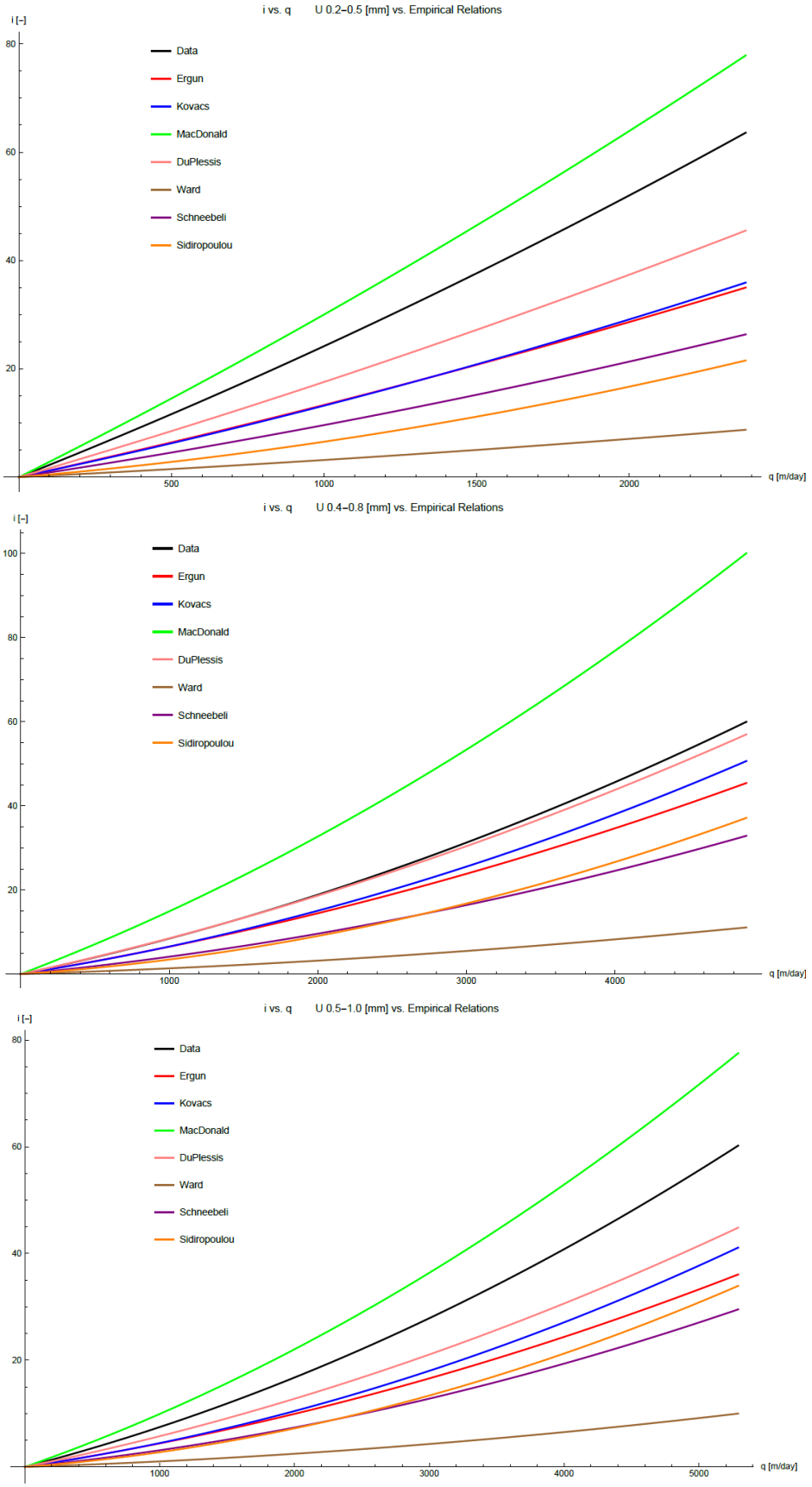

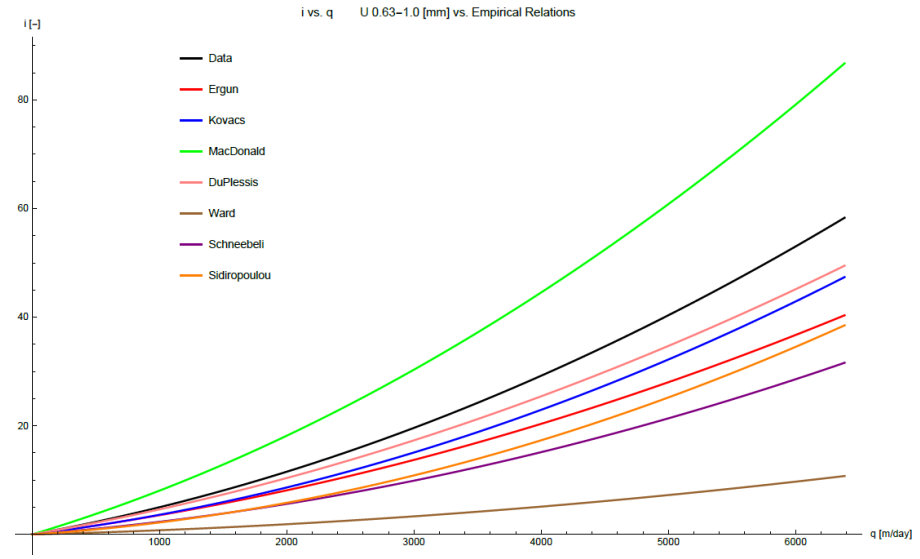
i vs. q U 0.63−1.0 [mm] vs. Empirical Relations
i [−]
Data
Ergun
Kovacs
MacDonald
DuPlessis
Ward
Schneebeli
Sidiropoulou
20
40
60
80
1000
2000
3000
4000
5000
6000
q [m/day]

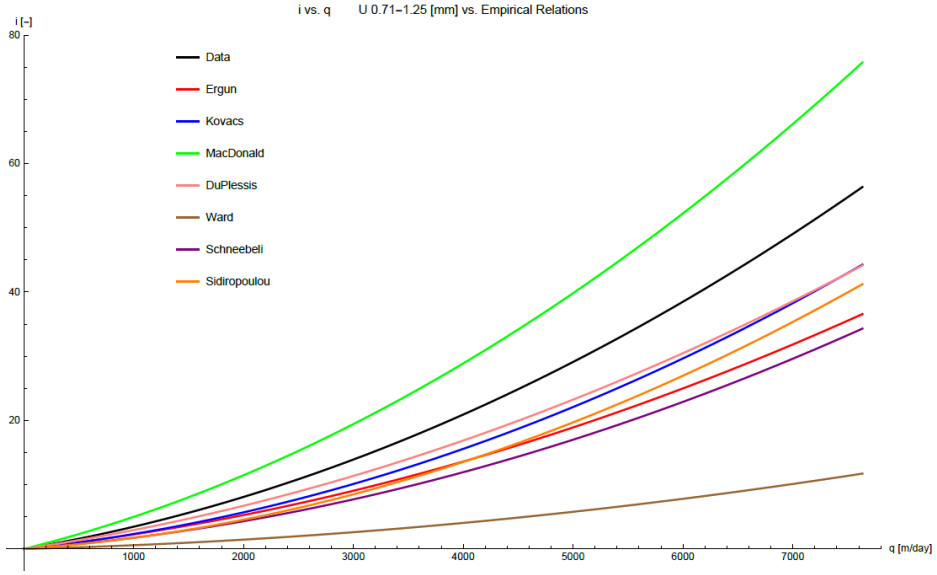
i vs. q U 0.71−1.25 [mm] vs. Empirical Relations
i [−]
Data
Ergun
Kovacs
MacDonald
DuPlessis
Ward
Schneebeli
Sidiropoulou
20
40
60
80
1000
2000
3000
4000
5000
6000
7000
q [m/day]

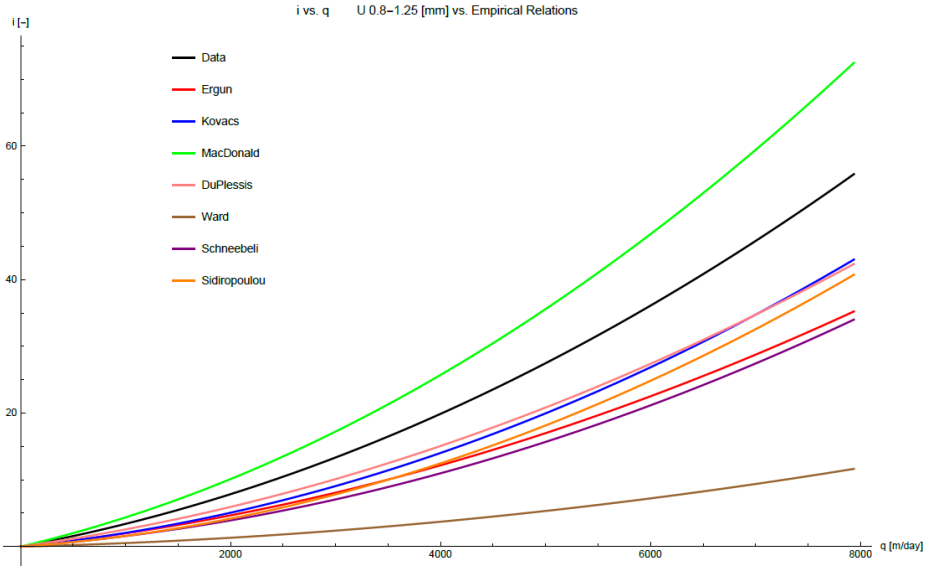
i vs. q U 0.8−1.25 [mm] vs. Empirical Relations
i [−]
Data
Ergun
Kovacs
MacDonald
DuPlessis
Ward
Schneebeli
Sidiropoulou
20
40
60
2000
4000
6000
8000
q [m/day]

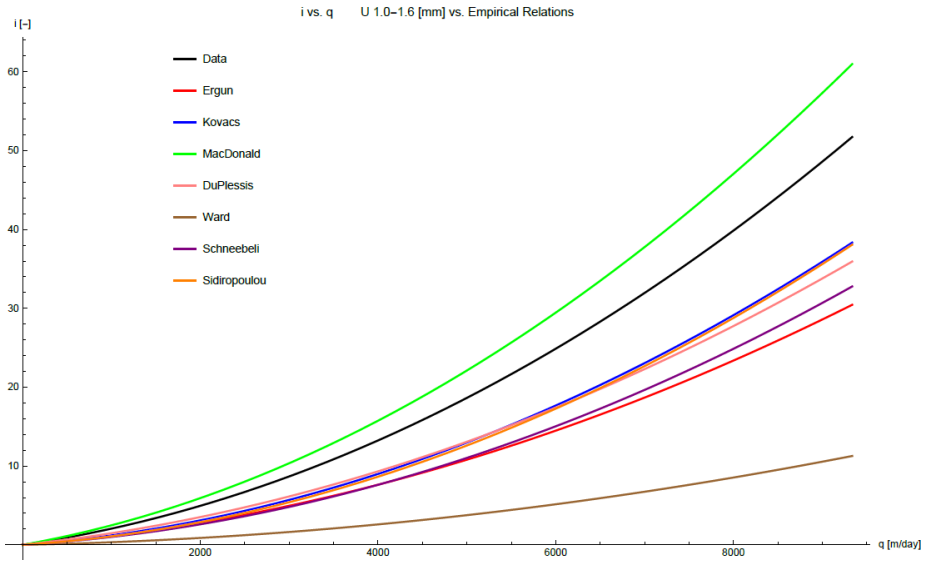
i vs. q U 1.0–1.6 [mm] vs. Empirical Relations
i [–]
Data
Ergun
Kovacs
MacDonald
DuPlessis
Ward
Schneebeli
Sidiropoulou
60
50
40
30
20
10
2000
4000
6000
8000
q [m/day]

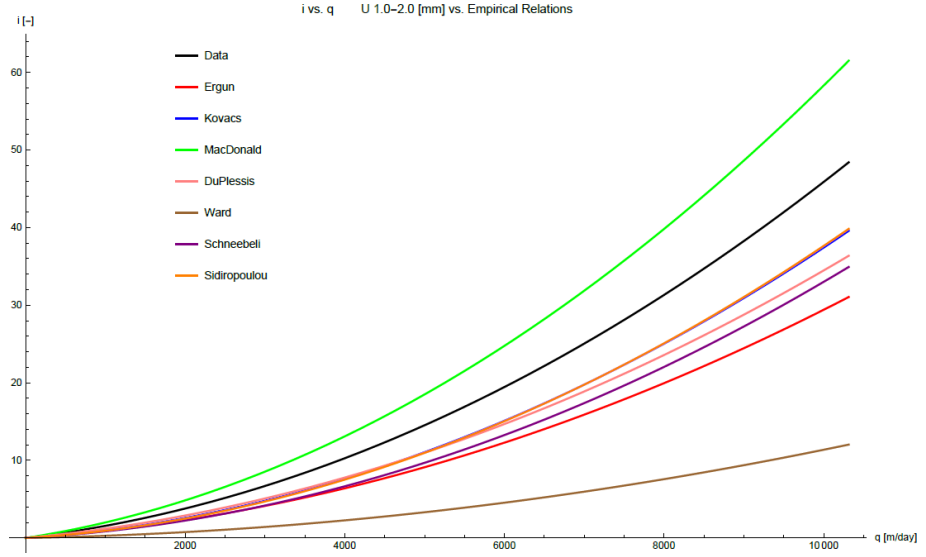
i vs. q U 1.0–2.0 [mm] vs. Empirical Relations
i [–]
Data
Ergun
Kovacs
MacDonald
DuPlessis
Ward
Schneebeli
Sidiropoulou
60
50
40
30
20
10
2000
4000
6000
8000
10000
q [m/day]

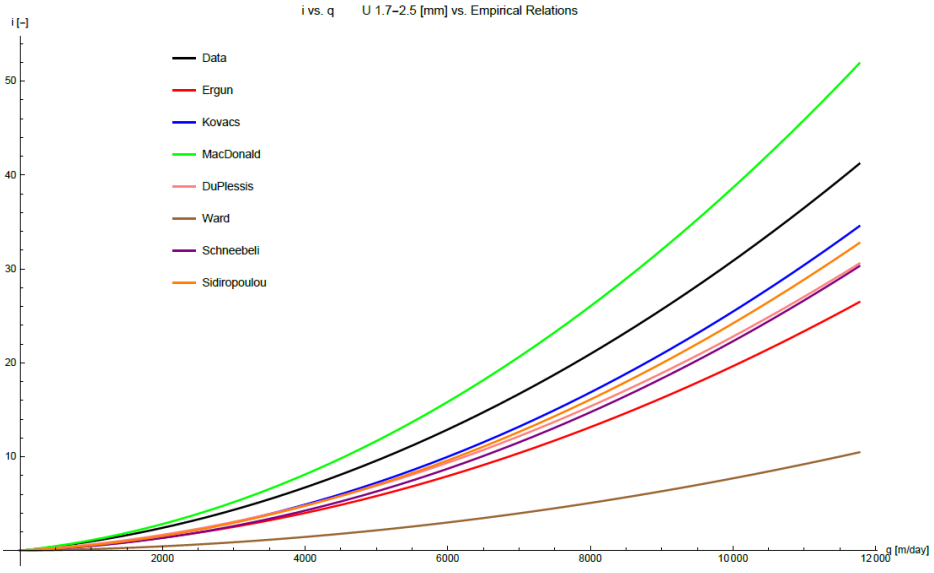
i vs. q U 1.7–2.5 [mm] vs. Empirical Relations
i [–]
Data
Ergun
Kovacs
MacDonald
DuPlessis
Ward
Schneebeli
Sidiropoulou
50
40
30
20
10
2000
4000
6000
8000
10000
12000
q [m/day]

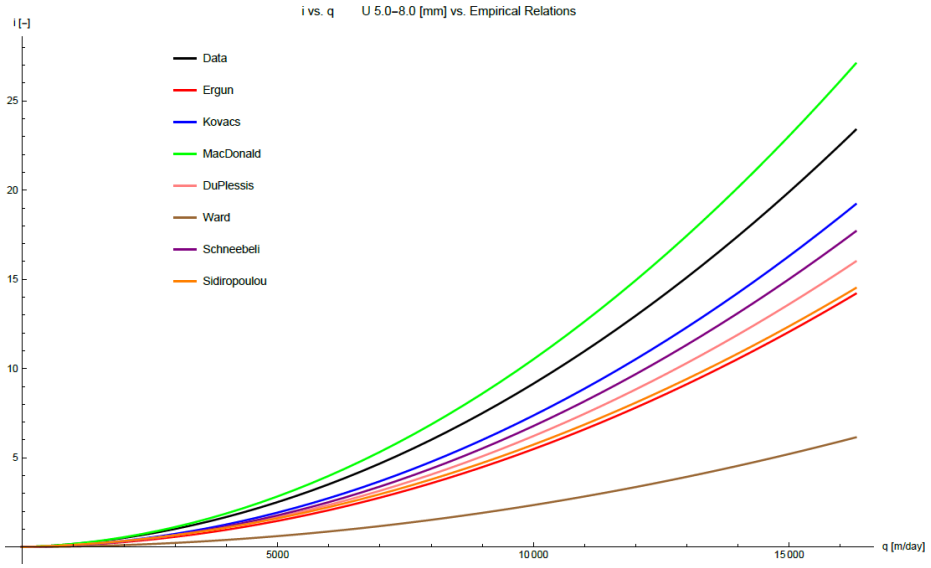
i vs. q U 5.0–8.0 [mm] vs. Empirical Relations
i [–]
Data
Ergun
Kovacs
MacDonald
DuPlessis
Ward
Schneebeli
Sidiropoulou
25
20
15
10
5
5000
10 000
15 000
q [m/day]

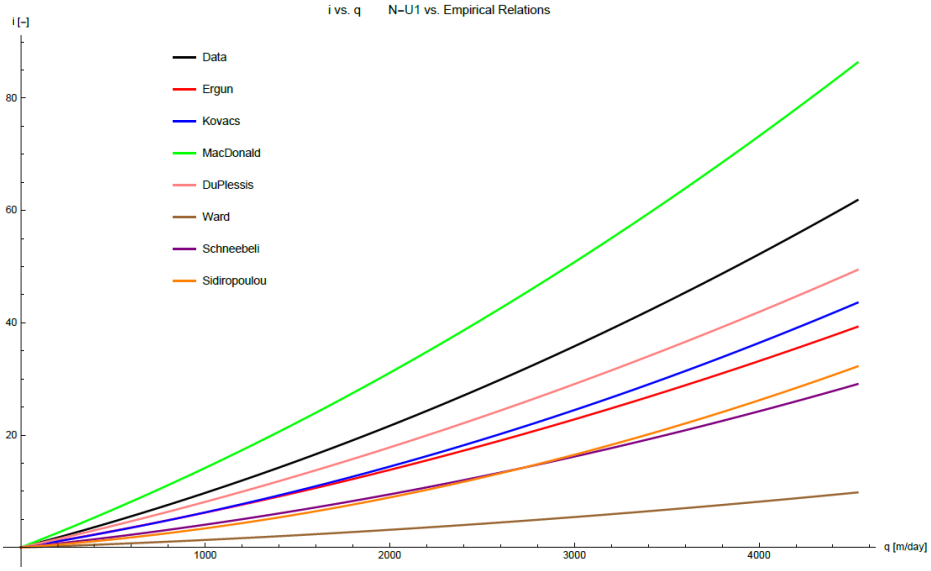
i vs. q N–U1 vs. Empirical Relations
i [–]
Data
Ergun
Kovacs
MacDonald
DuPlessis
Ward
Schneebeli
Sidiropoulou
80
60
40
20
1000
2000
3000
4000
q [m/day]

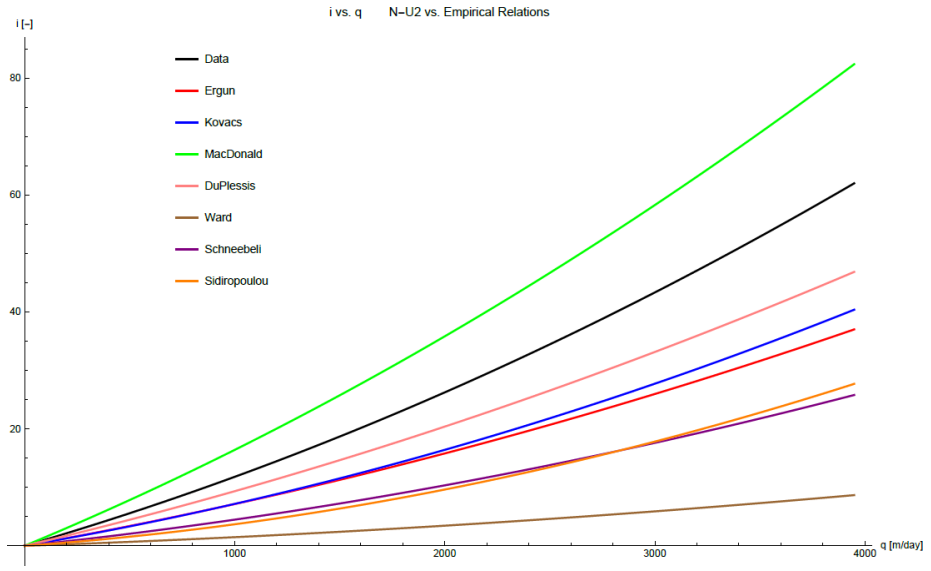
i vs. q N–U2 vs. Empirical Relations
i [–]
Data
Ergun
Kovacs
MacDonald
DuPlessis
Ward
Schneebeli
Sidiropoulou
80
60
40
20
1000
2000
3000
4000
q [m/day]

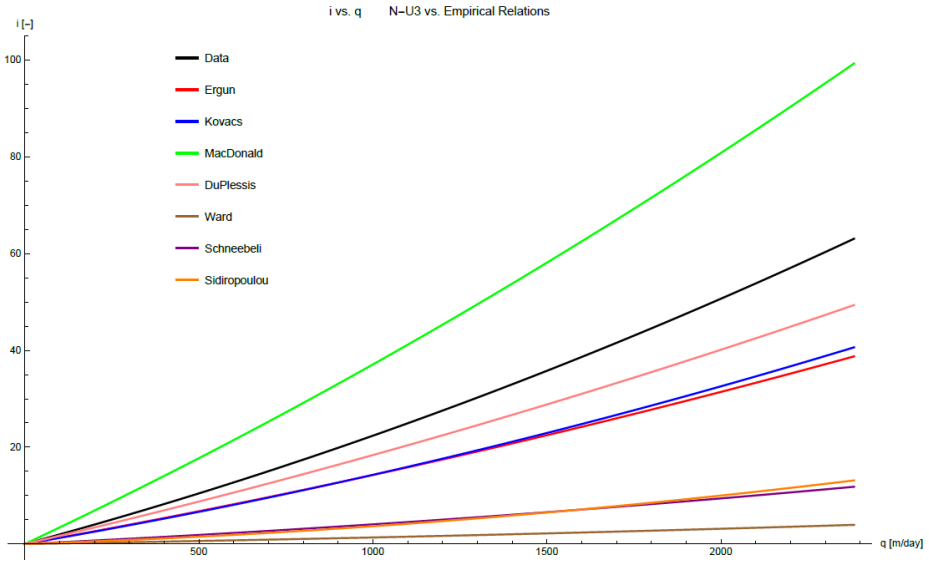
i vs. q N–U3 vs. Empirical Relations
i [–]
Data
Ergun
Kovacs
MacDonald
DuPlessis
Ward
Schneebeli
Sidiropoulou
100
80
60
40
20
500
1000
1500
2000
q [m/day]

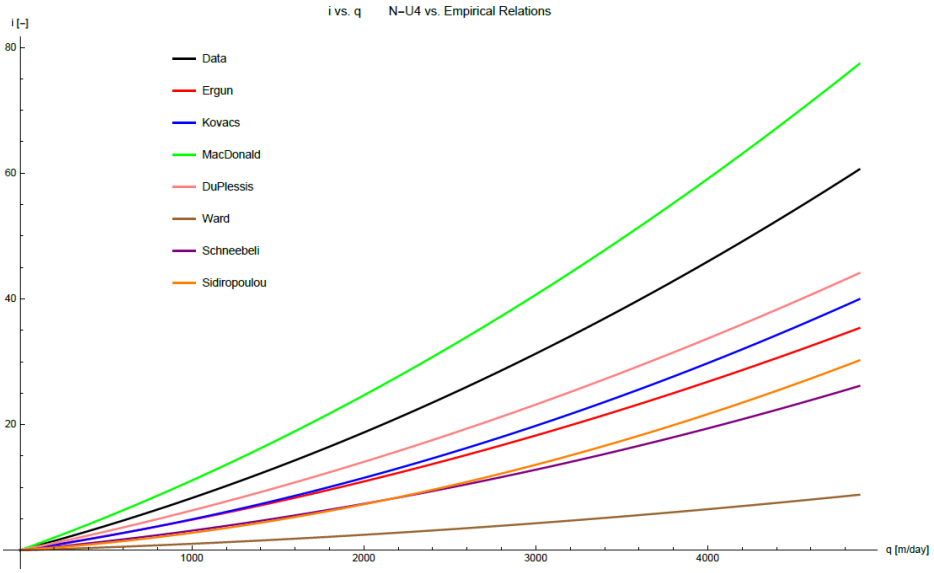
i vs. q N–U4 vs. Empirical Relations
i [–]
Data
Ergun
Kovacs
MacDonald
DuPlessis
Ward
Schneebeli
Sidiropoulou
80
60
40
20
1000
2000
3000
4000
q [m/day]

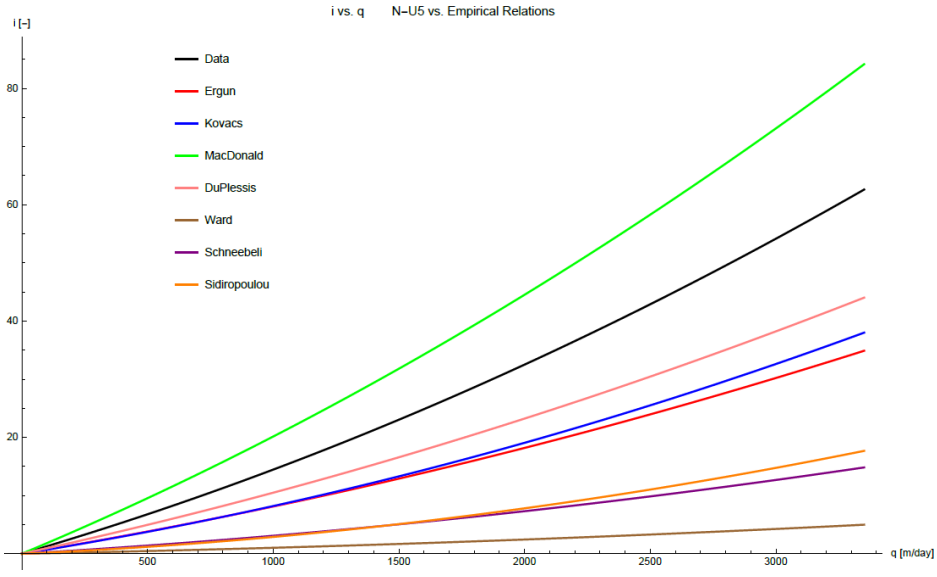
i vs. q N–U5 vs. Empirical Relations
i [–]
Data
Ergun
Kovacs
MacDonald
DuPlessis
Ward
Schneebeli
Sidiropoulou
80
60
40
20
500
1000
1500
2000
2500
3000
q [m/day]

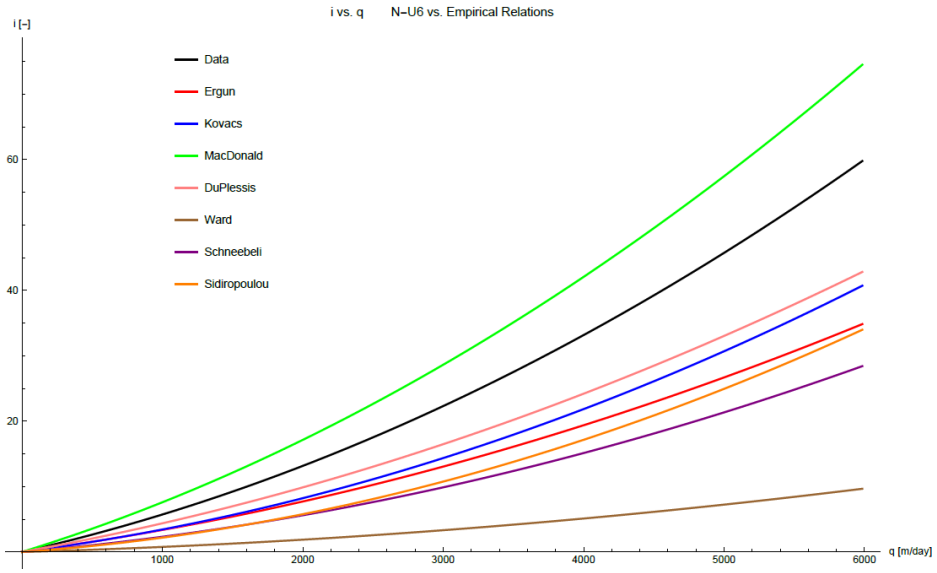
i vs. q N–U6 vs. Empirical Relations
i [–]
Data
Ergun
Kovacs
MacDonald
DuPlessis
Ward
Schneebeli
Sidiropoulou
60
40
20
1000
2000
3000
4000
5000
6000
q [m/day]

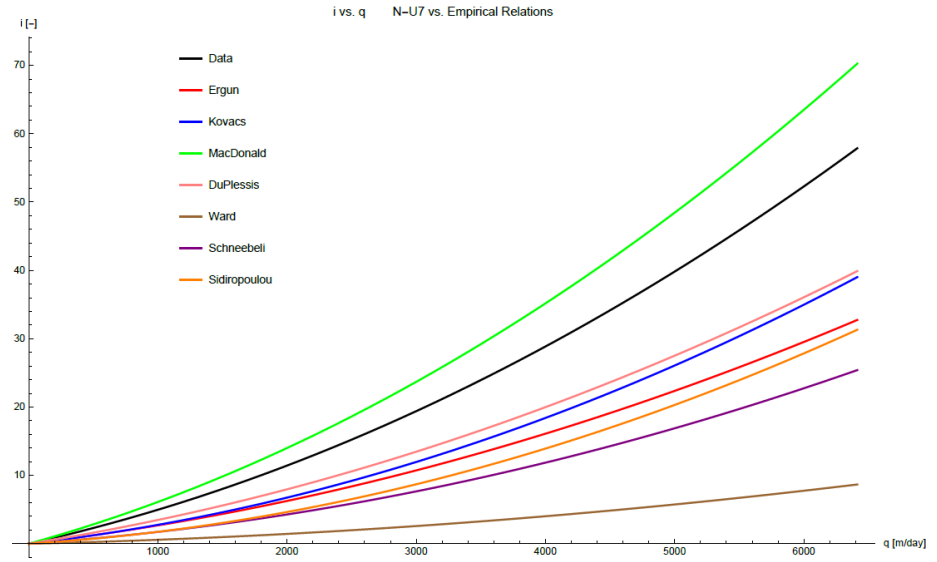
i vs. q N–U7 vs. Empirical Relations
i [–]
Data
Ergun
Kovacs
MacDonald
DuPlessis
Ward
Schneebeli
Sidiropoulou
70
60
50
40
30
20
10
1000
2000
3000
4000
5000
6000
q [m/day]

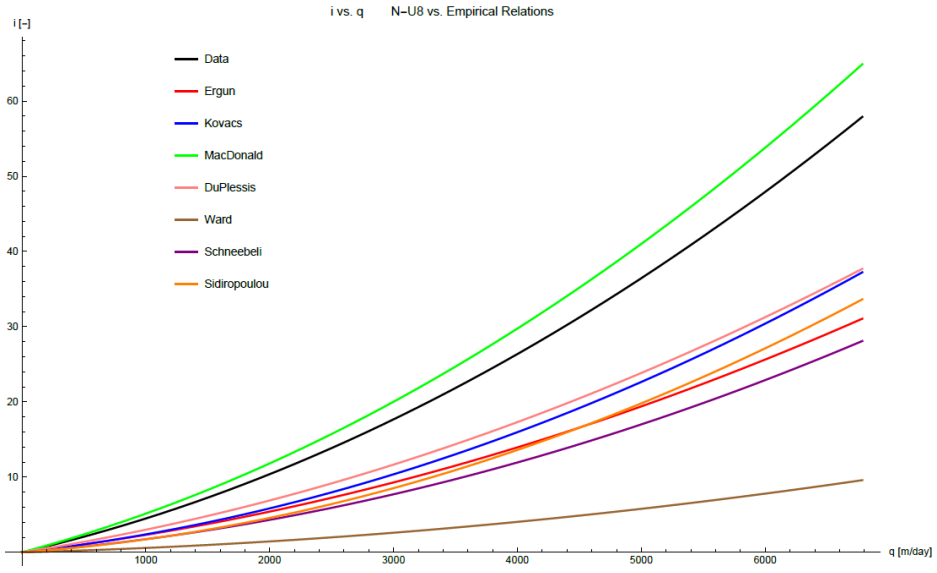
i vs. q N–U8 vs. Empirical Relations
i [–]
Data
Ergun
Kovacs
MacDonald
DuPlessis
Ward
Schneebeli
Sidiropoulou
60
50
40
30
20
10
1000
2000
3000
4000
5000
6000
q [m/day]

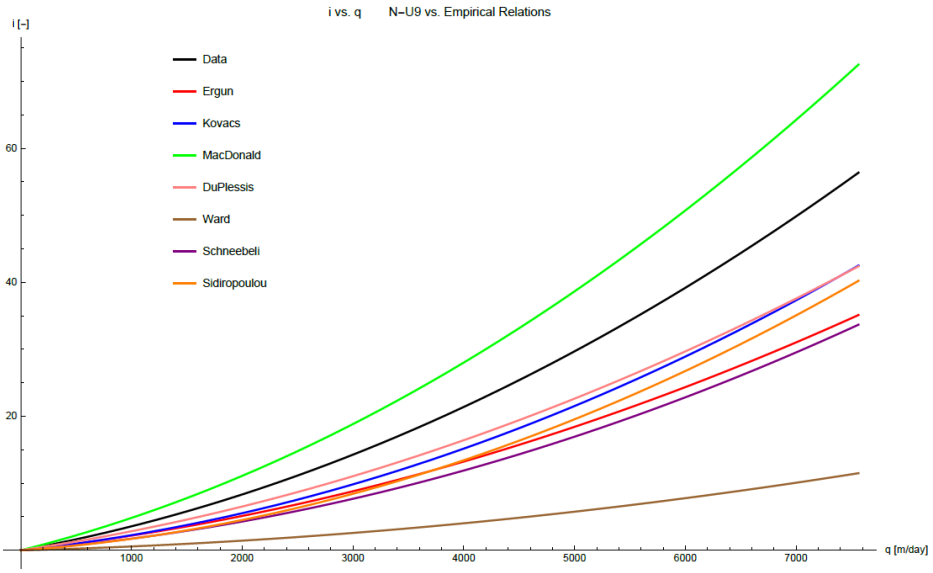
i vs. q N–U9 vs. Empirical Relations
i [–]
Data
Ergun
Kovacs
MacDonald
DuPlessis
Ward
Schneebeli
Sidiropoulou
60
40
20
1000
2000
3000
4000
5000
6000
7000
q [m/day]

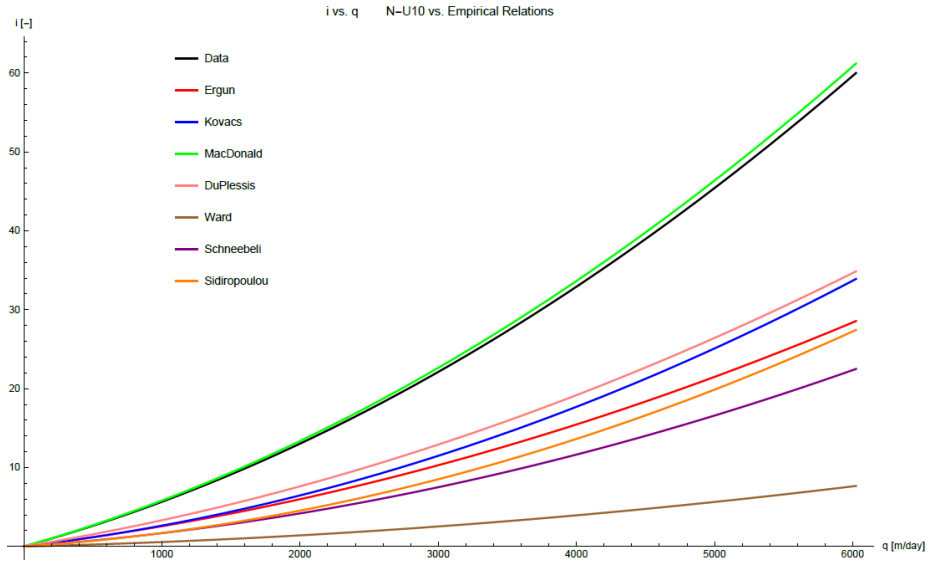
i vs. q N–U10 vs. Empirical Relations
i [–]
Data
Ergun
Kovacs
MacDonald
DuPlessis
Ward
Schneebeli
Sidiropoulou
60
50
40
30
20
10
1000
2000
3000
4000
5000
6000
q [m/day]

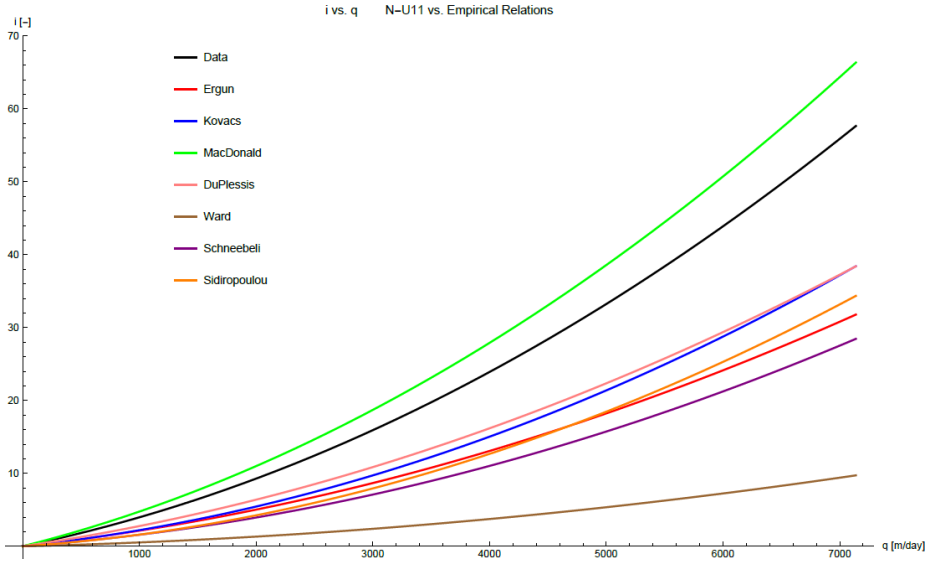
i vs. q N–U11 vs. Empirical Relations
i [–]
Data
Ergun
Kovacs
MacDonald
DuPlessis
Ward
Schneebeli
Sidiropoulou
70
60
50
40
30
20
10
1000
2000
3000
4000
5000
6000
7000
q [m/day]

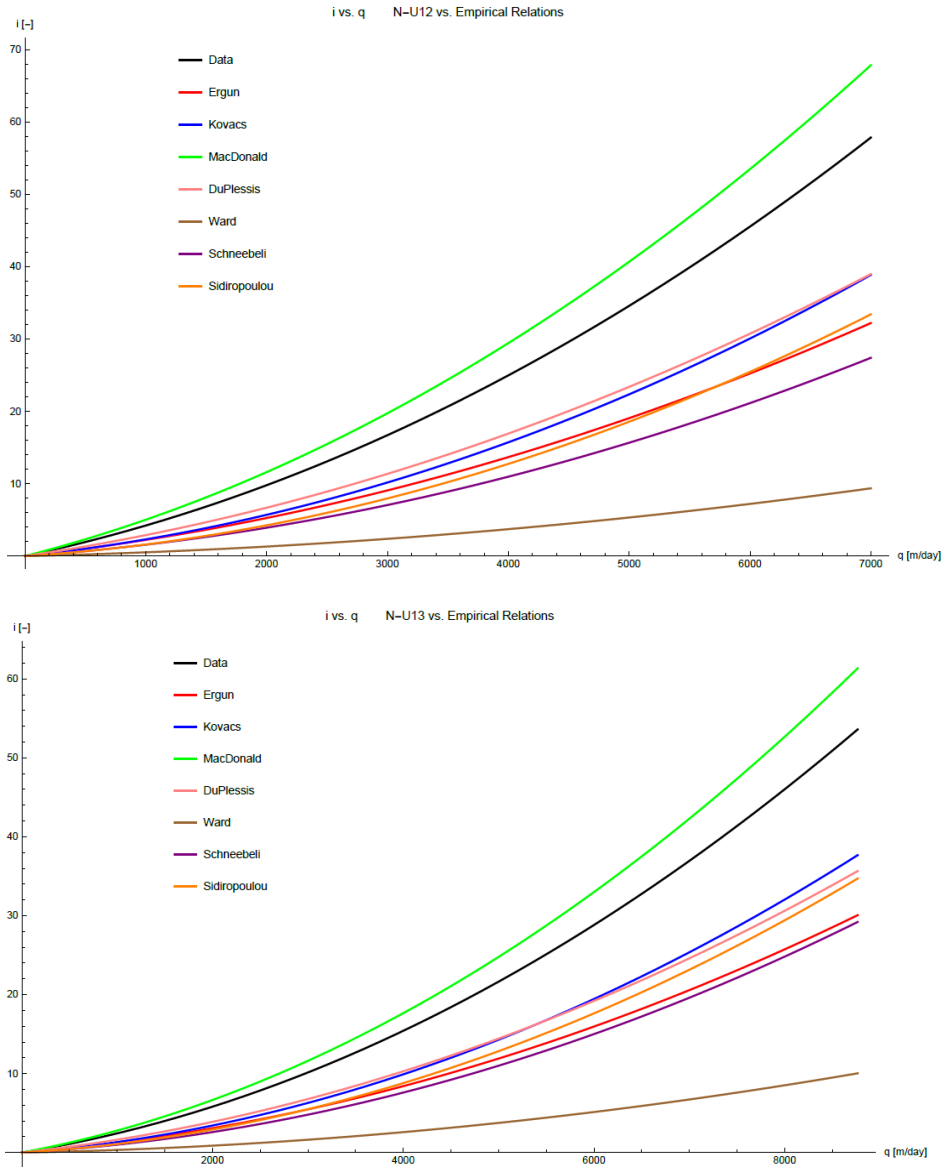

Figure A-8: Comparison between the empirical relations and the experimental data for all porous media.